PERFORMANCE ANALYSIS OF CHANNEL CODES IN MULTIPLE ANTENNA OFDM SYSTEMS

by

Oludare Ayodeji Sokoya

Submitted in partial fulfilment of the requirements for the degree

Philosophiae Doctor (Engineering)

in the

Department of Electrical, Electronic and Computer Engineering
Faculty of Engineering, Built Environment and Information Technology
UNIVERSITY OF PRETORIA

May 2012

UNIVERSITEIT VAN PRETORIA
UNIVERSITY OF PRETORIA
YUNIBESITHI YA PRETORIA

SUMMARY

PERFORMANCE ANALYSIS OF CHANNEL CODES IN MULTIPLE ANTENNA OFDM SYSTEMS

by

Oludare Ayodeji Sokoya

Promoter(s):	Professor B.T. Maharaj
Department:	Electrical, Electronic and Computer Engineering
University:	University of Pretoria
Degree:	Philosophiae Doctor (Engineering)
Keywords:	Equalisation, OFDM, multiple antenna techniques, space-time codes, space-frequency codes, pairwise error probability, fading channels

Multiple antenna techniques are used to increase the robustness and performance of wireless networks. Multiple antenna techniques can achieve diversity and increase bandwidth efficiency when specially designed channel codes are used at the scheme's transmitter. These channel codes can be designed in the space, time and frequency domain. These specially designed channel codes in the space and time domain are actually designed for flat fading channels and in frequency selective fading channel, their performance may be degraded. To counteract this possible performance degradation in frequency selective fading channel, two main approaches can be applied to mitigate the effect of the symbol interference due to the frequency selective fading channel. These approaches are multichannel equalisation and orthogonal frequency division multiplexing (OFDM). In this thesis, a multichannel equalisation technique and OFDM were applied to channel codes specially designed for multiple antenna systems.

An optimum receiver was proposed for super-orthogonal space-time trellis codes in a multichannel equalised frequency selective environment. Although the proposed receiver had

increased complexity, the diversity order is still the same as compared to the code in a flat fading channel.

To take advantage of the multipath diversity possible in a frequency selective fading channel, super-orthogonal block codes were employed in an OFDM environment. A new kind of super-orthogonal block code was proposed in this thesis. Super-orthogonal space-frequency trellis-coded OFDM was proposed to take advantage of not only the possible multipath diversity but also the spatial diversity for coded OFDM schemes. Based on simulation results in this thesis, the proposed coded OFDM scheme performs better than all other coded OFDM schemes (i.e. space time trellis-coded OFDM, space-time block coded OFDM, space-frequency block coded OFDM and super-orthogonal space-time trellis-coded OFDM). A simplified channel estimation algorithm was proposed for two of the coded OFDM schemes, which form a broad-based classification of coded OFDM schemes, i.e. trellis-coded schemes and block-coded schemes.

Finally in this thesis performance analysis using the Gauss Chebychev quadrature technique as a way of validating simulation results was done for super-orthogonal block coded OFDM schemes when channel state information is known and when it is estimated. The results obtained show that results obtained via simulation and analysis are asymptotic and therefore the proposed analysis technique can be use to obtain error rate values for different SNR region instead of time consuming simulation.

OPSOMMING

PRESTASIE-ONTLEDING VAN KANAALKODES IN MEERVOUDIGE ANTENNA OFDM

deur

Oludare Ayodeji Sokoya

Promotor(s):	Professor B.T. Maharaj
Departement:	Elektriese, Elektroniese en Rekenaar-Ingenieurswese
Universiteit:	Universiteit van Pretoria
Graad:	Philosophiae Doctor (Ingenieurswese)
Sleutelwoorde:	Gelykmakings, OFDM, meervoudige antenna, ruimte-tyd kodes, ruimte-frekwensiekodes, paarsgewyse fout waarskynlikheidkodes, vervaag kanale

Meervoudige-antennategnieke word gebruik om die robuustheid en werkverrigting van draadlose netwerke te verbeter. Meervoudige-antennategnieke kan diversiteit en verbeterde bandwydte-effektiwiteit teweegbring wanneer spesiaal ontwerpte kanaalkodes by die sender van die skema gebruik word. Die kanaalkodes kan in die ruimte, tyd- en frekwensiedomein ontwerp word.

Hierdie spesiaal ontwerpte kanaalkodes in die ruimte- en tyddomein word eintlik ontwerp vir plat deinende kanale en in ’n frekwensie-selektiewe deinende kanaal mag hulle werkverrigting swakker wees. Om hierdie moontlike werkverrigtingverswakking in frekwensie-selektiewe deinende kanaal teen te werk, kan twee hoofmetodes gebruik word om die effek van die simboolinmenging as gevolg van die frekwensie-selektiewe deinende kanaal te verminder. Hierdie benaderings is multikanaalvereffening en ortogonale frekwensiedivisiemultipleksering (OFDM). In hierdie tesis is ’n multikanaalvereffeningtegniek en OFDM toegepas op kanaalkodes wat spesiaal vir meervoudige-antennasisteme ontwerp is.

’n Optimumontvanger is voorgestel vir super-ortogonale ruimte-tydtraliekodes in ’n multik-

anaalvereffende frekwensieselektiewe omgewing. Hoewel die voorgestelde ontvanger meer kompleks was, is die diversiteitorde onveranderd vergeleke met die kode in ’n plat deinende kanaal.

Om die multiroetediversiteit wat in ’n frekwensieselektiewe plat deinende kanaal moontlik is te benut, is super-ortogonale blokkodes aangewend in ’n OFDM-omgewing. ’n Nuwe tipe super-ortogonale blokkode is in die tesis voorgestel. Super-ortogonale ruimte-tydtraliegekodeerde OFDM is voorgestel om voordeel te trek uit nie alleen die moontlike multiroetediversiteit nie, maar ook die ruimtelike diversiteit vir gekodeerde OFDM-skemas. Volgens simulasieresultate in hierdie tesis is die werkverrigting van die voorgestelde gekodeerde OFDM-skema beter as diè van alle ander gekodeerde OFDM-skemas (nl. ruimte-tydtraliegekodeerde OFDM, ruimte-tydblokgekodeerde OFDM, ruimte-frekwensieblokgekodeerde OFDM en super-ortogonale ruimte-tydtraliegekodeerde OFDM). ’n Vereenvoudigede kanaalskattingalgoritme is voorgestel vir twee van die gekodeerde OFDM-skemas, wat ’n breë klassifikasie van gekodeerde OFDM-skemas vorm, nl. traliegekodeerde skemas en blokgekodeerde skemas.

Ten slotte is in hierdie tesis werkverrigtinganalise gedoen deur die Gauss Chebychev-kwadratuurtegniek te gebruik as ’n metode om simulasieresultate te bevestig vir super-ortogonale blokgekodeerde OFDM-skemas met bekende en geskatte kanaalstatusinformasie. Die resultate wat verkry is, toon dat resultate wat deur simulasie en analise verkry is, asimptoties is en die voorgestelde analisetegniek, eerder as tydrowende simulasie, kan dus gebruik word om foutvoorkomswaardes vir verskillende sein-tot-geraasstreke vas te stel.

To the ALPHA and OMEGA: The present help in times of need

ACKNOWLEDGEMENT

My thanks goes to my supervisor, Professor B.T. Maharaj, for his inspiration with the topic of this thesis, careful guidance, constant support and sustained encouragement during the course of my studies.

My parents, Bldr. and Dr (Mrs.) E.O. Sokoya, and siblings, are owed many thanks for their support and their keen interest in my well-being. They have always prayerfully supported me in whatever challenge I have taken up in my life and my PhD was no exception. I would also like to thank my wife, Temitope, and my sons, Toluniyin and Ibukunoluwa, for all their support and encouragement throughout the time I worked on this thesis.

Thanks are also owed to the University of Pretoria, the Sentech Chair in Broadband Wireless Communication and Meraka Institute (managed by the CSIR) for their much appreciated financial support and for providing the equipment necessary for the completion of my PhD.

Last, but definitely not least, I would like to thank all my friends at RCCG Mt Zion Parish and all my postgraduate colleagues for their assistance and for making our time together enjoyable.

I give thanks unto the LORD; for He is good: for His mercy endures for ever.

LIST OF ABBREVIATIONS

1-D	One-dimensional
1G	First Generation
2G	Second Generation
2.5G	Second and half Generation
3G	Third Generation
AWGN	Additive White Gaussian Noise
BER	Bit Error Rate
BPSK	Binary Phase Shift Keying
CIR	Channel Impulse Response
COD	Complex Orthogonal Design
CSI	Channel State Information
DAB	Digital Audio Broadcasting
DLST	Diagonally Layered Space Time
DSL	Digital Subscriber Line
E-UTRAN	Evolved Universal Telecommunication Service Terrestrial Radio Access Network
FER	Frame Error Rate
FFT	Fast Fourier Transform
FS	Frequency Selective
GSM	Global System for Mobile Communication
HLST	Horizontally Layered Space Time
IEEE	Institute for Electrical and Electronic Engineers
IFFT	Inverse Fast Fourier Transform
LMS	Least Mean Square
LOS	Line of sight
LS	Least Squares

LST	Layered Space Time
LTE	Long-term Evolution
MIMO	Multiple-Input-Multiple-Output
MMSE	Minimum Mean Square Error
OFDM	Orthogonal Frequency Division Multiplexing
OFDMA	Orthogonal Frequency Division Multiple Access
PAM	Pulse Amplitude Modulation
PEP	Pairwise Error Probability
PSK	Phase Shift Keying
QAM	Quadrature Amplitude Modulation
QPSK	Quadrature Phase Shift Keying
SDR	Software Defined Radio
SISO	Single-Input-Single-Output
SOSTTC	Super-Orthgonal Space-Time Trellis Code
SOSFTC	Super-Orthgonal Space-Frequency Trellis Code
SNR	Signal-to-Noise Ratio
STBC	Space-Time Block Code
STTC	Space-Time Trellis Code
TCM	Trellis-Coded Modulation
UP	University of Pretoria
WiMAX	Wireless Interoperability for Microwave Access

NOTATION

$(.)^T$	The transpose operation
$(.)^H$	The hermitian transpose operation
$\mathbf{I}_N$	The $N \times N$ identity matrix
j	The imaginary unit (j= $\sqrt{-1}$)
$\log(.)$	The natural logarithm
$\log_2(.)$	The binary logarithm
$\max(.)$	The maximum
$\|.\|$	The norm of an element
$(.)^*$	The complex conjugate
$E(.)$	The expectation operation or mean value
$\det(.)$	The determinant of matrix element
f_n	The frequency of the nth subscriber
$\delta(.)$	The Dirac delta function
$\otimes$	The Kronecker operator
$Q(.)$	The Q-function
$\text{erfc}(.)$	The complementary error function

LIST OF SYMBOLS

P_R	The probability distribution of the Rayleigh distribution
σ^2	Variance of the Rayleigh distribution
N_t	Number of transmit antennas
N_r	Number of receive antennas
N	Number of subcarrier
$r_{ij(n)}$	The received vector from the i^{th} transmit antenna to the j^{th} receive antenna on the n^{th} subcarrier
$H_{ij}(n)$	Channel frequency response from the i^{th} transmit antenna to the j^{th} receive antenna on the n^{th} subcarrier
$\eta_j(n)$	AWGN vector from the j^{th} receive antenna on the n^{th} subcarrier
L	Total number of independent fading channel paths
C	The channel capacity of a fading channel
E_s	Energy per symbol
E_b	Energy per bit
N_o	Single-sided power spectral density of AWGN
τ	Delay spread
Δf	The tone spacing of an OFDM system
θ	Angular rotation of orthogonal block code matrix
O	Number of trellis state
$\hat{h}_{ij}(l,t)$	The complex amplitude of the l^{th} non-zero tap at time t for the i^{th} transmit and j^{th} receiver
$m(\mathbf{R},\mathbf{X})$	The decoding metric when $\mathbf{X}$ is transmitted and $\mathbf{R}$ is received
$P(\mathbf{X} \rightarrow \hat{\mathbf{X}}\|\mathbf{H})$	The conditional probability of choosing $\hat{\mathbf{X}}$ when in fact $\mathbf{X}$ was transmitted

TABLE OF CONTENTS

CHAPTER 1

INTRODUCTION

1.1 BRIEF HISTORY OF WIRELESS COMMUNICATION SYSTEMS

Owing to the need to transfer information (i.e. voice and data) in a fast, reliable and affordable way, the wireless communication world has been experiencing exponential growth to keep up with today's demand. This is evident in the historical progression growth from the first generation technologies (1G) to second generation (2G) technologies then to third generation (3G) technologies and now the much talked about fourth generation (4G) wireless technologies [1], [2].

The 1G wireless technologies are based on cellular telephone standard (i.e. analogue signals that are voice only). Examples of such standards are Nordic Mobile Telephone, Advanced Mobile Phone System, Nippon Telephone and Telegraph and Total Access Communication System [3].

The 2G technologies emerged in the 1990s and are based on digital transmission. Examples of the 2G technologies are Global System for Mobile Communication, Digital Advanced Mobile Phone System, Interim Standard-95 and Personal Digital Cellular [4].

The main difference between the 1G and 2G technologies is their mode of transmission and signalling. 2G technologies use digital transmission and have introduced advanced fast phone-to-network signalling, while 1G uses analogue transmission [2].

As the demand for 2G technologies increased, it became clearer that the demand for data

services was growing and consequently, the need for 3G technologies, i.e. high-speed internet protocol (IP) data networks. The three major 3G standards that provide high-speed IP networks are Universal Mobile Telecommunication Standard, Code Division Multiple Access 2000 (CDMA2000) and Time-Division Synchronous CDMA [5].

In-between 2G and 3G technologies, the 2.5G technologies were introduced as an extension of the 2G technologies. The 2.5G technologies describes a 2G technologies with a General Packet Radio Service, or other services not generally found in 2G or 1G networks. Examples of 2.5G technologies are Enhanced Data Rates for GSM Evolution, High-Speed Circuit Switched Data and Interim Standard for CDMA, i.e. IS-95B [6].

The main difference between the 2G and the 3G technologies is the method used to control digital signals used in transmitting data between specific points in the network, i.e. the switching method used. Packet-switching is used for data transmission in 3G, while circuit-switching is used for data transmission in 2G [1].

As the end of the first decade in the new millennium approaches, it has become clearer that the 3G network will be overwhelmed by the need for bandwidth-intensive applications such as streaming media and mobile applications, which place emphasises on the quality of services. Bandwidth-intensive devices marked the need to consider evolution towards the 4G, which promises data optimisation techniques with speed improvement up to 10-fold over the existing 3G technologies. The first two commercially available technologies billed as 4G are the Worldwide Interoperability for Microwave Access (WiMAX) standard [7] and the Long Term Evolution (LTE) [8] standard.

1.1.1 Worldwide Interoperability for Microwave Access

WiMAX is a wireless technology that promises to revolutionise wireless broadband service delivery. WiMAX promises a replacement for or an alternative to the digital subscriber line (DSL) and provides a long-range connection for private networks. For a fixed station, WiMAX can provide bit rates up to 40 Mbits/s according to the 2011 speed test by the WiMAX forum [9].

WiMAX is based on the IEEE 802.16 standard that uses Orthogonal Frequency Division Multiplexing (OFDM) with provision for Orthogonal Frequency Division Multiple Access

(OFDMA) and the multiple antenna system.

1.1.2 Long Term Evolution

LTE came about because of mobile subscribers' preference for an increase in the capacity and speed of wireless data network that can support new applications such as online gaming, mobile television and streaming content. LTE uses new digital signal processing (DSP) techniques, physical layer technologies e.g. OFDM, multiple-input-multiple-output (MIMO) and smart antennas to achieve an increased data rate and better subscriber experience. LTE is based on standards developed by the 3rd Generation Partnership Project and ensures a competitive edge over other cellular technologies. The radio access of LTE is called Evolved Universal Mobile Telecommunication Service Terrestrial Radio Access Network and is use to increase end-user throughput and sector capacity and reduce user plane latency, bringing about improved user experience with full mobility [10]. LTE promised a peak data rate of 100 Mbit/s and 50 Mbit/s for downlink and uplink, respectively.

1.2 CHALLENGES IN WIRELESS COMMUNICATION SYSTEM

Some challenges are faced in designing robust networks that can yield the performance necessary to support emerging trends in wireless communication. These challenges are [11]:

1. Traffic patterns, user locations and network conditions change constantly.

2. Wireless applications are heterogeneous with hard constraints that must be met by the network.

3. Privacy and security issues of the network present problems.

4. Energy and delay constraints change design principles across all layers of the protocol stack.

5. Wireless channels are difficult to model when compared with wired channels and their

capacity is limited.

As mentioned ealier, the wireless communication channel is an unpredictable and difficult communication medium as opposed to the wired one. As signals propagate through a wireless channel, they experience random fluctuation and arrive at the destination along a number of different paths, collectively referred to as multipath.
These paths arise from scattering, reflection and diffraction, as defined below.

1. Scattering – This happens when the medium through which the wave propagates is a rough surface, e.g. foliage, street signs and lamp posts.

2. Reflection – This occurs when a travelling wave strikes an object which has very large dimensions compared with the wavelength of the transmitting wave.

3. Diffraction – This happens when the path between the transmitter and the receiver is blocked by a surface that has sharp edges.

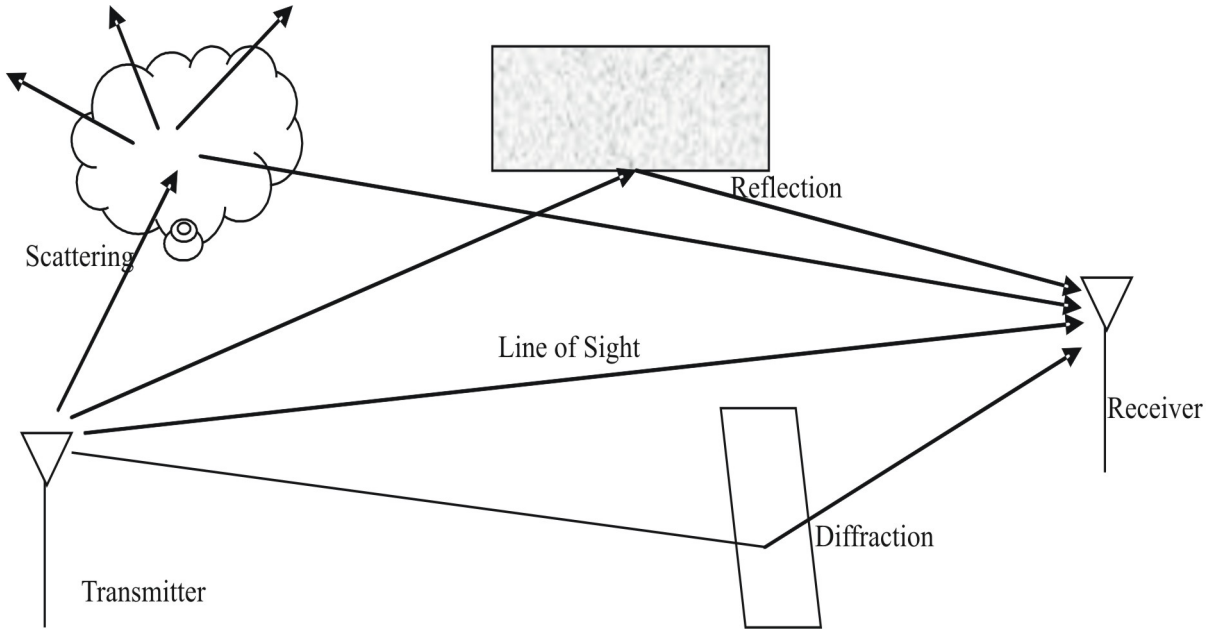

Figure 1.1: Different paths in wireless communication channel

Figure 1.1 shows the different paths in wireless communication channel. There is a non-obstructive path between the transmitter and the receiver i.e. line of sight (LOS) and other obstructive paths caused by scattering, reflection and diffraction of the transmitted signal

before it reaches the receiver.

1.3 FADING

Fading occurs when two or more versions of the transmitted signal i.e. multipath waves, arrive at the receiver at slightly different times, producing signals that vary widely in amplitude and phase. The multipath waves cause a rapid change in signal strength over a small travel distance, random frequency modulation and time echoes due to the propagation delay [12]. In radio wave propagation, many factors influence fading. These include multipath propagation, speed of the mobile subscriber (i.e. the relative motion between mobile station and the base station can result in different Doppler shifts on each of the multipath waves), speed of near objects and the signal's transmission's bandwidth; when the bandwidth of the multipath channel is less than that of the transmitting radio signal, the receiver signal will be affected, but not much, to cause local fading.

1.4 CHARACTERISTICS OF MULTIPATH CHANNEL

The different multipath wireless channels can be analysed and quantified based on some parameters. These parameters can be determined from the power delay profile. The power delay profile is a profile that shows the plot of the arrival time in seconds of different path waves versus the received power in dBm. These parameters can be divided into two:

1. Time dispersion parameters – These include the root-mean-square delay spread, excess delay spread and the mean delay spread;

2. Frequency dispersion parameters – These include the coherence bandwidth and the coherence time.

Fading channels can be characterised based on the time dispersion parameters as:

1. Frequency non-selective fading – This occurs when the channel has a constant gain and linear phase response over a bandwidth that is greater than the bandwidth of the

transmitted signal. The spectral characteristics of the transmitted signal are preserved at the receiver. The time delay spread is equal to zero.

2. Frequency selective (FS) fading – This occurs when the channel possesses a constant gain and linear phase over a bandwidth that is smaller than the bandwidth of the transmitted signal. The received signal is distorted and the channel induces intersymbol interference (ISI). This wideband channel model is usually approximated by a number of delta functions which fade independently.

Fading can also be characterised based on the frequency dispersion parameters as:

1. Slow fading – The channel impulse response changes at a rate much slower than the transmitted baseband signal. The channel may be assumed to be static over one or several reciprocal bandwidth intervals. Based on the coherence time, if a signal duration is smaller than the coherence time, the channel is said to be a slow fading channel.

2. Fast fading – The channel impulse response changes rapidly within the symbol duration. When the signal duration is greater that the coherence time, the channel is said to be a fast fading channel.

1.5 FADING CHANNEL MODEL

The nature of the multipath wireless channel is such that the amplitude and power of the received signal are random. This randomness necessitates a brief introduction of the various statistical models in the literature [6].

1.5.1 Rayleigh Fading Model

This is a commonly used channel model in wireless communication systems. The Rayleigh fading channel model is widely used when there is no LOS between the transmitter and the receiver. This model assumes that the magnitude of the received signal fades according to a Rayleigh distribution, i.e. the radial component of the sum of two uncorrelated Gaussian

random variables. The probability density function (pdf) of a Rayleigh random variable is given by [13]:

$$P_{RA}(r) = \frac{r}{\sigma^2} \exp\left(\frac{-r^2}{2\sigma^2}\right), \qquad r \geq 0 \tag{1.1}$$

where r is the amplitude of the equivalent baseband signal, σ^2 is the variance of zero mean random variable A and B, which are independently identical distributed Gaussian variables. The Rayleigh fading model is the worst fading case because it does not consider any LOS between the transmitter and receiver.

1.5.2 Rician Fading Model

This type of channel fading model is used when an LOS signal is present between the transmitter and the receiver. In Rician fading, the magnitude of the received signal is characterised by a Rician distribution. The pdf of Rician distribution is given by [6]:

$$P_{RI}(r) = \frac{r}{\sigma^2} \exp\left(\frac{-(r^2+q^2)}{2\sigma^2}\right) I_o\left(\frac{qr}{\sigma^2}\right), \qquad r \geq 0 \tag{1.2}$$

where q is the peak amplitude of the dominant signal and $I_o(\bullet)$ is the modified Bessel function of the first kind and of the zero-order. The Rician distribution converges to a Rayleigh distribution when the dominant signal disappears.

1.6 DIVERSITY

The various challenges of signals in a wireless communication channel can cause severe attenuation, i.e. fading, making it impossible for the receiver to determine the transmitted signals. One way of overcoming this challenge is using a technique called diversity, i.e. providing the receiver with different replicas of the transmitted signal. If these different replicas fade independently, it is less probable to have all copies of the transmitted signal in deep fade simultaneously. Therefore the receiver can reliably decode the transmitted signal using the received signal.

This can be done, for example, by picking the signal with the highest signal-to-noise ratio

(SNR) or by combining the multiple received signals. Diversity causes lower outages, which is a scenario where the effective SNR at the receiver goes through a deep fade and drops below the receiver threshold for reliable recovery of the transmitted signal, when compared with a network where it does not exist [14]. Examples of diversity techniques are:

1. Time diversity – This occurs when the transmitted information is replicated in different time slots. The time slots have a spacing that exceeds the coherence time of the channel. The main disadvantages of time diversity are that it requires a long, slow fading channel and does not utilise bandwidth efficiently. To combat these disadvantages, error-correcting codes and interleavers can be used with time diversity [11].

2. Frequency diversity – This occurs when the same information is transmitted or received simultaneously on two or more independently fading carrier frequencies. To achieve frequency diversity, the carrier frequencies should be separated by more than the coherence bandwidth of the channel. The main disadvantage of frequency diversity is that it is not bandwidth efficient owing to redundancy [14].

3. Antenna diversity – This occurs when multiple antennas are used at either the receiver or the transmitter side of the communication network. The multiple antennas need to be separated sufficiently (i.e. more than half of the wavelength) to achieve a level of performance that a single antenna cannot achieve [6]. Forms of antenna diversity are:

   (a) Spatial diversity: This is the use of multiple antennas to eliminate signal fading from a multipath environment. When multiple antennas are placed at the receiving end of a communication system it is called receive diversity, while when placed at the transmitting end it is called transmit diversity [15].

   (b) Pattern diversity: This is the use of two or more antennas with minimal overlapping patterns to provide greater overall pattern coverage [15].

   (c) Polarisation diversity: This is the use of vertically or horizontally polarised signals to achieve diversity. As a result of the scattering, the arriving signal, which is not polarised, can be split into two orthogonal polarisations. If the signal goes through

random reflections, its polarisation state can be independent of the transmitted polarisation. Polarisation diversity can only provide a diversity of an order of two and not more [15].

1.7 COMBINING METHODS

The multiple versions of the signals provided at the receiver by the various diversity techniques need to be properly combined to improve the performance of the system. There are three main combining methods [16] that can be used at the receiver:

1. Maximum ratio combining (MRC) – In this method, multiple versions of the same information-bearing signal received over different diversity branches are combined so as to maximise the instantaneous SNR at the combiner output. It is a classical and powerful technique that mitigates the effects of severe fading at the receiver [17].

2. Selection combining – In this method, amongst the multiple versions of the different diversity branches, the signal with the highest SNR is selected for decoding [17].

3. Hybrid combining or generalised selection combining – This is a method in which a subset of available diversity branches is selected based on the branch SNR and combined per MRC rule [18].

1.8 CAPACITY OF MULTIPLE ANTENNA SYSTEMS IN FADING ENVIRONMENT

In multiple antenna wireless systems, the basic model and the possible channel capacity are of great importance in wireless network design and performance measurement. The basic model of a multiple antenna system is shown below in Figure 1.2.

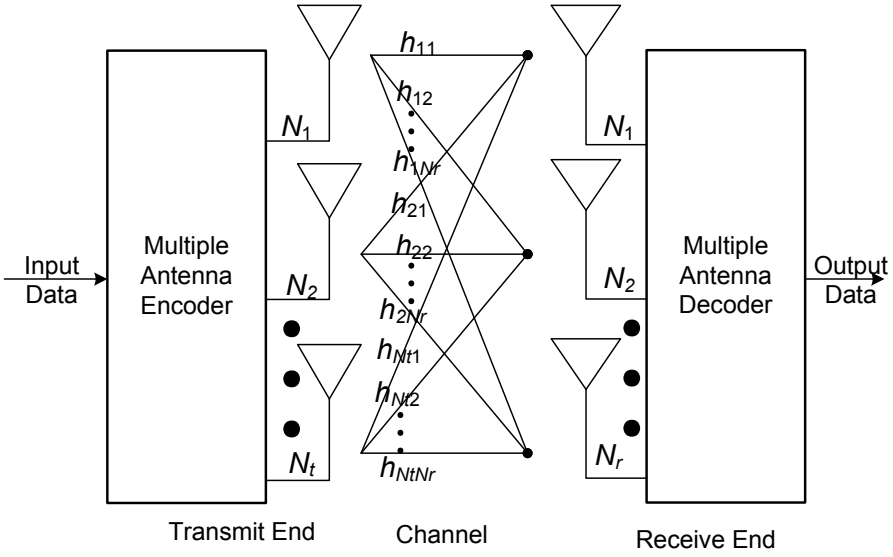

Figure 1.2: Multiple antenna system

Figure 1.2 shows the block diagram of a multiple antenna wireless system with N_t transmit antennas and N_r receive antennas. The channel matrix $\mathbf{H}$ that characterises the multiple antenna wireless system can be represented by:

$$\mathbf{H} = \begin{bmatrix} h_{11} & \dots & h_{N_t 1} \\ \vdots & \ddots & \vdots \\ h_{1N_r} & \dots & h_{N_t N_r} \end{bmatrix} \tag{1.3}$$

where h_{ij} is the complex channel gain between transmitter i and receiver j.

The channel capacity of a communication system can be defined as the measure of the amount of information transmitted and received in the system with a negligible probability of error. Wireless systems require high channel capacity so that large amounts of information can be transmitted and received. Communication systems which operate over a single transmitter and a single receiver channel (also known as single-input-single-output (SISO) systems) have limited capacities in a wireless channel when compared to transmission over multiple antenna wireless channels.

Earlier works in literature [19], [20] have shown that very high capacities can be obtained by employing multiple antenna elements at both the transmitter and the receiver of a wireless

system. This is demonstrated below by enumerating the ergodic capacity for a SISO system and a MIMO system. The ergodic capacity of a SISO system (*i.e.* $N_t = N_r = 1$) with a random complex channel is given by [20];

$$C = E\left\{\log_2\left(1 + SNR \bullet |h|^2\right)\right\} \tag{1.4}$$

where E denotes the expectation of the ensemble statitistic of the channel vector h and SNR is the average signal-to-noise ratio at the receiver side. If $|h|$ is Rayleigh then $|h|^2$ follows a chi-squared distribution with two degrees of freedom.

The ergodic capacity for an $N_t \times N_r$ MIMO system [19] [20] is expressed as:

$$C = E\left\{\log_2\left(\det\left[\mathbf{I}_{N_r} + \frac{SNR}{N_t} \bullet \mathbf{H}\mathbf{H}^H\right]\right)\right\} \tag{1.5}$$

where $\mathbf{H}$ is the MIMO channel matrix of $N_t \times N_r$ dimension given in equation (1.3), $(\bullet)^H$ denotes the transpose conjugate of the matrix element and $\mathbf{I}_{N_r}$ is the identity matrix of order N_r. In the case represented by (1.5) the transmitter has no knowledge of the channel, but the receiver has perfect knowledge of the channel and the noise samples are assumed to be uncorrelated.

The expression in equation (1.5) can be reduced further according to the law of large numbers [21]. Using the law of large numbers, the term $\frac{1}{N_t} \bullet \mathbf{H}\mathbf{H}^H$ tends to $\mathbf{I}_{N_r}$ as N_t gets large and N_r is fixed. Thus the capacity can be expressed as:

$$C = E\left\{N_r\left(\log_2\left[1 + SNR\right]\right)\right\}. \tag{1.6}$$

It was shown in [22] that the total capacity of the MIMO channel is made up by the sum of parallel additive white Gaussian noise (AWGN) SISO sub-channels and that the number of parallel sub-channels is determined by the rank of the channel matrix, which is given by $min\left(N_t, N_r\right)$.

Further analysis of equation (1.5) shows that it is possible to decompose $\mathbf{H}\mathbf{H}^H$ as a function of the eigenvalues of the diagonal equivalent matrix of $\mathbf{H}\mathbf{H}^H$ so that equation (1.5) becomes

equation (1.7), i.e

$$C = E\left\{\sum_{i=1}^{m}\log_2\left(1+\frac{SNR}{N_t}\lambda_i\right)\right\}, \tag{1.7}$$

where m is the number of the non-zero eigenvalues, i.e. λ_i of $\mathbf{H}$.
When the channel is known at the transmitter, the maximum capacity of a MIMO channel can be achieved by using the water-filling principle [23] and equation (1.5) becomes:

$$C = E\left\{\sum_{i=1}^{m}\log_2\left(1+\beta_i\frac{SNR}{N_t}\lambda_i\right)\right\}, \tag{1.8}$$

where β_i is a scalar that represents the portion of the available transmit power going into the ith sub-channel. In water-filling, more power is allocated to the "better" sub-channels with higher SNR so as to maximise the sum of the data rate in all sub-channels.

Figure 1.3 shows the channel capacity plot for a Rayleigh fading SISO channel as calculated by equation (1.4) and that of a Rayleigh fading MIMO channel in equation (1.5) for various transmit and receive antennas. In general 10000 channel realisations are used in the capacity plot shown in Figure 1.3. According to Figure 1.3, as the number of antennas increases, the capacity increases significantly. Also at 15dB, the channel capacity increases from 4 bits/sec to 10 bits/sec to 15 bits/sec and 30 bits/sec for $N_t = N_r = 1$, $N_t = N_r = 2$, $N_t = N_r = 3$ and $N_t = N_r = 6$, respectively.

1.9 SPACE-TIME CODING

As mentioned earlier, multiple antenna wireless systems can be used to achieve antenna diversity. However, this diversity is at the expense of bandwidth efficiency. In order not to compromise diversity at the expense of bandwidth efficiency, channel codes can be specially designed for multiple antenna wireless systems.
Space-time codes are bandwidth-efficient channel codes that are suitable for multiple antenna systems without compromising the diversity over wireless channels. These codes use the combination of conventional channel coding design criteria, modulation techniques and

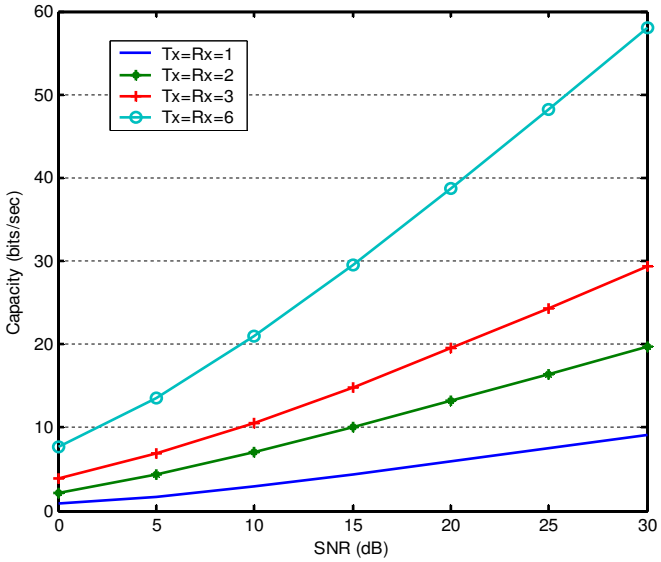

Figure 1.3: Channel capacity of a SISO channel compared with the ergodic capacity of a Rayleigh fading MIMO channel with a diferent number of transmit and receive antennas

multiple antenna diversity techniques in their design. Space-time coding schemes give a better error rate performance when compared with an uncoded scheme [24].
Various forms of space-time coding schemes that can be used for multiple antenna systems are discussed below.

1.9.1 Layered Space-Time Codes

Layered space-time (LST) codes are channel codes designed according to LST architecture. The LST architecture is a point-to-point communication architecture that employs an equal number of antennas elements at both ends of a multiple antenna system [25], [26]. The encoded codewords used in the LST architecture can be assigned horizontally i.e. horizontally layered space-time (HLST) or diagonally, i.e. diagonally layered space-time (DLST) [27]. In LST architecture, input bits are first demultiplexed into N_t and then encoded by a one-dimensional convolution encoder. The output of the encoder contains symbols that can be layered horizontally or diagonally in the transmitted codeword matrix with the aim of reducing receiver complexity. When comparing HLST codes and DLST codes in a slow fading

channel, DLST codes achieve better error rate performance than HLST codes [27].

1.9.2 Space-Time Block Code

Alamouti first presented a transmit diversity technique, for two transmit antennas, with a simplified decoding algorithm [28]. This scheme was later called space time block codes (STBC) in [24] and [29]. Based on these later works, the Alamouti codes were extended to more than two transmit antennas using the theory of orthogonal design [30]. The theory of orthogonal design enables the use of a simple maximum-likelihood decoder that is based on linear combining at the receiver. Based on this theory, two types of STBC can be generated. The first type, i.e. real orthogonal design, is based on real constellation such as pulse amplitude modulation, while the second type, i.e. complex orthogonal design, is based on complex constellations, e.g. phase-shift keying and quadrature amplitude modulation.

1.9.2.1 Real Orthogonal Design

A real orthogonal design of size n is an $n \times n$ orthogonal matrix whose rows are permutations of real numbers $\pm x_1, \pm x_2, \ldots, \pm x_n$. For example, real orthogonal designs for $n = 2$, expressed as $\mathbf{O}_2$ and $n = 4$, expressed as $\mathbf{O}_4$ are given below as :

$$\mathbf{O}_2 = \begin{bmatrix} x_1 & x_2 \\ -x_2 & x_1 \end{bmatrix} \tag{1.9}$$

and

$$\mathbf{O}_4 = \begin{bmatrix} x_1 & x_2 & x_3 & x_4 \\ -x_2 & x_1 & -x_4 & x_3 \\ -x_3 & x_4 & x_1 & -x_2 \\ -x_4 & -x_3 & x_2 & x_1 \end{bmatrix}. \tag{1.10}$$

Obtaining a real orthogonal matrix for different values of n is known as the Hurwitz-Radon problem in mathematics [30]. Based on the Hurwitz-Radon theory, the maximum rate for a real orthogonal designed matrix can only be obtained for n =2, 4 or 8.

A set of $n \times n$ real matrices $\mathbf{B}_1, \ldots, \mathbf{B}_k$ is called a size k Hurwitz-Radon matrices if:

$$\mathbf{B}_i^T \mathbf{B}_i = \mathbf{I} \tag{1.11}$$

$$\mathbf{B}_i^T = -\mathbf{B}_i \qquad i = 1, \ldots, k \tag{1.12}$$

$$\mathbf{B}_i \mathbf{B}_j = -\mathbf{B}_i \mathbf{B}_j \qquad 1 \leq i,\ j \leq k \tag{1.13}$$

where $(\bullet)^T$ is the transpose of the matrix element.

If $n = 2^a b$ is a positive integer , where b is an odd number and $a = 4c + d$ with $0 \leq d \leq 4$ and $0 \leq c$, the Hurwitz-Radon family of matrices contains strictly fewer than $\rho(n) = 8c + 2^d$ matrices. From the expression of $\rho(n)$, one can show that a Hurwitz-Radon family of $n - 1$ matrices of size $n \times n$ exists if and only if $n = 2,\ 4$ or 8 .

Therefore to construct a STBC of length p, a Hurwitz-Radon family of integer matrices with $\rho(p) - 1$ members $\{\mathbf{A}_1, \mathbf{A}_2, \ldots, \mathbf{A}_{\rho(p)-1}\}$ is chosen. Let $\mathbf{A}_o = \mathbf{I}$ and denote $\mathbf{X} = (x_1, \ldots, x_p)$; one can construct a $p \times n$ generalised real orthogonal design ϕ by setting the jth column of ϕ to be $\mathbf{A}_{j-1}\mathbf{X}^T$. The real orthogonal matrix ϕ explained above is full-ranked.

1.9.2.2 Complex Orthogonal Design

A complex orthogonal design (COD) of size n is an orthogonal matrix $\mathbf{C}$ whose rows are permutations of $\pm x_1, \pm x_2, \ldots, \pm x_n$, their conjugates $\pm x_1^*, \pm x_2^*, \ldots, \pm x_n^*$, or products of the complex indeterminants with the imaginary unit i where $i = \sqrt{-1}$, such that:

$$\mathbf{C}\mathbf{C}^H = \sum_{v=1}^{n} |x_v|^2 \mathbf{I}. \tag{1.14}$$

If the elements of $\mathbf{C}$ are complex symbols $x_1, x_2, \ldots, x_n$ from a signal constellation, such as binary phase shift keying (BPSK) or quadrature phase shift (QPSK) and are to be transmitted through N_t transmit antennas in m time slots, the transmission rate R of $\mathbf{C}$ is given by:

$$R = \frac{n}{m}. \tag{1.15}$$

A higher rate means that more information is being carried by **C** at a given time slot.
The propose code by Alamouti [28] is an example of an STBC from COD of rate 1 for $N_t = 2$. In [29] more STBCs were proposed based on a systematic rate 1/2 COD construction for any number of transmit antenna using rate 1 real orthogonal design. Later works [31] and [32] on COD proposed STBCs for different rates and for various transmit antennas but none of these codes is full rate. One can therefore generalise that the STBC in [28], whose matrix is given below in equation (1.16), is a special case of COD with full rate.

$$\mathbf{C} = \begin{bmatrix} x_1 & x_2 \\ -x_2^* & x_1^* \end{bmatrix}. \tag{1.16}$$

1.9.3 Space-Time Trellis Code

Space-time trellis coding (STTC) was invented by Tarokh et al. [24] as a way of combining signal processing with a multiple antenna system to produce a system with an improved gain over the earlier transmit diversity schemes [33] [34]. Baro et al. [35] showed that although the STTC presented in [24] achieves maximum possible diversity, it does not necessarily provide full coding advantage because it was handcrafted. Subsequent computer searches in [35] and [36] have yielded new STTC with an improved coding advantage.
In [37], using generator matrices, various optimum STTCs were proposed. The proposed STTCs provide maximum diversity and coding gain for various states and antennas for a phase shift keying (PSK) modulation. By comparing the STTC that was handcrafted (i.e. [24]) and the ones generated by a generator matrix (i.e. [35], [36] and [37]), one can observe that the STTC that was handcrafted gives the best compromise in terms of constellation size, data rate, diversity advantage and trellis complexity.
The encoder system of an STTC is based on a one-input symbol at a time and a sequence of output symbols, whose length represents the number of transmit antennas.
To understand the functionality of an STTC, an example of the handcrafted STTC using a QPSK signal constellation is presented below.
A wireless communication system that is equipped with N_t and N_r transmit and receive antennas respectively is considered. Information data are encoded by the space-time trellis

encoder; the encoded data go through a serial-to-parallel converter, and are divided into N_t streams of data. Each stream of data is used as the input to a transmit antenna. At each time slot t, the output of the transmitted signal x_i^t is transmitted using transmit antenna i for $1 \leq i \leq N_t$. The trellis diagram for a four-STTC is shown in Figure 1.4 below.

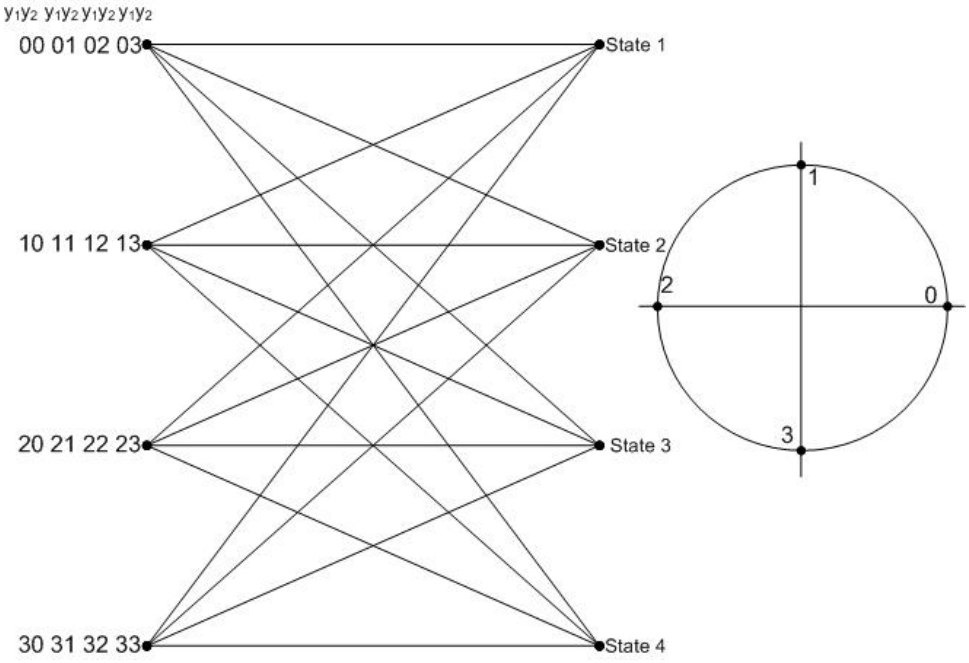

Figure 1.4: Four-state QPSK STTC

At each time t , the encoder is in a generic state. The input bit streams to the space-time encoder are divided into groups of two bits, a_1a_2 . Each group 00, 01, 10 or 11 then selects one of the four branches originating from the corresponding state. The branches are then mapped for every transmit antenna into one of the four constellation points. The edge labels y_1y_2 in the above figure are associated with the four transitions from top to bottom and indicate that symbols y_1 and y_2 are transmitted simultaneously over the first and second antennas, respectively. The encoder moves to the next state after transmission of the couple of symbols. At the decoder, based on the received estimate and using the maximum likelihood (ML) method, a decoding algorithm is then used to search for the best path. Viterbi algorithm is a good decoding algorithm for trellis-based codes [38].

1.9.4 Super-Orthogonal Space-Time Trellis Code

By combining the advantages of both STTC and STBC, a new channel code for multiple antenna systems called super-orthogonal space- time trellis code (SOSTTC) was developed [39], [40]. The SOSTTC uses sets of super-orthogonal block code (SOBC) and set partitioning technique in its construction. The sets of SOBCs are obtained by rotating the original block code by an angle θ. This code gives an improved coding gain and diversity order when compared with other space-time coding schemes, i.e. STTC [24] and STBC [28]. The SOSTTC provides a scheme that shows how to systematically design a channel code for multiple antenna systems of any code rate and maximum coding gain when compared with other space-time coding schemes.

The main idea behind SOSTTC is to consider STBCs as a modulation scheme for multiple transmit antennas and assign an STBC with specific constellation symbols to transitions emanating from a state. For a $T \times N_t$ STBC, picking a trellis branch emanating from a state is equivalent to transmitting TN_t symbols from the N_t transmit antennas in T time intervals. By doing so, it is guaranteed that the diversity of the corresponding STBC is preserved.

The super-orthogonal transmission matrix used in the design of SOSTTC for $N_t = 2$ is given by:

$$\mathbf{X}(x_1, x_2, \theta) = \begin{bmatrix} x_1 e^{j\theta} & x_2 \\ -x_2^* e^{j\theta} & x_1^* \end{bmatrix}. \tag{1.17}$$

In equation (1.17) $x_i \in e^{j\frac{2\pi a}{M}}$ represent the M-PSK signal constellation. The angular rotation θ is equivalent to $2\pi\acute{a}/M$ where $\acute{a} = 0, 1, \cdots, M-1$. Despite the angular rotation of the transmitted signal, the matrix elements of equations (1.17) are still members of the M-PSK constellation and the signal constellation is not expanded. For BPSK signal constellation, $\theta = 0$ or π while for a QPSK signal constellation, $\theta = 0$ or $\pi/2$ or π or $3\pi/2$. When θ in equation (1.17) is zero, the Alamouti code is obtained.

The trellis diagram for a two-state and a four-state SOSTTC scheme is given in Figure 1.5.

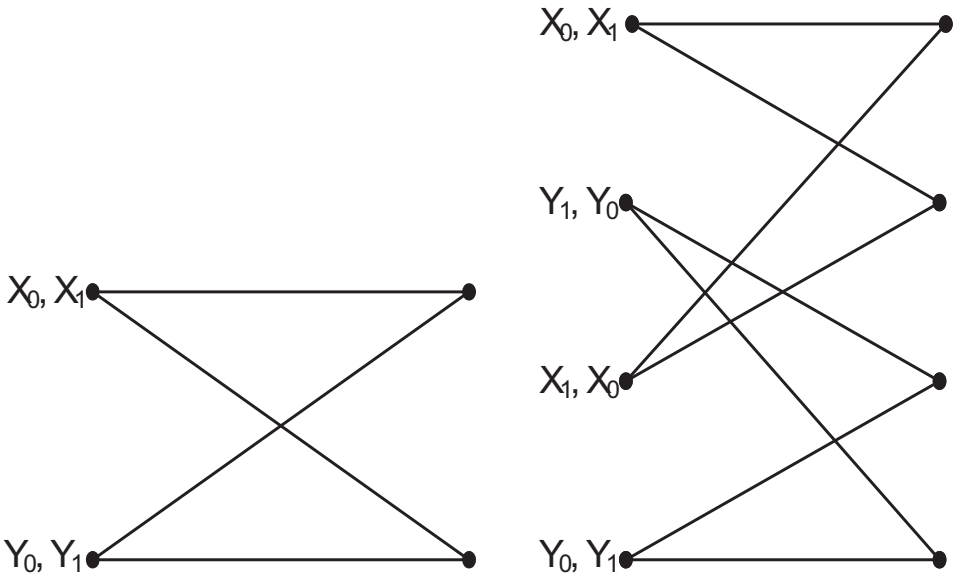

Figure 1.5: Two-state and four-state QPSK SOSTTC

In the trellises in Figure 1.5, each path converging and diverging to a state consists of eight parallel paths. The state labels, i.e. $\mathbf{X}_i$ and $\mathbf{Y}_i$ are sets of SOBC given in equation (1.18).

$$\begin{aligned}
\mathbf{X}_0 &\equiv \{(\pm 1, \pm 1, 0), (\pm j, \pm j, 0)\} \\
\mathbf{X}_1 &\equiv \{(\pm 1, \pm j, 0), (\pm j, \pm 1, 0)\} \\
\mathbf{Y}_0 &\equiv \{(\pm 1, \pm 1, \pi), (\pm j, \pm j, \pi)\} \\
\mathbf{Y}_1 &\equiv \{(\pm 1, \pm j, \pi), (\pm j, \pm 1, \pi)\}
\end{aligned} \tag{1.18}$$

In each set of the SOBC e.g. $\mathbf{X}_i$, eight different block codes are possible. These block codes are obtained by substituting the symbol elements $\{+1, -1, j, -j\}$, for a QPSK symbol constellation into the orthogonal matrix given in equation (1.17). The correspondent orthogonal block codes are then transmitted on the trellis branch.

Although this SOSTTC was designed by hand and achieves a better coding gain when compared with the other space-time codes, a new representation of SOSTTCs based on a gen-

erator matrix that allows a systematic and exhaustive search of all possible codes was developed in [41], [42] . The generator matrix representation of the SOSTTCs allows for a more compact representation of the code, making the implementation of the encoder and decoder easier.

1.10 MOTIVATION AND OBJECTIVE OF THESIS

A Multiple antenna system can be used to increase the measure of information transmitted with negligible error in a wireless system significantly without the need to increase bandwidth or transmit power. Actually, multiple antenna systems provide a high-capacity wireless network, since they allow for an increase in rate, improvement in robustness and more users in a cell.

For multiple antenna systems to provide the kind of performance promised above, the system needs to be constructed in a way that improves the power and bandwidth efficiency by using specially designed channel codes, i.e. STBC [28], [29], STTC [24] and SOSTTC [39].

These specially designed channel codes have been designed with the assumption that the fading of the channel is frequency non-selective. The performance of these codes in FS fading channel is therefore of research importance in this thesis. Generally, to combat the effect of frequency selectivity of a fading channel, two main methods are employed in literature i.e. equalisation and OFDM. OFDM is a physical layer technique that uses multicarrier transmission to increase the robustness against FS fading or narrowband interference, while equalisation is a process of extracting transmitted information from the received signal.

This research attempts to answer questions on the main challenges facing the design and performance of the channel codes that are used for multiple antenna systems in FS fading channel by using multichannel equalisation and OFDM. These challenges include the performance of the channel codes in FS fading channel, channel estimation algorithm and an analytical method to validate simulation results with and without channel state information.

1.11 AUTHOR'S CONTRIBUTION AND OUTPUT

1.11.1 Research Contribution

The main research contribution by the author's is outlined as follows:

- The author presents a new decoding trellis structure for two-state and four-state SOSTTCs in FS fading channel when multichannel equalisation is employed. The error rate performance of the trellises were compared with similar code in frequency non-selective fading channel.

- A new channel coded OFDM scheme was proposed for super-orthogonal codes in an OFDM environment i.e. super-orthogonal space-frequency coded OFDM.

- A unique non-overlapping pilot symbol arrangement was proposed as a simplified channel estimation algorithm for a space-time trellis-coded OFDM scheme when channel state information has to be estimated at the receiver.

- Using the super orthogonal code structure in an OFDM environment, a channel estimation algorithm was proposed for super-orthogonal space-frequency block-coded OFDM and super-orthogonal space-time block-coded OFDM.

- A mathematical model based on Gauss-Chebychev quadrature technique was developed to analyse the bit error rate (BER) performance of the SOBC-OFDM schemes with perfect channel estimation and channel estimation error.

1.11.2 Journal Publication

Parts of the work presented in this thesis have been published by the author as part of his research activities.

1. O.A. Sokoya and B.T. Maharaj, "Super-orthogonal block codes with multichannel equalisation and OFDM in frequency selective fading," EURASIP Journal on Wire-

less Communications and Networking, vol.1, 2010.

1.11.3 Conference Proceedings

The author's research work as reflected in this thesis, yielded the following outputs through publications in the following peer-reviewed and accredited conference proceedings:

1. O.A. Sokoya and B.T. Maharaj, "Performance of super-orthogonal space-time trellis code in a multipath environment," Proceedings of IEEE AFRICON Conference, Windhoek, Namibia, September 2007.

2. O.A. Sokoya and B.T. Maharaj, "Performance of space-time coded orthogonal frequency division multiplexing schemes with delay spread," Proceedings of IEEE Mediterranean Electrotechnical Conference (MELECON), Ajaccio, France, May 2008.

3. O.A. Sokoya and B.T. Maharaj, "Channel estimation for space-time trellis coded-OFDM systems based on non-overlapping pilot structure," Proceedings of Southern African Telecommunication Networks and Applications Conference (SATNAC), Wild Coast Sun, South Africa, September 2008.

4. O.A. Sokoya and B.T. Maharaj, "Channel estimation algorithm for super-orthogonal space-time trellis coded OFDM system," Proceedings of IEEE Wireless and Mobile Computing, Networking and Communication (WIMOB) Conference, Avignon, France, October 2008.

5. O.A. Sokoya and B.T. Maharaj, "Performance analysis of super-orthogonal space-frequency trellis coded OFDM system ," Proceedings of IEEE Pacific Rim Conference on Communications, Computers and Signal Processing (PACRIM), University of Victoria, Canada, August 2009.

1.12 OUTLINE OF THESIS

This thesis is divided into six chapters. Chapter 1 enumerates some of the challenges faced in a wireless communication network. The causes of multipath propagation and various ways in which the transmitted signals spread in the multipath environment are discussed. Diversity techniques as a means of reducing the effect of multipath propagation, i.e. fading, are also discussed. The capacity advantage that is possible in a multiple antenna system is explained and lastly various types of space-time coding schemes employed in multiple antenna systems are mentioned.

Chapter 2 is an enumeration of the performance of space-time coded schemes in multipath channel. Two main approaches to enhancing the performance of space-time coded schemes in multipath channel are discussed i.e. multichannel equalisation with maximum likelihood sequence estimation and OFDM.
A new decoding trellis is proposed for a SOBC scheme with multichannel equalisation and a new form of SOBC OFDM scheme that fully exploits the frequency diversity available in a FS channel is proposed.

Chapter 3 focuses on the channel estimation algorithms for space-time coded OFDM schemes, i.e. STTC-OFDM and SOBC OFDM. A new pilot symbol arrangement is proposed for STTC-OFDM, while an orthogonal pilot symbol is used for the SOBC OFDM schemes. A simplified estimation is done at the pilot instance, and interpolation done for other frequency instances.

In Chapter 4 a mathematical analysis for calculating the performance of an SOBC OFDM scheme in FS Rayleigh fading channels is proposed. This simple numerical technique is useful in observing the asymptotic behaviour of super-orthogonal space-frequency trellis coded OFDM schemes at high SNR. The analytical results of this code are compared with the simulated results and various conclusions are reached, depending on the error length.

In Chapter 5 the mathematical analysis proposed in Chapter 4 is also used to calcu-

late the performance of a SOBC OFDM scheme when channel estimation is used to estimate the channel at the pilot instance. The analytical results of this code are compared with the simulated results and various conclusions are reached depending on the error length.

Lastly, Chapter 6 presents the conclusions drawn in this thesis and possible future research work.

CHAPTER 2

CHANNEL CODES FOR MULTIPLE ANTENNAS IN FADING CHANNEL

2.1 INTRODUCTION

In this chapter the performance of channel codes that were designed for multiple antenna systems is enumerated in both FS and frequency non-selective (i.e. flat) fading channels. These channel codes were primarily designed for frequency non-selective fading channel and their performance in FS fading channel is investigated in this chapter. The FS fading channel is a more realistic channel for determining the real performance of a code, as it takes into account the effect of multipaths.

The design and performance of channel-coded schemes for multiple antenna systems, i.e. STBC [28], STTC [24] and SOSTTC [39], are based on two main important assumptions of the fading channel.

Firstly, the antennas are assumed to be located at a minimum distance of $\lambda/2$ from each other so that the fading coefficient between the transmit and receive antenna have independently identically distributed random variables [43].

Secondly, it was assumed that the fading channel is frequency non-selective. This means that the wireless fading channel does not have intersymbol interference. This assumption will not hold in an outdoor environment, since the delay spreads will be very large because of the multipath interference of the fading channel. Multipath interference can greatly

affect the performance of channel codes for multiple antenna systems, when such codes are not designed to take advantage of the full diversity possible in such an environment [44], [45], [46].

Generally, to enhance the performance of codes with multiple interference due to the frequency selectivity of fading channel, two main methods are used. They are:

- equalisation, and
- OFDM, i.e. FS fading channel, with adequate Cyclic prefic, is converted to parallel flat fading subchannels, thereby reducing the effect of intersymbol interference.

To mitigate the effect of FS fading channel on channel codes for multiple antenna systems, an equalisation method, multichannel equalisation, is proposed. Secondly, by using OFDM, the performance of these channel codes is enumerated in the second part of this chapter.

2.2 MULTICHANNEL EQUALISATION OF CHANNEL CODES FOR MULTIPLE ANTENNA SYSTEMS

In this section, the effect of applying multichannel equalisation to channel codes designed for multiple antenna systems is discussed.

Multichannel equalisation can be used to mitigate the distortive channel effects caused by the frequency selectivity of wireless fading channel in multiple antenna systems. Multichannel equalisation minimises the distortive channel effect so as to maximise the probability of decoding correctly at the receiver.

2.2.1 Multichannel Equalisation in Space-Time Trellis Code

STTC is an example of channel codes designed for multiple antenna systems. Their design and performance analysis in quasi-static frequency non-selective fading channel have been studied in [24], [47]. The code design criterion/performance was provided in [35]. The code performance is dependent on maximising the minimum rank and the minimum product of the non-zero eigenvalues of the distance matrix. Using these design criteria, various STTC were

proposed using systematic search [48], [49]. In FS channel, STTC suffers from unreduceable floors of error probability due to the effect of intersymbol interference on the multipath fading channel [50]. To improve the performance of the STTC in FS fading channel, additional processing at the receiver may be employed [51]. One of such additional processing is the use of multichannel equalisation to design an optimum receiver. This optimum receiver can be combined with a maximum likelihood sequence estimator (MLSE) for the STTC in multipath fading channel so as to combat the negative effect of the ISI. The optimum receiver makes use of all the signals from all the rays in each subchannel in its decoding decision making. For a four-state QPSK STTC [24] given in Figure 2.1(a), the optimum receiver decoding trellis is given in Figure 2.1(b), when the multipath ISI spans $L = 2$ symbols.

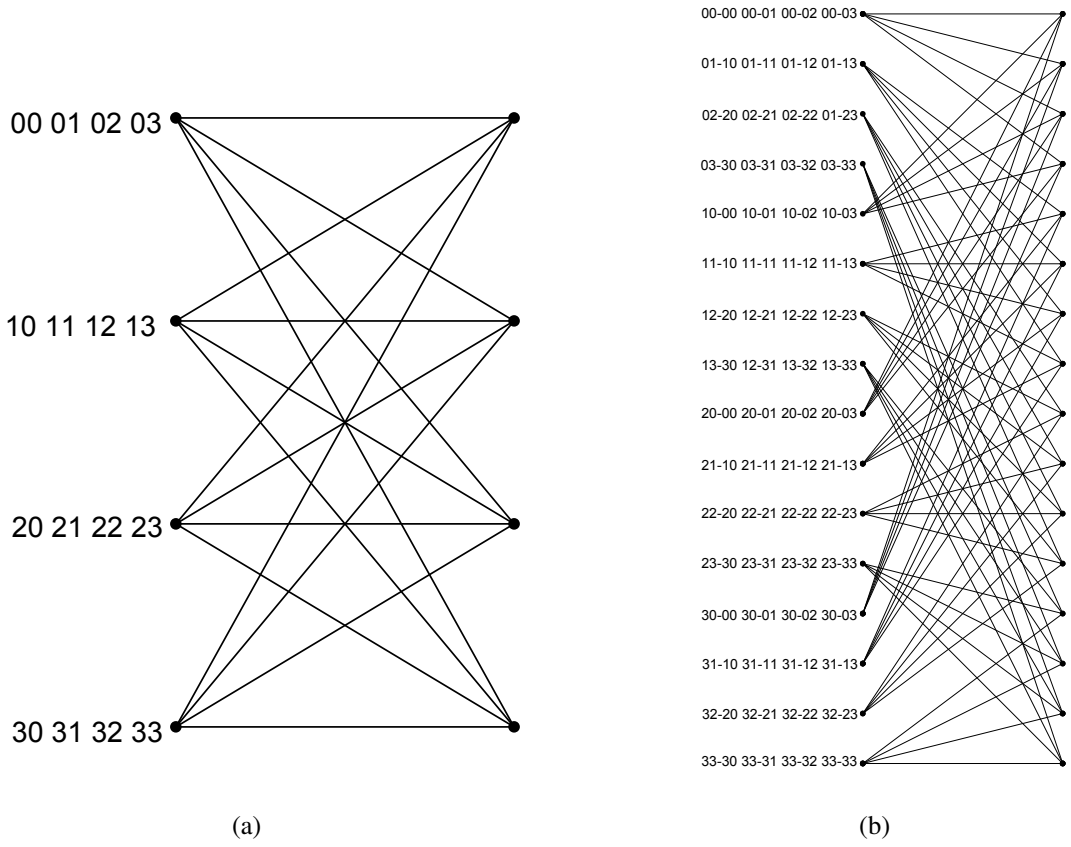

Figure 2.1: Four-state transmitting trellis (a) and sixteen-state decoding trellis (b) in FS fading channel

In Figure 2.1, the sixteen-state space time trellis decoder is obtained by using multichannel equalisation. At each trellis branch, the transmitted symbols are $x_1^1 x_1^1 - x_2^1 x_2^2$, where x_l^i is the

symbol transmitted from the i^{th} antenna at subchannel l.

2.2.2 Multichannel Equalisation in Space-Time Block Code

As mentioned earlier, channel codes for multiple antennas were originally developed for frequency non-selective fading channel. Since STBC is an example of such a code, applying it over FS fading channel becomes a design challenge. Various techniques to equalise STBC over FS fading channel have been proposed [52], [53], [54].

In [52], an equalised STBC is proposed over large blocks of data such as a frame. This achieves diversity gain on an FS channel, but with shortcomings. The design suffers from increased complexity due to the doubling of the front end convolution of the overall system. Also, the channel needs to be static over the entire larger block of coded data as opposed to only two coded-symbol periods as in the original Alamouti scheme [28]. Static channel assumption over an entire block of data is not valid, especially for high-speed mobile terminal. In order to reduce the complexity of the scheme proposed in [52], [53] proposed a frequency domain space time detector with decision feedback equaliser while [54] proposed a whitening filter followed by a decision feedback sequence estimator.

An easier way of reducing the overall system complexity is to assume that the additional processing done at the receiver, i.e. equalisation, is based on the transmission of the original STBC, i.e. two-symbol block. This concept is applicable to all orthogonal-based channel codes for a multiple antenna system and its detailed explanation is given in the multichannel equalisation for super-orthogonal block code.

2.2.3 Multichannel Equalisation in Super-Orthogonal Block Code

SOSTTCs were initially designed for flat fading channels but in FS fading channel this channel code may suffer from performance degradation due to symbol interference. In this thesis a method to reduce the effect of symbol interference caused by the frequency selectivity of the fading channel is proposed. This method combines a multichannel equalisation process at the receiver to design the decoder trellis with a maximum likelihood sequence estimator (MLSE) [55].

The block diagram of the proposed scheme is shown in Figure 2.2.

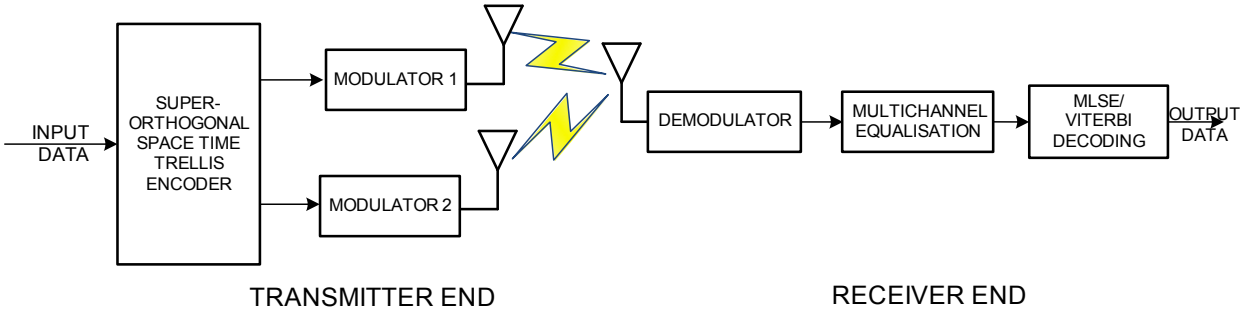

Figure 2.2: Block diagram of an SOSTTC with multichannel equalisation for $N_t = 2$ and $N_r = 1$

Figure 2.2 shows the block diagram of a two-transmiter and one-receiver SOSTTC in a FS fading channel. At the receiver end of the scheme, additional processing is involved to decode the transmit data. The additional processing involves multichannel equalisation and MLSE. The multichannel equalisation process involves designing the decoder trellis. Once the decoder trellis has been designed, MLSE is used to obtain the branch metric of the decoder trellis. Using the branch metric, a Viterbi decoder is used to obtain the path with the least accumulated branch metric. This scheme can be extended to more than one receive antenna.

The signal received at the t^{th} super-orthogonal block code can be written in matrix form for $N_t = 2$ as:

$$\begin{aligned}\begin{bmatrix} r_{11}(t) \\ r_{21}(t) \end{bmatrix} &= \begin{bmatrix} x_{11}(t)e^{j\theta} & x_2(t) \\ -x_{21}^*(t)e^{j\theta} & x_{11}^*(t) \end{bmatrix} \cdot \begin{bmatrix} h_{11}(0,t) \\ h_{21}(0,t) \end{bmatrix} \\ &+ \begin{bmatrix} -x_{21}^*(t-1)e^{j\theta} & x_{11}^*(t-1) \\ x_{11}(t)e^{j\theta} & x_{21}(t) \end{bmatrix} \cdot \begin{bmatrix} h_{11}(1,t) \\ h_{21}(1,t) \end{bmatrix} \\ &+ \cdots + \nu \cdot \begin{bmatrix} h_{11}(L-1,t) \\ h_{21}(L-1,t) \end{bmatrix} + \begin{bmatrix} \eta_{11}(t) \\ \eta_{21}(t) \end{bmatrix} \end{aligned} \tag{2.1}$$

where L is the number of non-zero delay taps, $h_{ij}(l,t)$ is the channel impulse response in the time domain for the l^{th} channel tap at block code t from the i^{th} transmit antenna to the j^{th} receive antenna, $r_{ij}(t)$ is the signal received from the i^{th} transmit antenna to the j^{th} receive antenna and $x_{ij}(t)$ represents the transmitted signal from the i^{th} transmit antenna to the j^{th} receive antenna at block code t. The AWGN component in equation (2.1) i.e. $\eta_{ij}(t)$ is the noise element from the i^{th} transmit antenna to the j^{th} receive antenna on the t^{th} coded block. These noise components are zero-mean vectors and variance $\sigma^2/2$ per dimension with Rayleigh fading channel coefficient.

The transmission matrix term ν in equation (2.1) is expressed for odd values of L i.e. ν_o and even values of L i.e. ν_e, in equations (2.2) and (2.3), respectively.

$$\nu_o = \begin{bmatrix} x_{11}((2t-L+1)/2)e^{j\theta} & x_{21}((2t-L+1)/2) \\ (-x_{21}((2t-L+1)/2))^* e^{j\theta} & (x_{11}((2t-L+1)/2))^* \end{bmatrix} \tag{2.2}$$

$$\nu_e = \begin{bmatrix} (-x_{21}((2t-L)/2))^* e^{j\theta} & (x_{11}((2t-L)/2))^* \\ x_{11}((2t-L)/2)e^{j\theta} & x_{21}((2t-L)/2) \end{bmatrix} \tag{2.3}$$

A multichannel equalised trellis is needed at the receiver for MLSE. To design a multichannel equalised decoder trellis for a SOBC with multipath interference that spans two consecutive symbols, all symbols due to the channel delay spread need to be used. Examples of the

multichannel equalised decoder trellises of a two-state and a four-state SOSTTC for $L = 2$ are given in Figure 2.3.

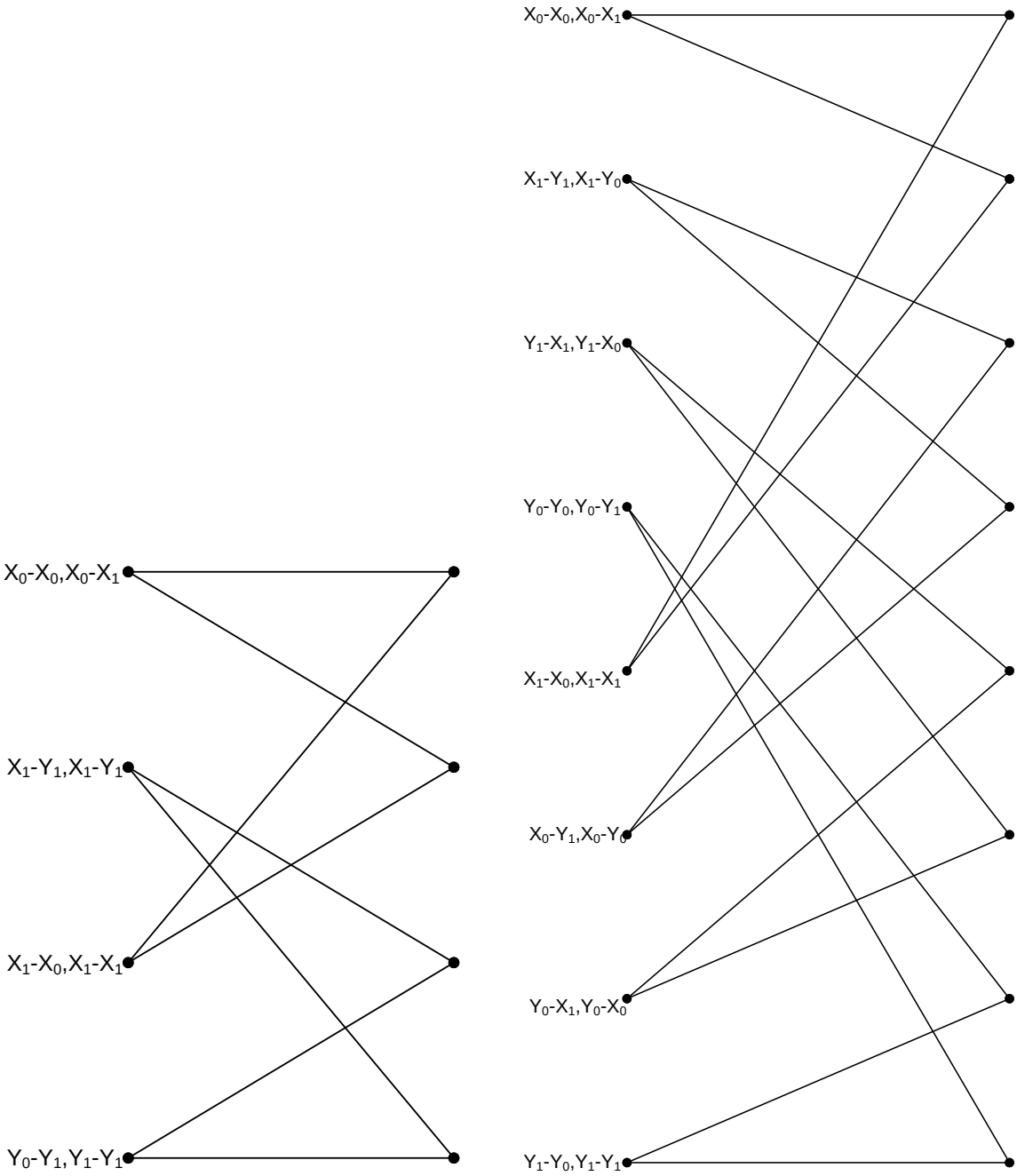

(a) 4-State Decoding Trellis (b) Eight-state Decoding Trellis

Figure 2.3: Decoding trellises for the two-state and four-state SOSTTC in FS fading channel

Figure 2.3 shows the multichannel equalised decoder trellis for a two-state and a four-state

super-orthogonal space-time trellis coding system in an FS fading channel. The multipath interference in the FS fading channel spans a two-symbol block. In each of the trellis branches, two block codes are represented. For example, in a trellis branch represented by, X_i-Y_j, Y_j is the delayed version of the two-symbol block code that is affected by the second subchannel and X_i is the two-symbol block affected by the first subchannel.

From the example given above, one can deduce that the number of states of a multichannel equalised decoder trellis is a function of the number of subchannel delay taps used and the original state of the super-orthogonal space time trellis code encoder. The number of states is given as:

$$N_s = 2*(L-1)*O \tag{2.4}$$

where L is the number of subchannel tap delays and O is the original number of states of the super-orthogonal space time trellis code encoder.

The multichannel equalised decoding scheme proposed above can be generalised to more than four-state transmission trellis for any form of trellis-based orthogonal block code scheme in FS fading channel.

2.3 SIMULATION RESULTS AND DISCUSSION

In this section, the frame error rate (FER) simulation results of channel codes for a multiple antenna system (i.e. STBC, STTC and SOSTTC) with multichannel equalisation for FS fading channel and without multichannel equalisation for frequency non-selective (i.e. flat) fading channel is presented. For both FS and flat fading channel, a quasi-static fading scenario is adopted, i.e. fading coeficients are constant per frame of the transmitted symbols and changes from one frame to the other. For FS fading channel $L = 2$ is used, while for flat fading channel $L = 0$. Each frame consists 260 transmitted symbols from $N_t = 2$ antennas. At the decoding stage of the system, in flat fading condition, a normal maximum likelihood estimator is used while in FS fading channel, the multichannel equalised decoder trellis is combined with the maximum likelihood sequence estimator the SOSTTC and STTC schemes. After obtaining the branch metric from the multichannel equalised decoder trel-

lis, Viterbi algorithm [38] is then used to obtain the lowest accumulated metric in a given frame.

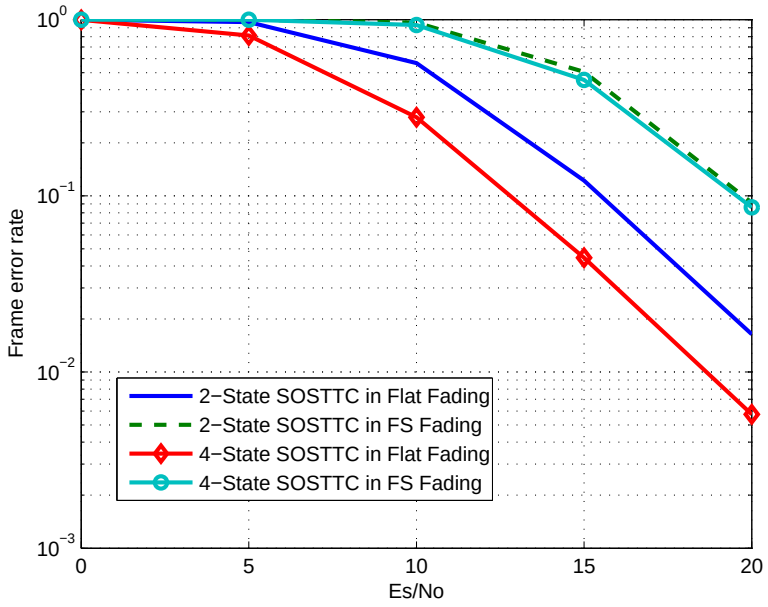

Figure 2.4: FER of two and four state SOSTTC in both flat and FS fading channel.

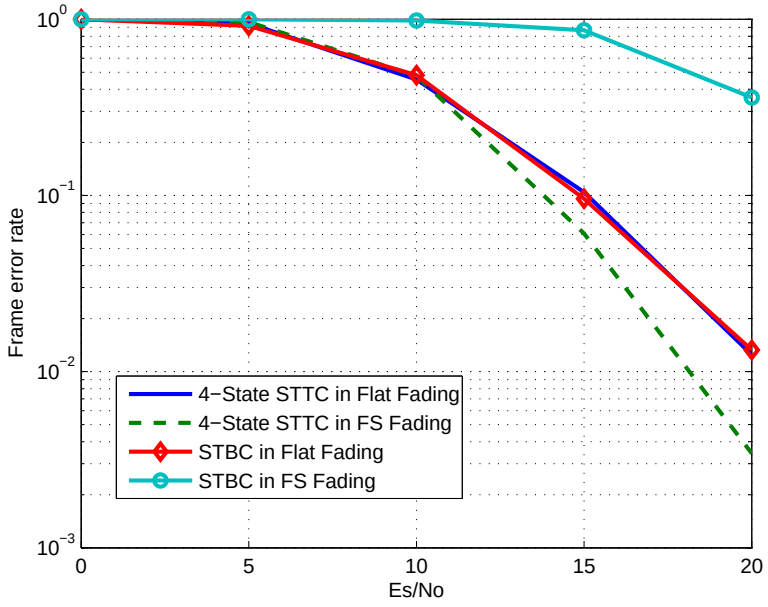

Figure 2.5: FER of four-state STTC and STBC in both flat and FS fading channel

Figure 2.4 shows the FER simulated results for a two-state and four-state SOSTTC in both FS and flat fading channel with and without multichannel equalisation, respectively. The

simulation parameters used were chosen purposely to compare the diversity advantage of the scheme with a similar scheme in [39]. The slope of an error rate curve represents the diversity order, while the shift downward in the curve represents the coding gain. In Figure 2.4, the slope of the FER curve for the two-state and four-state SOSTTC in the FS channel is the same as for the scheme in flat fading channel for the high SNR region. This corresponds to the scheme having the same diversity order in both flat and FS fading channel. In FS fading channel, SOSTTC displays performance degradation in its coding gain (i.e. shift backward of the FER curve). The performance loss for SOSTTC in FS channel is due to the increase in parallel paths converging/diverging from a state in the multichannel equalised decoder trellis. To prove this, one can compare the scheme's decoder trellis in FS and flat fading channel. In a flat fading decoder, there are 16 parallel paths coverging/diverging from a state, i.e. the probability of decoding a path correctly is $\frac{1}{8} \times \frac{1}{8} = \frac{1}{64}$, while in the FS multichannel equalised decoder, there are 128 parallel paths converging/diverging from a state, i.e. the probability of decoding a path correctly is $\frac{1}{64} \times \frac{1}{64} = \frac{1}{4096}$. From these two probabilities, $\frac{1}{64}$ for flat fading and $\frac{1}{4096}$ for the FS fading channel, there is a higher probability of decoding correctly in a flat fading channel than an FS channel. This is why there is a coding gain loss for the SOSTTC in an FS fading channel. Also, in designing SOSTTC for an FS channel, minimal parallel paths should be used.

In Figure 2.5, the four-state STTC code in FS fading channel outperforms both the four-state in flat fading channel and the STBC schemes. The main reason for this is the increase in the number of states and the absence of parallel paths in the decoding trellis.

2.4 MULTIPLE ANTENNA SYSTEM WITH OFDM

Although multichannel equalisation did not really perform well for some channel codes designed for a multiple antenna system in FS fading channel, other physical layer techniques can be combined with these codes to achieve better performance. Some of the other physical layer techniques that can be used with these channel codes to achieve better performance includes ultra wideband communication [56], cognitve radios [57] and OFDM [58]. In this thesis, OFDM is combined with channel codes for a multiple antenna system to achieve better performance in FS fading channel.

Multiple antenna systems can be combined with OFDM in a wireless network to produce a system that can achieve spectral efficiency and increase throughput in such a network. The block diagram of a multiple antenna OFDM system is shown in Figure 2.6.

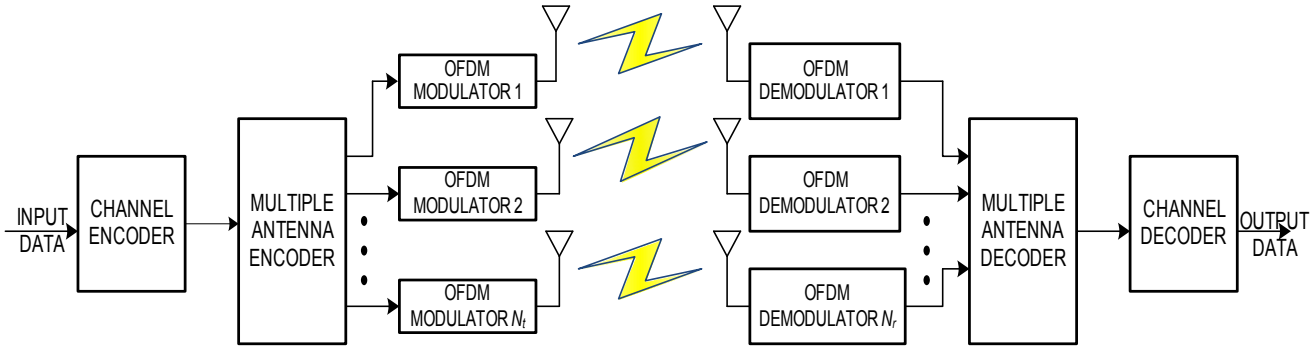

Figure 2.6: Multiple antenna OFDM system

In Figure 2.6, the multiple antenna system with OFDM transmits independent OFDM modulated data from multiple antennas at the same time. At the receiver, after OFDM demodulation, multiple antenna system decoding is done on each of the subchannels by extracting the data from all the transmit antennas on all the subchannels.

2.4.1 Brief Description of OFDM

OFDM is a physical layer technique for high data rate wireless networks that has been used in several wireless standards. These standards include digital audio broadcasting [59], digital video broadcasting [60], the IEEE 802.11a [61] and the IEEE 802.16a [62].

In FS fading channel, OFDM divides an FS channel into a number of equally spaced frequency bands. Each user's information is transmitted in a subcarrier. The subcarriers are orthogonal (i.e. independent) with each other. This is the main difference between an OFDM system and the commonly used frequency division multiplexing. An OFDM signal consists of N orthogonal subcarriers modulated by N parallel data streams. Each baseband subcarrier is of the form:

$$\phi_k(t) = e^{j2\pi f_n t} \tag{2.5}$$

where f_n is the frequency of the n^{th} subcarrier. One baseband OFDM symbol (without cyclic prefix) multiplexes N modulated subcarriers:

$$s(t) = \frac{1}{\sqrt{N}} \sum_{n=0}^{N-1} x_n e^{j2\pi f_n t} \quad 0 \leq t \leq NT \tag{2.6}$$

where x_n is the n^{th} complex data symbol (typically taken from a PSK or quadrature amplitude modulation (QAM) symbol constellation) and NT is the length of the OFDM symbols.

OFDM converts an FS channel into a parallel collection of frequency flat subchannels. The subcarriers have the minimum frequency separation required to maintain orthogonality of their corresponding time domain waveforms, yet the signal spectral corresponding to the different subcarriers overlap in frequency. Hence, the available bandwidth is used very efficiently.

To generate parallel subcarriers in OFDM, an inverse fast Fourier transform (IFFT) is applied to a block of data symbols. To avoid ISI due to the channel delay spread, a few cyclic prefix symbols, which are greater than the length of the impulse response, are inserted in the block. The cyclic prefix eliminates the ISI and converts the convolution between the transmit symbols and the channel to a circular convolution. At the receiver, the cyclic prefixes are removed and a fast Fourier transform (FFT) is applied to the data block to recover the received symbols.

2.4.2 Channel Codes for Multiple Antenna in OFDM

In flat fading channel, channel codes for multiple antenna systems (i.e. STTC, STBC and SOSTTC) exploit the spatial diversity present in the multiple transmit/receiver antennas to produce codes that are effective in combating fading and enhancing the data rate. The maximum diversity gain possible in a flat fading channel is the product of the number of transmit and receive antennas.

In FS fading channel, channel codes for multiple antenna systems and OFDM can potentially exploit the multipath diversity possible in the FS fading channel. As a result of the multipath diversity, the maximum diversity possible for the channel codes in an OFDM environment is therefore a product of the number of transmit antennas and receive antennas and the channel

impulse response length.

Some of the channel codes designed for multiple antenna sytems with OFDM that have been introduced in the literature include STTC-OFDM [63], STBC-OFDM [64] and SOSTTC-OFDM [65].

The performance of STTC-OFDM schemes has been investigated in the literature, [63], [66] and [67]. In [63] the performance of STTC-OFDM without interleavers in quasi-static FS fading channel was presented. The coding gain of the STTC-OFDM under various channel conditions was presented. The analysis gives two main conditions that can be used to maximise the minimun determinant of the STTC-OFDM system over multiple tap channels. These are maximising the minimum determinant of the tap delay channel and increasing the memory order of the STTC system. Based on these conditions, a new STTC-OFDM was designed in [66].

Conventional orthogonal block codes can be combined with OFDM to form either STBC-OFDM or space-frequency block-coded OFDM (SFBC-OFDM) schemes [64], [68] . These schemes exploit the simplified decoding algorithm used for conventional orthogonal block code that is based on linear combining.

SOBCs can also be combined with OFDM. Earlier work on SOBCs with OFDM have only emphasised one possible transmit diversity scheme [65]. This scheme is capable of realising only space and time diversity in multiple antenna systems. In this thesis, an SOBC-OFDM scheme that is capable of realising space and frequency diversity in a multiple antenna system is proposed.

2.4.2.1 System Model

A multiple antenna-OFDM system is considered with N_t transmit antennas, N_r receive antennas and N subcarriers. The transmitted frame consists of an $N_t \times N$ M-PSK super-orthogonal block of coded symbols. The channel impulse response in the time domain from the i^{th} transmit antenna to the j^{th} receive antenna is expressed as:

$$h_{ij}(\tau_s,t) = \sum_{l=0}^{L-1} h_{ij}(l,t)\delta(\tau_s - \frac{n_l}{N\Delta f}) \tag{2.7}$$

where $\delta(\bullet)$ is the Dirac delta function, n_l is the normalised time delay for the l^{th} tap, Δf is the subcarrier separation and $h_{ij}(l,t)$ represents the complex amplitude of the l^{th} non-zero tap with a delay of t. The complex amplitudes are modelled by the wide sense stationary and narrowband complex Gaussian processes, which are independent of each other with $E[|h_{ij}(l,t))|^2] = \sigma_l^2$ and the channel power is normalised such that $\Sigma_{l=0}^{L-1}\sigma_l^2 = 1$.

The channel representation in the frequency domain, for an OFDM system with adequate cyclic prefix, can be expressed as:

$$\begin{aligned} H_{ij}(n) &= \sum_{l=0}^{L-1} h_{ij}(l,t)exp(-j2\pi n(l)/N) \\ &= \mathbf{h}_{ij}\mathbf{f}(n) \end{aligned} \tag{2.8}$$

where $\mathbf{h}_{ij}$ comprises channel vectors $[h_{ij}(0,t),\ h_{ij}(1,t),\ h_{ij}(2,t),\ \cdots,\ h_{ij}(L-1,t)]$ and $\mathbf{f}(n)$ consists of the FFT coeficients $[1, \cdots, \exp(-j2\pi n(L-2)/N), \exp(-j2\pi n(L-1)/N)]^T$. For notation convenience, the time index t will be ignored in the rest of the analysis.

The transmitted SOBC symbols in matrix form for a full-rate $N_t = 2$ are expressed as:

$$\mathbf{X}(x_1,x_2,\theta) = \begin{bmatrix} x_1 e^{j\theta} & x_2 \\ -x_2^* e^{j\theta} & x_1^* \end{bmatrix}. \tag{2.9}$$

Based on the orthogonal transmission matrix given above, two main transmit diversity techniques are possible.

For a SOBC-OFDM scheme with the channel impulse response in the frequency domain that is constant over N_t continuous symbol intervals, an SOSTTC-OFDM scheme is produced [65] while in this thesis, a scheme in which the channel impulse response in the frequency domain is similar across the N_t adjacent subcarrier is proposed. The proposed scheme is called super-orthogonal space frequency trellis coded-OFDM (SOSFTC-OFDM) scheme .

The received equation for an SOSTTC-OFDM scheme, at the j^{th} receive antenna, on the n^{th} subcarrier and for two time intervals t and $t+1$, is expressed as:

$$r_j^t(n) = x_{1j}(n)e^{j\theta}H_{1j}(n) + x_{2j}(n)H_{2j}(n) + \eta_j^t(n)$$

$$r_j^{t+1}(n) = -x_{2j}^*(n)e^{j\theta}H_{1j}(n) + x_{1j}^*(n)H_{2j}(n) + \eta_j^{t+1}(n), \quad (2.10)$$

while the received equation for the SOSFTC-OFDM scheme at the j^{th} received antenna on the n^{th} subcarrier and for two time intervals t and $t+1$, is expressed as:

$$\begin{aligned} r_j^t(n) &= x_{1j}(n)e^{j\theta}H_{1j}(n) + x_{2j}(n)H_{2j}(n) + \eta_j^t(n) \quad (2.11)\\ r_j^{t+1}(n+1) &= -x_{2j}^*(n+1)e^{j\theta}H_{1j}(n+1) + x_{1j}^*(n+1)H_{2j}(n+1) + \eta_j^{t+1}(n+1), \end{aligned}$$

where $H_{ij}(n)$ is the channel impulse vector from the i^{th} transmit antenna to the j^{th} receive antenna on the n^{th} subcarrier. The noise components $\eta_j^t(n)$ are complex additive white Gaussian variables with zero mean and a variance of $N_o/2$ per dimension.

The received equation in (2.11) for the SOSFTC-OFDM scheme can be written for a frame of N subcarrier as:

$$\mathbf{R}_j = \mathbf{H}_{1j}\mathbf{X}_{1j} + \mathbf{H}_{2j}\mathbf{X}_{2j} + \tilde{\mathbf{N}}_j \quad (2.12)$$

where:

$$\mathbf{R}_j = \left[r_j^1(1), \; r_j^2(2), \; \cdots, \; r_j^N(N) \right], \quad (2.13)$$

$$\mathbf{H}_{ij} = \left[H_{ij}(1), \; H_{ij}(2), \; \cdots, \; H_{ij}(N) \right], \quad (2.14)$$

$$\tilde{\mathbf{N}}_j = \left[\eta_j^1(1), \; \eta_j^2(2), \; \cdots, \; \eta_j^N(N) \right], \quad (2.15)$$

$$\mathbf{X}_{1j} = \left[x_{1j}(1)e^{j\theta}, \; -x_{2j}^*(2)e^{j\theta}, \; \cdots, \; x_{1j}(N-1)e^{j\theta}, \; -x_{2j}^*(N)e^{j\theta} \right]^T, \quad (2.16)$$

and

$$\mathbf{X}_{2j} = \left[x_{2j}(1), \; x_{1j}^*(2), \; \cdots, \; x_{2j}(N-1), \; x_{1j}^*(N) \right]^T. \quad (2.17)$$

The design of channel codes for multiple antenna systems are based on the pairwise error probability (PEP) of the code. The PEP of a code is the probability that an originally transmitted codeword is mistaken for a different codeword. To get an optimum channel code based on the PEP, the minimum rank of the codeword sequence matrix is maximised and the minimum determinant of the codeword sequence matrix of the code is maximised. The minimum rank of the codeword sequence matrix corresponds to the diversity order, i.e. slope of the error rate curve, while the determinant of the codeword matrix corresponds to the coding gain, i.e. shift in the error rate curve.

The process of obtaining the PEP of SOSFTC-OFDM system is given below as a way of knowing the design criteria for the code.

To obtain the PEP of the SOSFTC-OFDM scheme, the originally transmitted codeword sequence and the erroneously decoded codeword sequence are used. Assuming the originally transmitted codeword sequence as $\mathbf{X} = [x(1), x(2), x(3), x(4), x(5), \cdots, x(N)]$ and erroneously decoded codeword sequence as $\hat{\mathbf{X}} = [\hat{x}(1), \hat{x}(2), \hat{x}(3), \hat{x}(4), \hat{x}(5), \cdots, \hat{x}(N)]$, the ML decision metric can be obtained based on the received equation in (2.12). The ML decision metric, i.e. $m(\mathbf{R}, \mathbf{X})$, which corresponds to the originally transmitted SOSFTC-OFDM codeword sequence, is given as:

$$m(\mathbf{R}, \mathbf{X}) = ||\mathbf{R}_j - (\mathbf{H}_{1j}\mathbf{X}_{1j} + \mathbf{H}_{2j}\mathbf{X}_{2j})||^2, \tag{2.18}$$

while the ML decision metric, i.e. $m(\mathbf{R}, \hat{\mathbf{X}})$ corresponding to the erroneously decoded SOSFTC-OFDM codeword is given as:

$$m(\mathbf{R}, \hat{\mathbf{X}}) = ||\mathbf{R}_j - (\mathbf{H}_{1j}\hat{\mathbf{X}}_{1j} + \mathbf{H}_{2j}\hat{\mathbf{X}}_{2j})||^2. \tag{2.19}$$

The PEP is given below based on the decision metric for a given channel impulse $\mathbf{H} = [\mathbf{H}_{1j} \;\; \mathbf{H}_{2j}]$ in the frequency domain as:

$$\begin{aligned} P(\mathbf{X} \rightarrow \hat{\mathbf{X}}|\mathbf{H}) &= Pr\{m(\mathbf{R}, \mathbf{X}) > m(\mathbf{R}, \hat{\mathbf{X}})\} \\ &= Pr\{(m(\mathbf{R}, \mathbf{X}) - m(\mathbf{R}, \hat{\mathbf{X}})) > 0\}. \end{aligned} \tag{2.20}$$

The decision metric of the transmitted (i.e. equation (2.18)) and erroneously decoded codeword (i.e. equation (2.19)) can be substituted into equation (2.20) to give equation (2.21).

$$\begin{aligned} P(\mathbf{X} \rightarrow \hat{\mathbf{X}}|\mathbf{H}) &= Pr\{||\mathbf{H}_{1j}(\mathbf{X}_{1j} - \hat{\mathbf{X}}_{1j})||^2 + ||\mathbf{H}_{2j}(\mathbf{X}_{2j} - \hat{\mathbf{X}}_{2j})||^2\} \\ &= Pr\{||\mathbf{H}_j\mathbf{\Delta}||^2 > 0\}, \end{aligned} \tag{2.21}$$

where $\mathbf{\Delta}$ is the codeword difference matrix that characterises the SOSFTC-OFDM scheme whose expression is given as:

$$\mathbf{\Delta} = \begin{bmatrix} \mathbf{X}_{1j} - \hat{\mathbf{X}}_{1j} \\ \mathbf{X}_{2j} - \hat{\mathbf{X}}_{2j} \end{bmatrix}, \tag{2.22}$$

and $||.||$ represents the norm of the matrix element.

The conditional PEP written in equation (2.21) can be expressed in terms of the Gaussian Q function [69] as:

$$P(\mathbf{X} \rightarrow \hat{\mathbf{X}}|\mathbf{H}) = Q\left(\sqrt{\frac{E_s}{2N_o}\sum_{j=1}^{N_r}\mathbf{H}_j\mathbf{\Delta}\mathbf{\Delta}^H\mathbf{H}_j{}^H}\right), \tag{2.23}$$

where $\mathbf{\Delta}\mathbf{\Delta}^H$ is a diagonal matrix written as:

$$\mathbf{\Delta}\mathbf{\Delta}^H = \begin{bmatrix} \Delta(1)(\Delta(1))^H & 0 & \dots & 0 \\ 0 & \Delta(2)(\Delta(2))^H & \dots & 0 \\ \vdots & \vdots & \ddots & \vdots \\ 0 & 0 & \dots & \Delta(N)(\Delta(N))^H \end{bmatrix}, \tag{2.24}$$

and $(\bullet)^H$ is the conjugate transpose of the matrix element.

The diagonal element of equation (2.24) is given in equation (2.25) as:

$$\Delta(n) = \begin{bmatrix} x_1(n) - \hat{x}_1(n) \\ x_2(n) - \hat{x}_2(n) \end{bmatrix}, \tag{2.25}$$

and further expansion of $\mathbf{H}_j$ is given in equation (2.26) as:

$$\begin{aligned}\mathbf{H}_j &= \begin{bmatrix} \mathbf{H}_{1j} & \mathbf{H}_{2j} \end{bmatrix}_{1\times N_t} \\ \mathbf{H}_j &= \begin{bmatrix} \mathbf{h}_j\mathbf{F}(0) & 0 & \dots & 0 \\ 0 & \mathbf{h}_j\mathbf{F}(1) & \dots & 0 \\ \vdots & \vdots & \ddots & \vdots \\ 0 & 0 & \dots & \mathbf{h}_j\mathbf{F}(N) \end{bmatrix}\end{aligned} \tag{2.26}$$

where:

$$\mathbf{F}(n) = \begin{bmatrix} \mathbf{f}(n) & 0 & \dots & 0 \\ 0 & \mathbf{f}(n) & \dots & 0 \\ \vdots & \vdots & \ddots & \vdots \\ 0 & 0 & \dots & \mathbf{f}(n) \end{bmatrix}_{LN_t\times N_t} \tag{2.27}$$

and

$$\begin{aligned}\mathbf{h}_j &= \begin{bmatrix} h_{1j}(0) & \dots & h_{1j}(L-1) & h_{2j}(0) & \dots & h_{2j}(L-1) \end{bmatrix}_{1\times LN_t} \\ \mathbf{h}_j &= [\mathbf{h}_{1j}\ \mathbf{h}_{2j}].\end{aligned} \tag{2.28}$$

The conditional probability in equation (2.23) can then be expressed as equation (2.29) by using equations (2.26) and (2.24).

$$P(\mathbf{X}\rightarrow\hat{\mathbf{X}}|\mathbf{H}) = Q\left(\sqrt{\frac{E_s}{2N_o}\sum_{j=1}^{N_r}\sum_{n=1}^{N}\mathbf{h}_j\mathbf{F}(n)\Delta(n)(\Delta(n))^H(\mathbf{F}(n))^H\mathbf{h}_j{}^H}\right). \tag{2.29}$$

The Q function [70] is defined as:

$$Q(t) = \frac{1}{\sqrt{2\pi}}\int_0^\infty e^{\frac{-t^2}{2}}dt, \tag{2.30}$$

and by using the Chernoff bound [71] of the Q-function:

$$Q(t) \leq \frac{1}{2}\exp\left(-t^2/2\right) \quad t\geq 0, \tag{2.31}$$

the conditional PEP written in equation (2.29) can be upper bounded as:

$$P(\mathbf{X}\rightarrow\hat{\mathbf{X}}|\mathbf{H}) \leq \frac{1}{2}\exp\left(-\frac{E_s}{4N_o}\sum_{j=1}^{N_r}\sum_{n=1}^{N}\mathbf{h}_j\mathbf{F}(n)\Delta(n)(\Delta(n))^H(\mathbf{F}(n))^H{\mathbf{h}_j}^H\right). \quad (2.32)$$

The conditional PEP given in (2.32) can be averaged over all possible channel impulses in the frequency domain as:

$$P(\mathbf{X}\rightarrow\hat{\mathbf{X}}) \leq E\left\{\frac{1}{2}\exp\left(-\frac{E_s}{4N_o}\sum_{j=1}^{N_r}\sum_{n=1}^{N}\mathbf{h}_j\mathbf{F}(n)\Delta(n)(\Delta(n))^H(\mathbf{F}(n))^H{\mathbf{h}_j}^H\right)\right\}. \quad (2.33)$$

Using [72], one can reduce the complexity of equation (2.33).

For a complex distributed Gaussian random row matrix $\mathbf{g}$ with mean $\boldsymbol{\mu}$ and covariance matrix $\sigma_{\mathbf{g}}^2 = E[\mathbf{g}\mathbf{g}^*] - \boldsymbol{\mu}\boldsymbol{\mu}^*$, and a Hermitian matrix $\mathbf{M}$, the expectation of the exponential term $(-\mathbf{g}\mathbf{M}(\mathbf{g}^*)^T)$ can be written as :

$$E\left[\exp(-\mathbf{g}\mathbf{M}(\mathbf{g}^*)^T)\right] = \frac{\exp\left[-\boldsymbol{\mu}\mathbf{M}(\mathbf{I}+\sigma_{\mathbf{g}}^2\mathbf{M})^{-}1((\boldsymbol{\mu}^*)^T)\right]}{\det(\mathbf{I}+\sigma_{\mathbf{g}}^2\mathbf{M})}. \quad (2.34)$$

Using the exponential terms in equation (2.34), one can solve the PEP equation in (2.33) as:

$$P(\mathbf{X}\rightarrow\hat{\mathbf{X}}) \leq \frac{1}{2}\bullet\prod_{j=1}^{N_r}\frac{1}{\det\left[\mathbf{I}+\frac{E_s}{4N_o}\sum_{n=1}^{N}\mathbf{F}(n)\Delta(n)(\Delta(n))^H(\mathbf{F}(n))^H\right]_j} \quad (2.35)$$

where:

$$\mathbf{I} = \mathbf{I}_{LN_t}, \quad (2.36)$$

$$\mathbf{g} = [\mathbf{h}_{1j}\ \mathbf{h}_{2j}], \quad (2.37)$$

and

$$\mathbf{M} = -\frac{E_s}{4N_o}\mathbf{F}(n)\Delta(n)(\Delta(n))^H(\mathbf{F}(n))^H. \quad (2.38)$$

Based on the above expressions, one can note that the left hand-side (LHS) of (2.38) is a diagonal matix and so **M** is a Hermitian matrix. Furthermore, if one assumes that **g** contains zero-mean Gaussian distribution, then the LHS numerator of equation (2.34) becomes 1 (since $\exp(0) = 1$). In a high SNR region (i.e. $E_s/N_o \gg 1$), the identity matrix in the denominator of equation (2.35) may be ignored and the PEP upper bound averaged over all possible channel impulses in the frequency domain derived as follows:

$$\begin{aligned} P(\mathbf{X} \to \hat{\mathbf{X}}) &\leq \frac{1}{2} \bullet \prod_{j=1}^{N_r} \frac{1}{\det\left[\frac{E_s}{4N_o} \sum_{n=1}^{N} \mathbf{F}(n)\Delta(n)(\Delta(n))^H(\mathbf{F}(n))^H\right]_j} \\ &\leq \frac{1}{2} \bullet \left[\frac{E_s}{4N_o}\right]^{-\alpha N_r} \left[\prod_{k=1}^{\alpha} \beta_k\right]^{-N_r} \end{aligned} \tag{2.39}$$

where α is the rank and β_k are the set of non-zero eigenvalues of matrix $\mathbf{F}(n)\Delta(n)(\Delta(n))^H(\mathbf{F}(n))^H$ for $k \leq (1, 2, \cdots, \alpha)$.

From equation (2.39), the design criteria for an SOSFTC-OFDM scheme for a high SNR region is therefore based on the rank and eigenvalue criteria. The rank criterion maximises the diversity of the SOSFTC-OFDM scheme while the eigenvalue criterion maximises the coding gain of the SOSFTC-OFDM scheme. The rank criterion is to maximise the minimum rank of $\mathbf{F}(n)\Delta(n)(\Delta(n))^H(\mathbf{F}(n))^H$ for any codeword $\mathbf{X}$ and $\hat{\mathbf{X}}$, and the eigenvalue criterion is to maximise the minimum product of the non-zero eigenvalues of $\mathbf{F}(n)\Delta(n)(\Delta(n))^H(\mathbf{F}(n))^H$.

2.5 SIMULATION RESULTS AND DISCUSSION

In this section the FER performance of channel codes designed for a multiple antenna system in the OFDM environment, i.e. SOSFTC-OFDM, SOSTTC-OFDM, STBC-OFDM, SFBC-OFDM and STTC-OFDM, is compared.

To compare these schemes, a sub-optimal two-state and four-state trellis with parallel paths, as shown in Figure 1.5, and an optimal 16-state trellis without parallel paths, as shown in Figure 2.7, are used for the SOBC-OFDM schemes (i.e. SOSTTC-OFDM and SOSFTC-OFDM). The 16-state trellis shown in Figure 2.7 maximises the space/frequency diversity and coding gain by minimising the number of parallel path for the SOBC-OFDM scheme.

The symbols on each trellis brach in Figure 2.7, (*i.e.* x_1 and x_2) 0, 1, 2 and 3, correspond to the QPSK signal constellations and the value of the rotation angle is denoted by 0 and π. For STTC-OFDM, the 16-state trellis proposed in [73] is used.

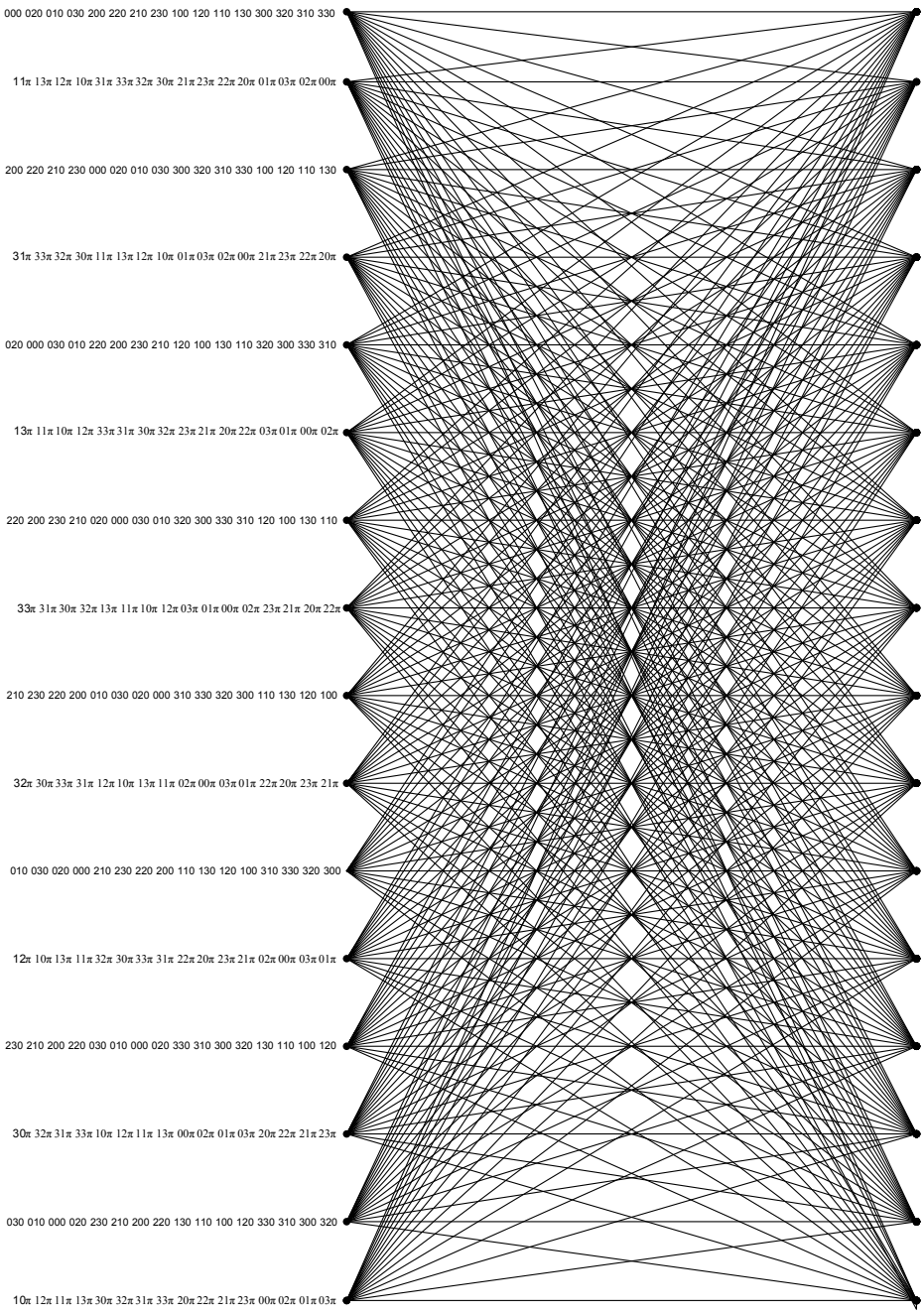

Figure 2.7: 16-State QPSK Trellis for SOBC-OFDM Scheme

A quasi-static FS Rayleigh fading channel with $N_t = 2$, $N_r = 1$, $L = 2$ and an equal delay profile is used in the simulation. The total power of the transmitted coded symbol was normalised to unity. The maximum Doppler frequency of 200 Hz was used in the simulation. The multipath channel undergoes independent Rayleigh fading and the receiver has perfect knowledge of the channel state information. The SOBC-OFDM scheme has a bandwidth of 1 MHz and 128 OFDM subcarriers. To eliminate ISI in the FS OFDM environment, a cyclic prefix that is greater than the channel delay spread is used.

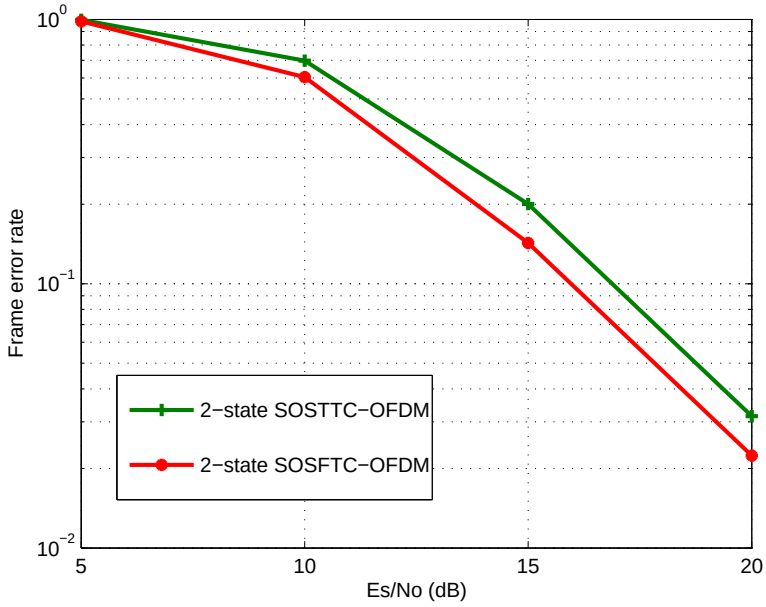

Figure 2.8: FER of a two-state SOBC-OFDM schemes

Figures 2.8 and 2.9 show the FER performance of SOBC-OFDM schemes in an OFDM environment. The two-state and four-state trellises used are both sub-optimal for an OFDM environment, since they contain parallel transition paths. The figures show that the proposed SOSFTC-OFDM scheme outperforms SOSTTC-OFDM and for a FER of 10^{-1}, the proposed SOSFTC-OFDM as about 1 dB gain over the SOSTTC-OFDM.

In Figures 2.10 and 2.11, the FER performance of the 16-state SOSTTC OFDM, 16-state SOSFTC-OFDM, 16-state STTC-OFDM, STBC-OFDM and SFBC-OFDM for 5μs and 40μs delay spreads between the two paths is shown. In both FER curves the proposed SOSFTC-OFDM scheme outperforms all other channel codes designed for multiple antennas in an OFDM environment, i.e. STTC-OFDM, STBC-OFDM, SFBC-OFDM and

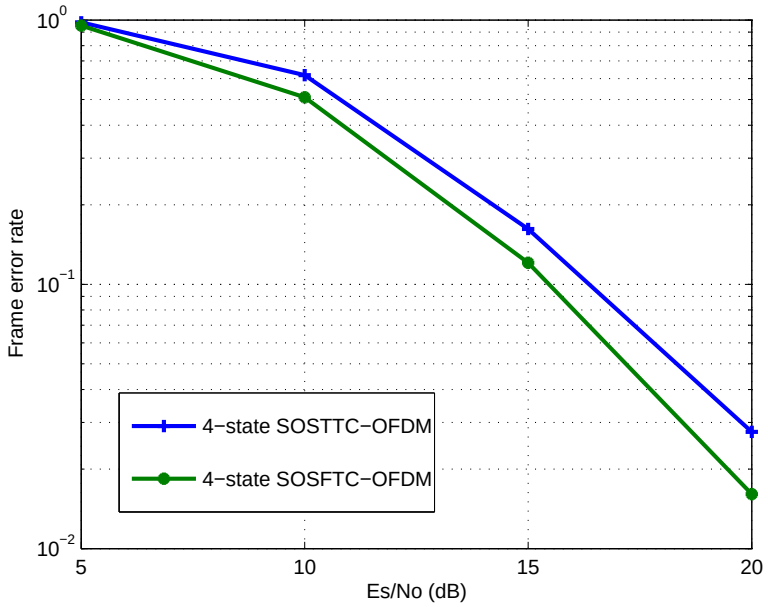

Figure 2.9: FER of a four-state SOBC-OFDM

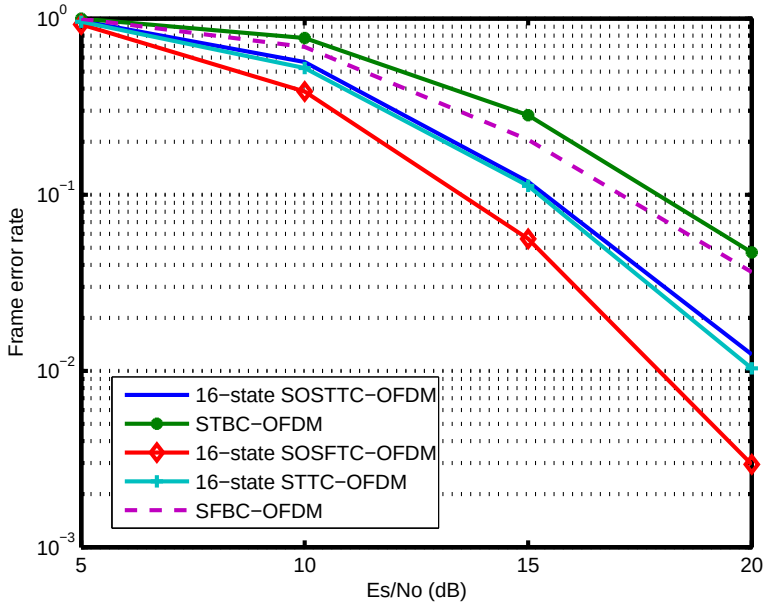

Figure 2.10: FER performance of coded schemes with OFDM and 5μs delay spread between the two paths

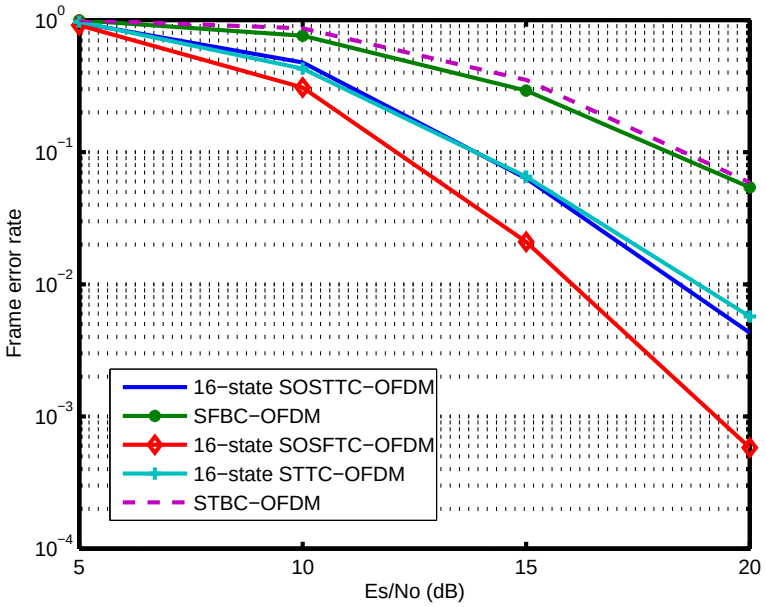

Figure 2.11: FER performance of coded schemes with OFDM and 40μs delay spread between the two paths

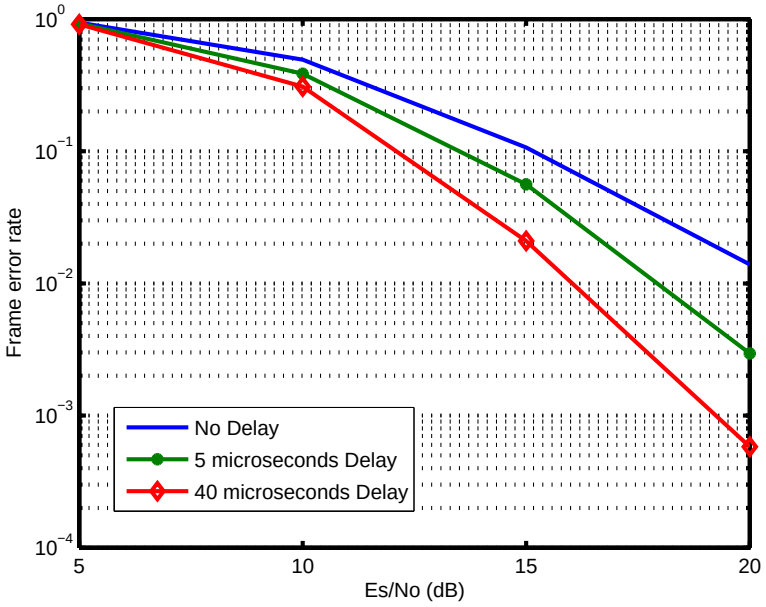

Figure 2.12: Effect delay spreads on 16-state SOSFTC OFDM scheme

SOSTTC-OFDM, in the two-channel delay spread scenario.

In both channel delay spread scenarios and at a FER of 10^{-2}, the proposed SOSFTC-OFDM schemes display more than 2 dB gain over all other schemes.

The effect of channel delay spread on SOSFTC-OFDM systems is shown in Figure 2.12. An increase in delay spread between the multipaths gives a better FER of the SOSFTC-OFDM systems.

2.6 SUMMARY

In this chapter the performance of channel codes for multiple antenna systems, with emphasis on the super-orthogonal block-coding scheme in fading channels, i.e. FS and flat fading channel, was discussed. The receiver structure of an SOSTTC and STTC in an FS fading channel is given when multichannel equalisation is used to mitigate the effect of multipath interference. New decoding trellises for two-state and four-state SOSTTC schemes were designed. The formula for the number of states of the SOSTTC in FS fading channel with multichannel equalisation was deduced as a function of the multipath rays and the original number of states of the super-orthogonal block-coding scheme. The simulation results proved that although the code was designed for flat fading channels, it provides at least the same diversity advantage when applied to an FS Rayleigh fading channel.

To investigate the performance of the multiple antenna system in an OFDM environment, various channel codes were combined with OFDM. A new super-orthogonal block coding scheme i.e. SOSFTC-OFDM, was proposed. This scheme outperforms all other channel codes designed for a multiple antenna OFDM system in various delay spreads, i.e. $5\mu s$ and $40\mu s$. Simulation result also show that increasing the delay spread of the multipath channel gives a better coding gain of the proposed code construction.

CHAPTER 3

CHANNEL ESTIMATION OF MULTIPLE ANTENNA OFDM SCHEMES

3.1 INTRODUCTION

In most wireless simulation models it is always assumed that the receiver has perfect knowledge of the channel so as to make coherent decoding possible, as discussed in previous chapter. This assumption is inappropriate when simulating a practical physical system, because in a real system the effect of the channel can never be known exactly: rather, some form of estimation is performed to find an approximation for the channel. Estimation algorithms can be grouped into three main methods [74], viz pilot/training-based channel estimation algorithm, blind channel estimation algorithm and semi-blind channel estimation.

In pilot/training channel estimation algorithm [75], [76], [77], known pilot symbols are sent at the transmitter and based on the known pilot symbols, the channel information is estimated.

To obtain channel information based on the blind channel estimation algorithm [78], [79], statistical information of the channel or property of the transmitted symbols is used.

The last method, called semiblind channel estimation, uses both pilot symbols and unknown data symbols for channel estimation [80], [81].

Although, the blind channel estimation method has litle or no overhead loss, the high complexity of such an algorithm prohibits it from being used in most communication systems.

Comparing all three estimation algorithms, training-based channel estimation algorithm has

the lowest complexity, as it requires a small data record for channel estimation [82]. Therefore, the focus in this thesis will be on the training-based channel estimation algorithms.

In single-antenna based OFDM schemes, channel estimation algorithms have been studied widely in the literature [83], [84] but in multiple-antenna based OFDM schemes, channel estimation can be complicated. This complication arises from the fact that transmitted signals from multiple antennas interfere with one another during the channel estimation instance [85].

In this chapter, in order to avoid interference of a transmitted signal in the channel estimation algorithms for multiple-antenna based OFDM schemes, a simplified channel estimation algorithm for the STTC-OFDM scheme is proposed. Also, based on the orthogonal structure of the transmitted signals in super-orthogonal block coded OFDM schemes, a simple channel estimation algorithm is proposed.

3.2 CHANNEL ESTIMATION FOR STTC-OFDM

Various channel estimation algorithms have been proposed in the literature for STTC-OFDM schemes [76], [86], [87]. In [76], a channel parameter estimation approach was proposed for STTC-OFDM scheme using the correlation of the channel parameters for different tones. The overall receiver performance of the channel coded multiple antenna OFDM scheme was demonstrated by extensive computer simulation. To reduce the high complexity of the scheme proposed in [76], a simplified channel estimation algorithm was proposed in [86]. The proposed approach in [86] is based on considering only significant taps, i.e. taps with large impulse power. This simplified channel estimation reduces the complexity of the overall system at the expense of performance degradation.

In the original, i.e. [76] and simplified scheme, i.e. [86], the channel state matrix (defined by $\mathbf{Q}$) must be invertible, i.e. $N_t = N_r$. The invertibility of the $\mathbf{Q}$ matrix is neccesary so that there will be a solution for the decision directed-minimum mean square estimator used. This channel estimation algorithm will not be suitable for schemes where $N_t \neq N_r$, as invertibility of the channel state matrix $\mathbf{Q}$ will not be possible.

In this thesis, a channel estimation algorithm that is independent of the number of transmit or receive antennas is proposed for STTC-OFDM. The independence of the proposed algorithm

on the number of transmit or receive antennas is based on the way the pilot symbols are inserted at the estimation stage. The channel estimation algorithm, which is explained more fully in the section below, is based on periodically inserting pilot symbols on the trasmitted frame. Once the pilot symbols are inserted, the least squares (LS) estimator can then be used to estimate the channel impulse in the frequency domain.

3.2.1 System Model

An STTC-OFDM transmission system with N_t transmit antennas, N_r receive antennas and N subcarriers is considered. The transmitted frame consists of $N_t \times N$ M-PSK STTC symbols, where the encoded symbol $x_i(n)$, $n \in \{0,1,2,,N-1\}$, $i \in \{0,1,2,,N_t-1\}$, is transmitted on the n^{th} subcarrier from the i^{th} transmitt antenna. The received STTC-OFDM signal at the j^{th} received antenna, on the n^{th} subcarrier is expressed as:

$$r_j(n) = \sum_{i=1}^{N_t} H_{ij}(n)x_i(n) + \eta_j(n) \tag{3.1}$$

where $H_{ij}(n)$ is the channel impulse in the frequency domain from the i^{th} transmit antenna to the j^{th} receive antenna for the n^{th} subcarrier. The noise component at the j^{th} receive antenna for the n^{th} subcarrier is given by $\eta_j(n)$. This noise component is an independent complex Gaussian random variable with zero-mean and a variance $N_o/2$ per dimension.
The channel impulse in the frequency domain can be expressed as a function of an L non-zero tap written as:

$$H_{ij}(n) = \sum_{l=0}^{L-1} h_{ij}(l) \exp\left(\frac{j2\pi n n_l}{N}\right) \tag{3.2}$$

where $h_{ij}(l)$ for $l = 0,1,2,,L-1$ are narrowband zero-mean complex Gaussian processes for different i and j.

3.2.2 Pilot System Description

Pilot-based channel estimation algorithms have been shown in the literature to be very attractive for wireless link where the channel varies with time [88], [89] and [90]. The two main approaches to pilot arrangement in pilot-based channel estimation are:

1. Block-type pilot arrangement, and

2. Comb-type pilot arrangement

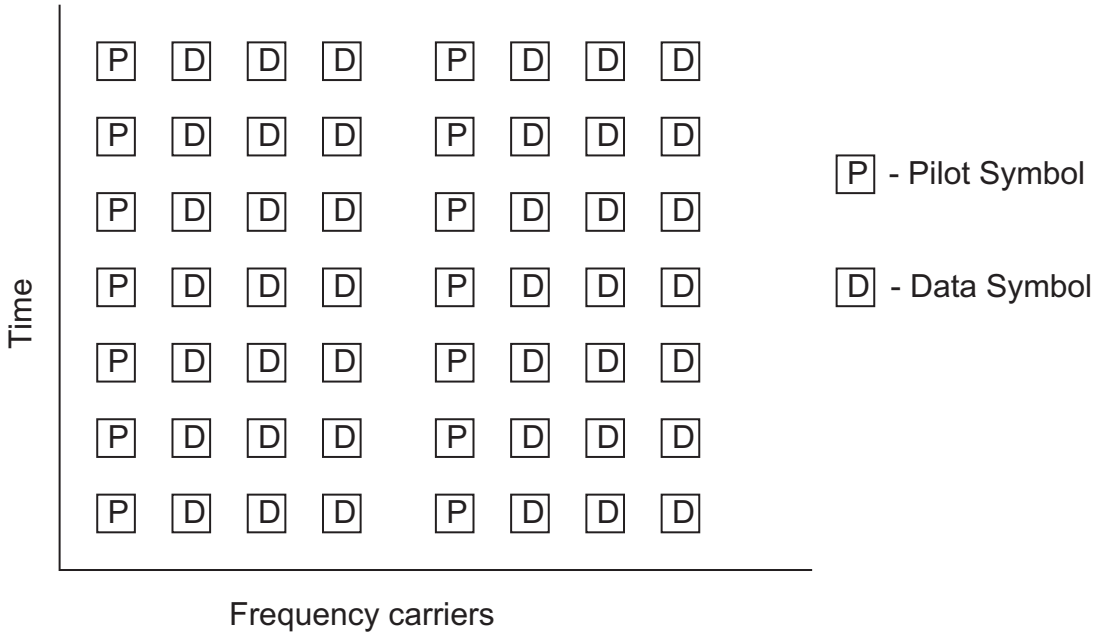

Figure 3.1: Block-type pilot arrangement

In block-type pilot arrangement, as shown in Figure 3.1, all subcarriers in a block are transmitted periodically as pilot symbols. Channel estimation is done based on the transmitted symbols. The channel estimation error will be zero if the channel is constant during the pilot block transmission, since all pilots are sent at all the carriers.

In block-type pilot arrangement various types of estimators can be used, this including LS, MMSE and modified MMSE. For optimum performance of a block-type pilot arrangement system, a slow fading channel model is always assumed.

Comb-type pilot channel estimation was introduced to satisfy the need for equalisation when the channel changes from one OFDM block to the subsequent one.

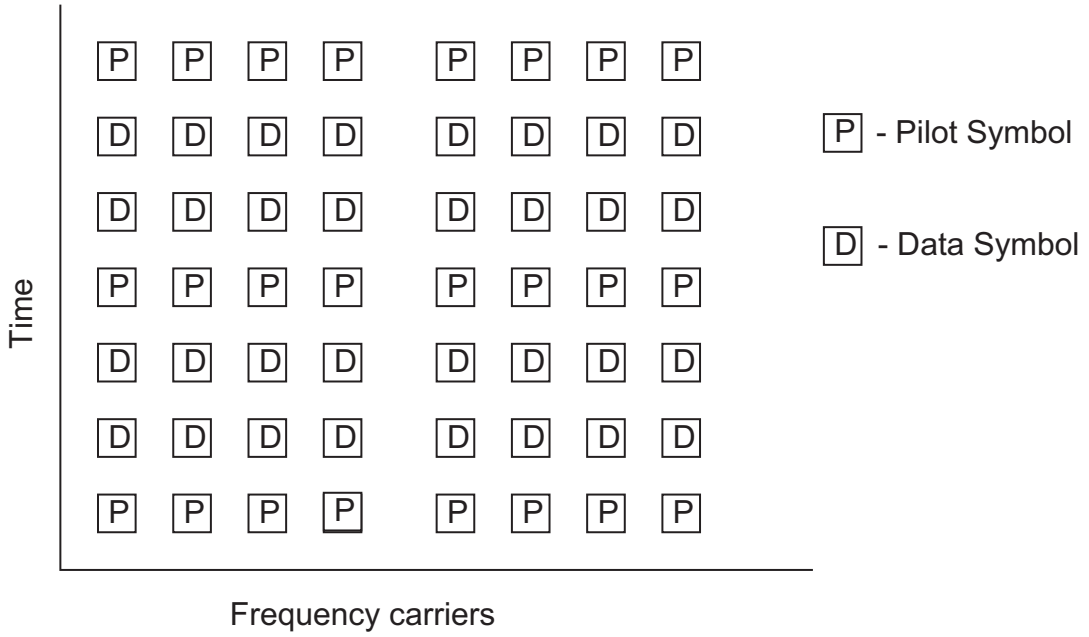

Figure 3.2: Comb-type pilot arrangement

In the comb-type pilot arrangement, as shown in Figure 3.2, pilot symbols are uniformly placed into the transmitted data sequence. Channel estimation is done at the pilot frequencies and interpolation is done to obtain estimates at the data subcarrier. The estimation at the pilot subcarrier can be based on known estimators, e.g. LS and MMSE. To obtain channel information at the data subcarriers, interpolation techniques used include linear interpolation, second-order interpolation, low-pass interpolation, spine-cubic interpolation and time/frequency-domain interpolation. In this part of the thesis, time/frequency-domain interpolation will be used, as it gives a lower BER when compared with other interpolation techniques [91], [92].

In the STTC-OFDM scheme, the different signals tend to interfere with one another. At the pilot instance, estimating the channel will be a case of having N_r equations and $N_r \times N_t$ unknowns, which has no exact solution. To obtain a solution for this case, some form of approximation is done. To obtain an exact solution without approximation, the number of unknowns needs to be equal to the number of equations i.e. N_r equal $N_r \times N_t$.

A non-overlapping pilot structure can be constructed for STTC-OFDM, as shown in Figure 3.3. The pilot construction avoids interference from other transmit antennas and so the task of channel estimation is simplified.

At the pilot instance, the received symbol contains a contribution from only one transmitted

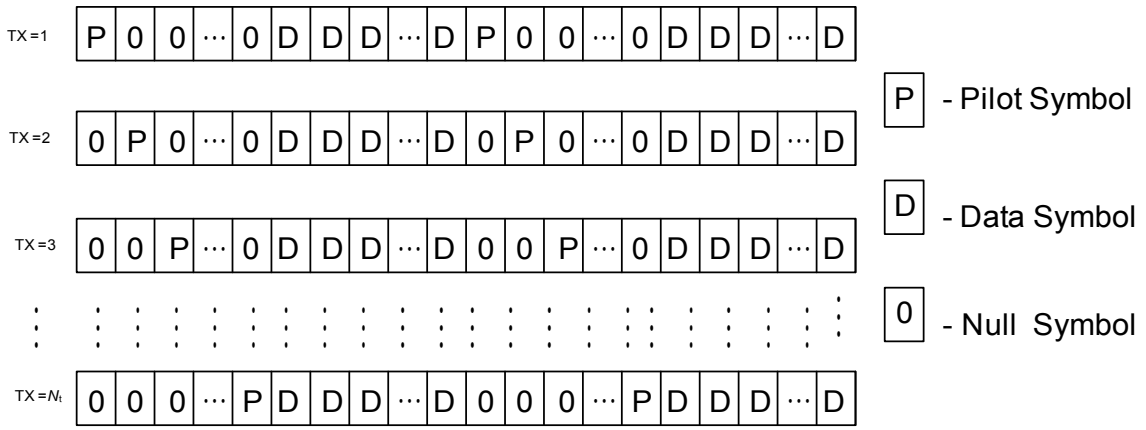

Figure 3.3: Non-overlapping pilot symbol pattern for STTC-OFDM

pilot symbol. Therefore, the channel impulse estimated in the frequency domain can easily be obtained. Using the LS estimator, the i^{th} channel impulse estimated in the frequency domain on the n_p^{th} subcarrier is written as:

$$\tilde{H}_i(n_p) = \frac{r_j(n_p)}{x_i(n_p)} \tag{3.3}$$

where $r_j(n_p)$ is the signal received on the j^{th} receive antenna and $x_i(n_p)$ is the transmitted pilot symbol for the i^{th} transmit antenna. Once the channel impulse estimate in the frequency domain has been obtained at the pilot subcarrier, the estimate at all other frequencies can be obtained by using the time/frequency-domain interpolation.

3.2.3 Time/Frequency-domain Interpolation

This interpolation technique is carried out in two domains, i.e. time and frequency domain by using zero padding and FFT/IFFT conversion [93].

Once the channel impulse estimates in the frequency domain have been obtained using the LS method at various pilot instances, the channel estimate will be converted to the time

domain by an IFFT operation on the various estimates as:

$$\tilde{h}(n_p) = \sum_{n_p=0}^{N_p-1} \tilde{H}(n_p) \exp\left(\frac{j2\pi n_p n_l}{N_p}\right), \qquad n_p = 0,1,\ldots,N_p-1, \tag{3.4}$$

where N_p is the total number of inserted pilot symbols. The antenna index i was ommited for notation convenience.

Once the estimate is in the time domain with zero padding, the signals can be transformed from N_p point into N point based on the multi-rate processing property of the signal [94]. The estimate of the channel at all frequencies is obtained by converting the time domain estimates into the frequency domain by FFT and this can be expressed as:

$$\tilde{H}(n) = \sum_{n=0}^{N} \tilde{h}(n) \exp\left(\frac{-j2\pi n n_l}{N}\right) \qquad 0 \leq n \leq N-1. \tag{3.5}$$

3.2.4 Simulation Results and Discussion

The FER of a 16-state QPSK STTC-OFDM scheme, whose trellis is shown in Figure 3.4, when the non-overlapping pilot arrangement is used to estimate the channel, is presented. The estimated channel is compared with the case of ideal channel state information (CSI) using different pilot intervals and delay spreads.

For the case of ideal CSI, the wireless channels used are quasi-static Rayleigh fading channels with $N_t = 2$, $N_r = 1$, $L = 2$ and an equal power delay profile. The two paths of the channel impulse in the time domain are separated by known delay spreads that are less than the cyclic prefix. The maximum Doppler frequency of 200 Hz was used in the simulation. The CSI is assumed to be perfectly known at the receiver, so that coherent decoding can be done.

In the estimated channel scenario, non-overlapping pilot symbols are used to estimate the channel. These pilot symbols have equal spacing from each other. Once the estimate of the channel at the pilot instance has been obtained, the time/frequency domain interpolation technique is then used for channels at other frequencies.

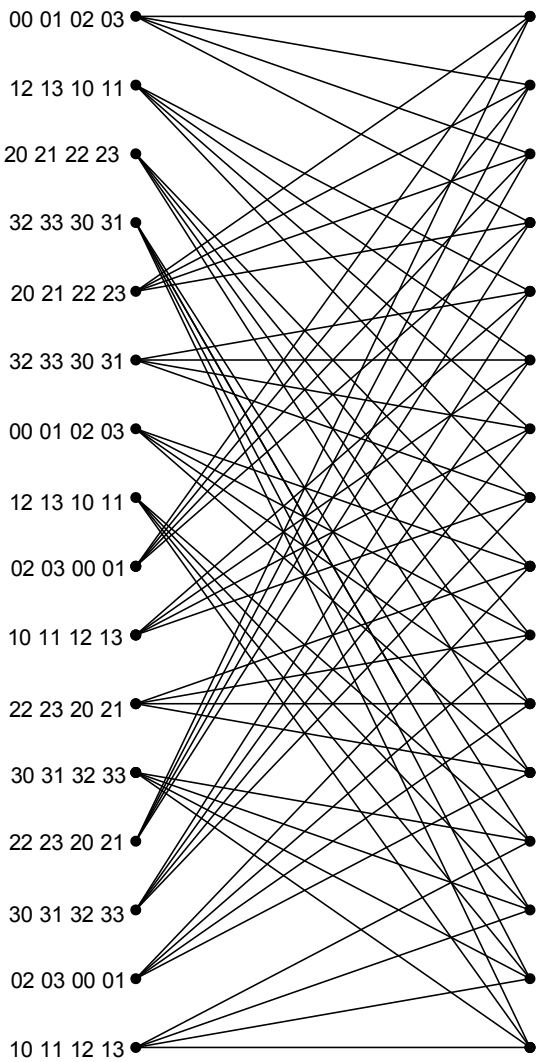

Figure 3.4: Trellis of a 16-state QPSK STTC -OFDM scheme

Figures 3.5 and Figure 3.6 show the FER for the 16-state QPSK STTC-OFDM scheme for different pilot intervals (i.e. 4, 16 and 32) with no delay spreads and 5μs delay spread, respectively. The delay spreads are assumed to be perfectly known at the receiver. Simulation results show that the closer the pilot symbols are to each other, the more accurate the channel estimate, while the farther the pilot symbols are from each other, the less the accuracy of the channel estimate. This is evident in the fact that for a pilot interval of 4, the ideal CSI curve is closer to the estimated graph, while for a pilot interval of 32, the ideal CSI curve is farther away from the estimate curve. The number of pilots used for channel estimation is a tradeoff between channel estimation accuracy and bandwidth efficiency. The lowest number of pilots should be used while keeping the error rate low for a predetermined SNR value.

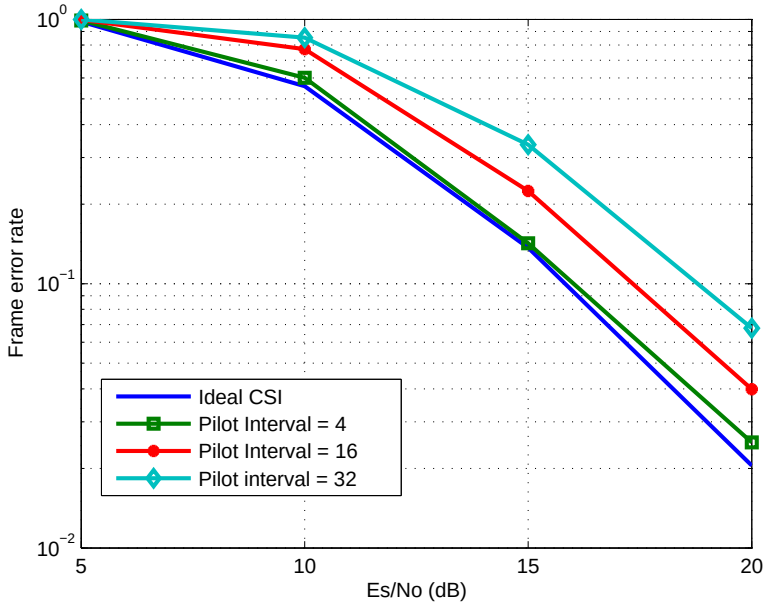

Figure 3.5: Frame error rate of STTC-OFDM with various pilot intervals and no delay spread

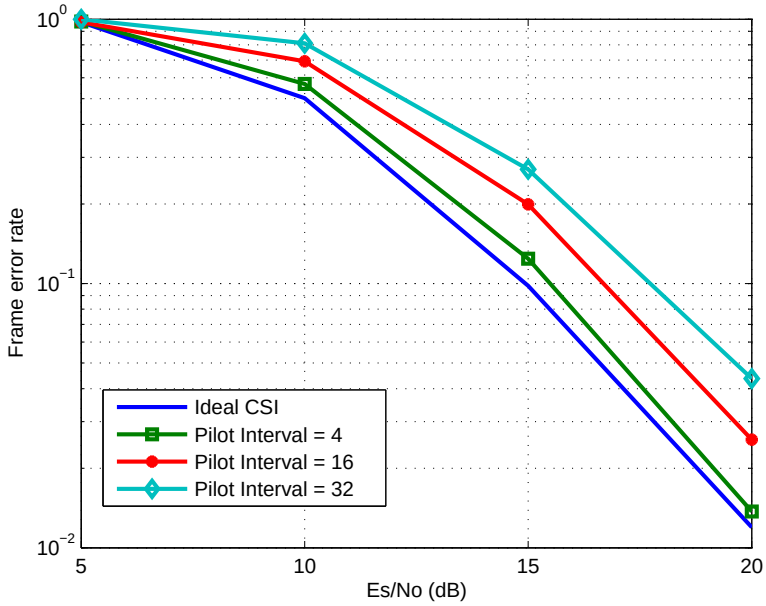

Figure 3.6: Frame error rate of STTC-OFDM with various pilot intervals and 5μs delay spread

3.3 CHANNEL ESTIMATION FOR SUPER-ORTHOGONAL BLOCK CODED OFDM SCHEMES

The transmit diversity schemes possible for SOBC-OFDM schemes, i.e. SOSFTC-OFDM and SOSTTC-OFDM, have been discussed earlier in this thesis. SOSTTC-OFDM schemes are capable of taking advantage of the space and time diversity possible for the SOBC-OFDM scheme, while SOSFTC-OFDM schemes are capable of taken advantage of the space and frequency diversity possible for the SOBC- OFDM scheme.
The channel estimation of these orthogonal-based schemes will be done by exploiting the orthogonal structure of the code or manipulating the code to be fully orthogonal at the pilot subcarrier and interpolation will be done to get estimates at other frequencies.

3.3.1 System Model

A full-rate SOBC-OFDM transmission system is considered with N_t transmit antennas, N_r receive antennas and N subcarriers.
The received signal at the j^{th} received antenna, on the n^{th} subcarrier and for $N_t = 2$ of an SOSTTC-OFDM, is written in matrix form for two time interval t and $t+1$ as:

$$\begin{bmatrix} r_j^t(n) \\ r_j^{t+1}(n) \end{bmatrix} = \begin{bmatrix} x_1(n)e^{j\theta} & x_2(n) \\ -x_2^*(n)e^{j\theta} & x_1^*(n) \end{bmatrix} \bullet \begin{bmatrix} H_{1j}(n) \\ H_{2j}(n) \end{bmatrix} + \begin{bmatrix} \eta_j^t(n) \\ \eta_j^{t+1}(n) \end{bmatrix}, \tag{3.6}$$

while the received signal at the j^{th} received antenna for the SOSFTC-OFDM scheme when $N_t = 2$ for two time interval t and $t+1$ is written as:

$$\begin{aligned} r_j^t(n) &= x_1(n)e^{j\theta}H_{1j}(n) + x_2(n)H_{2j}(n) + \eta_j^t(n) \\ r_j^{t+1}(n+1) &= -x_2^*(n+1)e^{j\theta}H_{1j}(n+1) + x_1^*(n+1)H_{2j}(n+1) + \eta_j^{t+1}(n+1) \end{aligned} \tag{3.7}$$

where $H_{ij}(n)$ is the channel impulse response in the frequency domain from the i^{th} transmit antenna to the j^{th} receive antenna on the n^{th} subcarrier. The noise elements $\eta_j^t(n)$ at the receive antenna j for subcarrier n and time t are complex additive white Gaussian variables with zero mean and variance of $N_o/2$ per dimension.

3.3.2 System Description

The channel estimation algorithm is based on taking advantage of the orthogonal nature of the transmitted N_t orthogonal matrix.

At the pilot instance of a SOSTTC-OFDM and on the n_p subcarrier, the received signal is given by:

$$\begin{bmatrix} r_j^t(n_p) \\ r_j^{t+1}(n_p) \end{bmatrix} = \begin{bmatrix} x_1(n_p)e^{j\theta} & x_2(n_p) \\ -x_2^*(n_p)e^{j\theta} & x_1^*(n_p) \end{bmatrix} \bullet \begin{bmatrix} H_{1j}(n_p) \\ H_{2j}(n_p) \end{bmatrix} + \begin{bmatrix} \eta_j^t(n_p) \\ \eta_j^{t+1}(n_p) \end{bmatrix}. \quad (3.8)$$

The estimate of the channel impulse in the frequency domain, at the pilot instance, can be expressed in matrix form as:

$$\begin{bmatrix} \tilde{H}_{1j}(n_p) \\ \tilde{H}_{2j}(n_p) \end{bmatrix} = \begin{bmatrix} \frac{r_j^{t+1}(n_p)x_2(n_p) - r_j^t(n_p)x_1^*(n_p)}{-x_2(n_p)x_2^*(n_p)e^{j\theta} - x_1^*(n_p)x_1(n_p)e^{j\theta}} \\ \frac{r_j^t(n_p)(-x_2^*(n_p)e^{j\theta}) - r_j^{t+1}(n_p)x_1(n_p)e^{j\theta}}{-x_2(n_p)x_2^*(n_p)e^{j\theta} - x_1^*(n_p)x_1(n_p)e^{j\theta}} \end{bmatrix} \quad (3.9)$$

For an SOSFTC-OFDM scheme, and based on an assumption that the channel is constant for the duration of the pilot insertion, i.e. $H_{ij}(n_p) \approx H_{ij}(n_p+1)$, the channel impulse in the frequency domain can be estimated. This assumption results in the number of received pilot equations being equal to the number of unknown channel impulse estimates in the frequency domain.

Hence, at the pilot instance of an SOSFTC-OFDM scheme, the received signal is given by:

$$\begin{bmatrix} r_j^t(n_p) \\ r_j^{t+1}(n_p) \end{bmatrix} = \begin{bmatrix} x_1(n_p)e^{j\theta} & x_2(n_p) \\ -x_2^*(n_p)e^{j\theta} & x_1^*(n_p) \end{bmatrix} \bullet \begin{bmatrix} H_{1j}(n_p) \\ H_{2j}(n_p) \end{bmatrix} + \begin{bmatrix} \eta_j^t(n_p) \\ \eta_j^{t+1}(n_p) \end{bmatrix}. \quad (3.10)$$

Solving for $H_{1j}(n_p)$ and $H_{2j}(n_p)$ in equation (3.10), the estimate of the channel impulse in

the frequency domain at each pilot subcarrier is expressed as:

$$\begin{bmatrix} \tilde{H}_{1j}(n_p) \\ \tilde{H}_{2j}(n_p) \end{bmatrix} = \begin{bmatrix} \frac{r_j^{t+1}(n_p)x_2(n_p) - r_j^t(n_p)x_1^*(n_p)}{-x_2(n_p)x_2^*(n_p+1)e^{j\theta} - x_1^*(n_p)x_1(n_p)e^{j\theta}} \\ \frac{r_j^t(n_p)(-x_2^*(n_p+1)e^{j\theta}) - r_j^{t+1}(n_p)x_1(n_p)e^{j\theta}}{-x_2(n_p)x_2^*(n_p)e^{j\theta} - x_1^*(n_p)x_1(n_p)e^{j\theta}} \end{bmatrix}. \quad (3.11)$$

The above channel estimation algorithm can be applied to SOBC-OFDM schemes with more than two transmit antennas by following the processes above outlined. After obtaining the channel estimation at the pilot instance, the time/frequency domain interpolation algorithm discussed earlier can be used to obtain the estimated channel at all other frequencies.

3.3.3 Simulation Result and Discussion

The FER for channel estimated SOBC-OFDM schemes is shown in this section. The channel at the pilot instance for the scheme is estimated based on transmission of orthogonal pilots at the pilot instance.

The trellis of a 16-state QPSK SOBC-OFDM shown in Figure 2.7 is used as the base trellis. A quasi-static FS Rayleigh fading channel with $N_t = 2$, $N_r = 1$, $L = 2$ and an equal delay profile is used in the simulation. The two paths of the channel impulse in the time domain are separated by known delay spreads that are less than the cyclic prefix. The maximum Doppler frequency of 200 Hz was used in the simulation.

The SOBC-OFDM schemes have a bandwidth of 1 MHz and 128 OFDM subcarriers. In Figures 3.7 to 3.10 , the effect of the equaly spaced pilots on SOSTTC-OFDM and SOSFTC-OFDM, when orthogonal pilots are transmitted at the pilot instance and interpolation is done to obtain the frequencies at the other channels, is given for various delay spread scenarios. Comparing the FER curves with no delay spread and once with a delay spread of 5μs, one can observe that the FER curves with a delay spread of 5μs give a better error rate performance for a similar pilot interval. This is expected, as delay spread increases the coding gain advantage of channel codes that are specially designed for multiple antenna OFDM systems. Also, the FER curves show that the farther away the pilot symbols are from each other, the less the accuracy of the channel estimation.

In system design, a choice needs to be made between many pilot symbols or more

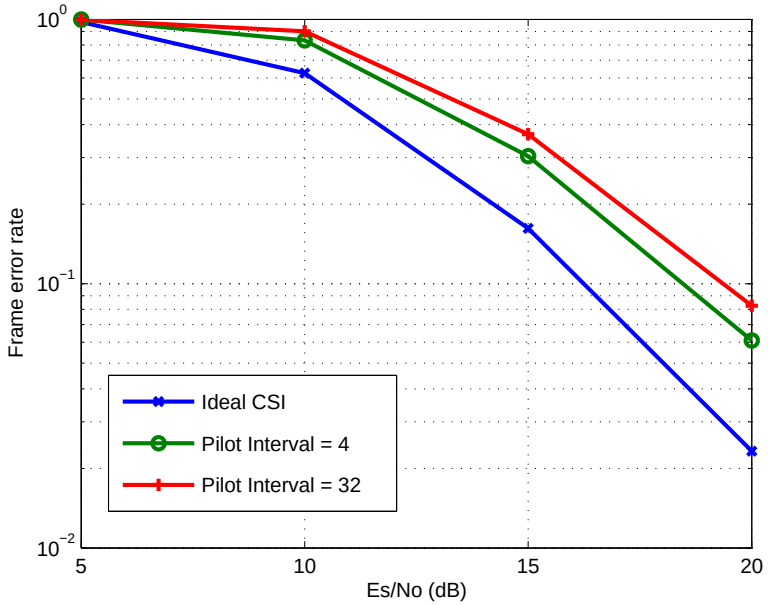

Figure 3.7: Frame error rate of SOSTTC-OFDM with various pilot intervals and no delay spread

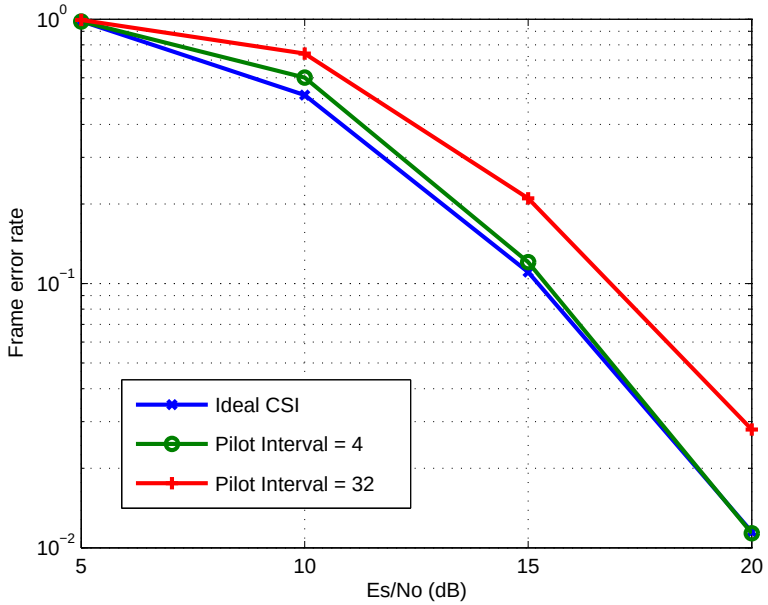

Figure 3.8: Frame error rate of SOSTTC-OFDM with various pilot intervals and 5μs delay spread

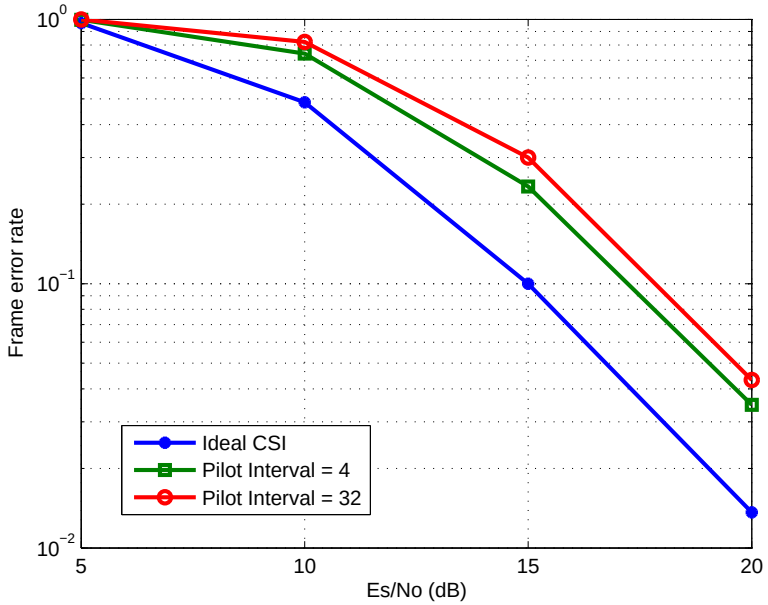

Figure 3.9: Frame error rate of SOSFTC-OFDM with various pilot intervals and no delay spread

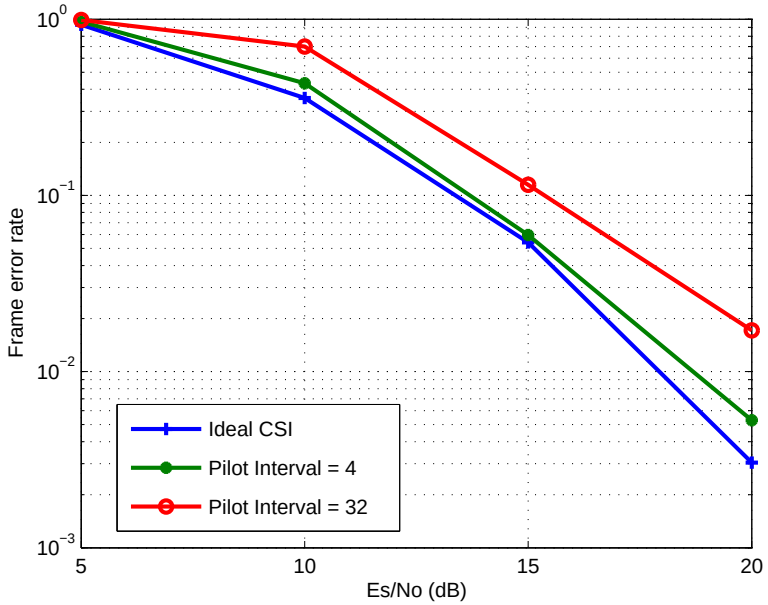

Figure 3.10: Frame error rate of SOSFTC-OFDM with various pilot intervals and 5μs delay spread

information-carrying symbols. This is because the more pilot symbols there are in a frame, the more accurate the channel estimation algorithm will be and the less efficient the bandwidth throughput is, while the fewer pilot symbols there are in the transmitted frame, the less accurate the channel estimation algorithm and the more efficient the bandwidth throughput will be.

3.4 SUMMARY

In this chapter, a pilot-based channel estimation algorithm was applied to STTC-OFDM and SOBC-OFDM schemes (i.e. SOSTTC-OFDM and SOSFTC-OFDM). A non-overlapping pilot structure was proposed for the STTC-OFDM and an orthogonal pilot structure was used for the SOBC-OFDM schemes.

The proposed pilot symbol algorithm was based on an equal number of receive equations and channels to be estimated at the pilot instance in the frequency domain. Simulation results show the effect of pilot interval on the accuracy of the channel estimation algorithm for various delay spread scenarios.

CHAPTER 4

BER ANALYSIS OF SOBC-OFDM SCHEMES WITH PERFECT CHANNEL ESTIMATION

SOBC were actually designed for flat fading channels. To mitigate the effect of FS fading channels on their performance, two main approaches have been discussed in this thesis, viz multichannel equalisation and OFDM [95].

SOBC-OFDM schemes have two main forms, viz SOSTTC-OFDM and SOSFTC-OFDM systems.

The SOSTTC-OFDM system provides space and time diversity, while the SOSFTC-OFDM system provides space and frequency diversity. Simulation results in Section 2.5, Chapter 2 of this thesis show that SOSFTC-OFDM outperforms SOSTTC-OFDM.

To validate the correctness of the simulated error rate for the high SNR region where simulations are time-consuming, performance analysis can be used to obtain the error rate perfomance.

In this chapter, a closed-form expression for the PEP of an SOBC-OFDM scheme under the assumption of perfect channel state information is obtained. This closed-form expression is based on a numerical anaysis method called the Gauss-Chebychev quadrature technique. The closed-form expression is then used to give an approximated BER for the SOBC-OFDM schemes. To validate the PEP and BER, an SOSFTC-OFDM is used as the base code.

In [24], the Chernoff upper bound of the PEP for STTC was derived. The derived bound considered all the available error events to give an expression for the error rate. In most SNR regions, the derived bound is very loose when compared with a simulated curve. After

the pioneering work in [24], other research work [96], [97], [98], [99] has been generated in order to find a tigher bound for channel codes that are specifically designed for multiple antenna systems.

The various methods that have been proposed in literature are explained below.

In [97], an exact expression of the PEP for STTC was derived using the residual method. The residual method used the characteristic function (*cf*) [100], [101] of the code to obtain the closed-form expression. An analytical estimate of the BER was obtained based on the closed-form expression by considering only dominant error events. The closed-form expression in [97] is actually the Chernoff bound in [24] with a correcting factor. The correcting factor is dependent on the poles of the *cf* of the quadratic form of the complex Gaussian random variable [72].

Another method that can be used to obtain a closed-form expression is the moment generating function (MGF) technique [98]. The MGF has been used previously in analysing the performance of SISO schemes and multiple antenna schemes. The MGF technique enables the derivation of the upper bound of the transfer function average bit error probability. In [69], the MGF-based method was used in analysing the PEP of the SOSTTC. It was shown that for both slow and fast fading channels it is possible to obtain a closed-form expression for the PEP in terms of the elements of the error signal difference matrix that characterised the super-orthogonal space-time block code.

As has been mentioned previously in this thesis, channel codes for multiple antenna systems can be combined with OFDM to give a system that has robust performance in FS channel. Most of the literature that examines the closed-form expression for OFDM schemes has concentrated on schemes with no transmit diversity and without giving any expression for the PEP [102], [103].

A technique for obtaining the exact expression of the PEP for channel codes that are specifically designed for a multiple antenna system in the OFDM environment is presented in this chapter. Although this technique is demonstrated using an SOBC-OFDM scheme in this chapter, it can be applied to other multiple antenna channel codes. This technique, the Gauss-Chebysev quadrature technique, has been used for channel codes without OFDM [104]. The performance of this technique for channel codes with OFDM is of importance and it is considered as novel in this thesis. This method combines both simplicity and accuracy in giving

an exact expression for the PEP and later the average BER is calculated by taking into account the dominant error event.

4.1 SYSTEM MODEL

A SOBC-OFDM transmission system with N_t transmit antennas, N_r receive antennas and N subcarriers is considered. The transmitted frame consists of $N \times N_t$ M-PSK multiple antenna channel codes. The encoded symbol $x_{ij}(n)$, $n \in \{0,1,2,,N-1\}$, $i \in \{0,1,2,,N_t-1\}$, is transmitted on the n^{th} subcarrier from the i^{th} transmit antenna to the j^{th} receive antenna. The signal received on each subcarrier is dependent on the type of SOBC-OFDM system.
For an SOSTTC-OFDM scheme, the signal received on the n^{th} over two time periods t and $t+1$ is given as:

$$\begin{aligned} r_j^t(n) &= x_{1j}(n)e^{j\theta}H_{1j}(n) + x_{2j}(n)H_{2j}(n) + \eta_j^t(n) \\ r_j^{t+1}(n) &= -x_{2j}^*(n)e^{j\theta}H_{1j}(n) + x_{1j}^*(n)H_{2j}(n) + \eta_j^{t+1}(n), \end{aligned} \tag{4.1}$$

while for an SOSFTC-OFDM, the signal received on two subcarriers n and $n+1$, and over two time periods t and $t+1$, is given as:

$$\begin{aligned} r_j^t(n) &= x_{1j}(n)e^{j\theta}H_{1j}(n) + x_{2j}(n)H_{2j}(n) + \eta_j^t(n) \\ r_j^{t+1}(n+1) &= -x_{2j}^*(n+1)e^{j\theta}H_{1j}(n+1) + x_{1j}^*(n+1)H_{2j}(n+1) + \eta_j^{t+1}(n+1), \end{aligned} \tag{4.2}$$

where $H_{ij}(n)$ is the channel impulse vector from the i^{th} transmit antenna to the j^{th} receive antenna on the n^{th} subcarrier. The noise components $\eta_j^t(n)$ are complex additive white Gaussian variables with zero mean and variance of $N_o/2$ per dimension.
The channel impulse vector used in equations (4.1) and (4.2) can be expressed as a function of an FFT coeficient as:

$$\begin{aligned} H_{ij}(n) &= \sum_{l=0}^{L-1} h_{ij}(l,t)exp(-j2\pi n(l)/N) \\ &= \mathbf{h}_{ij}\mathbf{f}(n) \end{aligned} \tag{4.3}$$

where $\mathbf{h}_{ij}$ comprises the channel vectors given in equation (4.4) as:

$$\mathbf{h}_{ij} = \left[h_{ij}(0),\ h_{ij}(1),\ h_{ij}j(2),\ \cdots,\ h_{ij}(L-1) \right], \tag{4.4}$$

and the FFT coefficient can be expressed as:

$$\begin{aligned} \mathbf{f}(n) &= [\exp(-j2\pi n(0)/N),\ \cdots,\ \exp(-j2\pi n(L-2)/N),\ \exp(-j2\pi n(L-1)/N)]^T \\ &= [1,\ \cdots,\ f(L-2),\ f(L-1)]^T. \end{aligned} \tag{4.5}$$

A generalised received equation for both SOBC-OFDM schemes at the j^{th} received antenna is written as:

$$\mathbf{R}_j = \mathbf{H}_j\mathbf{X}_j + \boldsymbol{\eta}_j \tag{4.6}$$

where

$$\mathbf{R}_j = \left[\mathbf{r}_j(1),\ \mathbf{r}_j(2),\ \mathbf{r}_j(3),\ \cdots,\ \mathbf{r}_j(N) \right], \tag{4.7}$$

$$\mathbf{H}_j = \left[\mathbf{H}_j(1),\ \mathbf{H}_j(2),\ \mathbf{H}_j(3),\ \cdots,\ \mathbf{H}_j(N) \right], \tag{4.8}$$

$$\mathbf{X}_j = \left[\mathbf{X}_j(1),\ \mathbf{X}_j(2),\ \mathbf{X}_j(3),\ \cdots,\ \mathbf{X}_j(N) \right]^T, \tag{4.9}$$

and

$$\boldsymbol{\eta}_j = \left[\boldsymbol{\eta}_j(1),\ \boldsymbol{\eta}_j(2),\ \boldsymbol{\eta}_j(3),\ \cdots,\ \boldsymbol{\eta}_j(N) \right]. \tag{4.10}$$

In equation (4.9), the transmitted block code at each subcarrier i.e. $\mathbf{X}_j(n)$ has a different form depending on the SOBC-OFDM scheme. For an SOSTTC-OFDM scheme, $\mathbf{X}_j(n)$ is

written as:

$$\mathbf{X}_j(n) = \begin{bmatrix} x_{1j}(n)e^{j\theta} & x_{2j}(n) \\ -x_{2j}^*(n)e^{j\theta} & x_{1j}^*(n) \end{bmatrix}, \tag{4.11}$$

while for an SOSFTC-OFDM scheme $\mathbf{X}_j(n)$ and $\mathbf{X}_j(n+1)$ is written as:

$$\mathbf{X}_j(n) = \begin{bmatrix} x_{1j}(n)e^{j\theta} \\ x_{2j}(n) \end{bmatrix}, \tag{4.12}$$

and

$$\mathbf{X}_j(n+1) = \begin{bmatrix} -x_{2j}^*(n+1)e^{j\theta} \\ x_{1j}^*(n+1) \end{bmatrix}. \tag{4.13}$$

4.2 PAIRWISE ERROR PROBABILITY OF SOBC-OFDM SCHEME

To obtain the BER via analysis for the SOBC-OFDM scheme, a closed form expression for the PEP need to be obtained first and later the PEP is used to calculate the BER.
The method used in this section is not limited to SOBC-OFDM schemes and can be extended to other coded OFDM schemes and for any number of transmit and receive antennas.

4.2.1 Mathematical Analysis

To obtain the PEP of an SOBC-OFDM scheme, the transmitted codeword and the erroneously decoded codeword are used. Assuming the transmitted codeword sequence as:

$$\mathbf{X} = \begin{bmatrix} x(1), & x(2), & x(3), & \cdots, & x(N) \end{bmatrix}, \tag{4.14}$$

and the erroneously decoded codeword sequence as:

$$\hat{\mathbf{X}} = \begin{bmatrix} \hat{x}(1), & \hat{x}(2), & \hat{x}(3), & \cdots, & \hat{x}(N) \end{bmatrix}, \tag{4.15}$$

the maximum likelihood decision metric will be used. The maximum likelihood decision metric corresponding to the transmitted SOBC-OFDM codeword is given as:

$$m(\mathbf{R},\mathbf{X}) = ||\mathbf{R}_j - (\mathbf{H}_j\mathbf{X}_j)||^2, \tag{4.16}$$

while the ML decision metric corresponding to the erroneously decoded SOBC-OFDM codeword is given as:

$$m(\mathbf{R},\hat{\mathbf{X}}) = ||\mathbf{R}_j - (\mathbf{H}_j\hat{\mathbf{X}}_j)||^2. \tag{4.17}$$

From the decision metrics, the PEP for a given channel impulse $\mathbf{H}_j$ in the frequency domain is expressed as:

$$\begin{aligned} P(\mathbf{X}\rightarrow\hat{\mathbf{X}}|\mathbf{H}_j) &= Pr\{m(\mathbf{R},\mathbf{X}) > m(\mathbf{R},\hat{\mathbf{X}})\} \\ &= Pr\{(m(\mathbf{R},\mathbf{X}) - m(\mathbf{R},\hat{\mathbf{X}})) > 0\}. \end{aligned} \tag{4.18}$$

The decision metric of the transmitted and erroneously decoded codeword can be substituted into equation (4.18) to give equation (4.19).

$$\begin{aligned} P(\mathbf{X}\rightarrow\hat{\mathbf{X}}|\mathbf{H}_j) &= Pr\{||\mathbf{H}_j(\mathbf{X}_j - \hat{\mathbf{X}}_j)||^2 > 0\} \\ &= Pr\{||\mathbf{H}_j\mathbf{D}||^2 > 0\} \end{aligned} \tag{4.19}$$

where $\mathbf{D}$ is the codeword difference matrix that characterises the SOBC-OFDM scheme whose expression is given as:

$$\mathbf{D} = \left[\ \mathbf{X}_j - \hat{\mathbf{X}}_j\ \right], \tag{4.20}$$

and $||.||$ represents the norm of the matrix element.

The conditional PEP written in equation (4.19) can be expressed in terms of the complementary error function (erfc) [104] as:

$$P(\mathbf{X} \rightarrow \hat{\mathbf{X}}|\mathbf{H}_j) = \frac{1}{2}\,\text{erfc}\left(\sqrt{\frac{E_s}{4N_o}\sum_{j=1}^{N_r}\mathbf{H}_j\mathbf{D}\mathbf{D}^H\mathbf{H}_j{}^H}\right), \tag{4.21}$$

where $\mathbf{D}\mathbf{D}^H$ is a diagonal matrix of the form:

$$\mathbf{D}\mathbf{D}^H = \begin{bmatrix} \mathbf{D}(1)(\mathbf{D}(1))^H & 0 & \dots & 0 \\ 0 & \mathbf{D}(2)(\mathbf{D}(2))^H & \dots & 0 \\ \vdots & \vdots & \ddots & \vdots \\ 0 & 0 & \dots & \mathbf{D}(N)(\mathbf{D}(N))^H \end{bmatrix}, \tag{4.22}$$

$(\bullet)^H$ is the conjugate transpose of the matrix element and E_s/N_o is the symbol SNR. The diagonal element of equation (4.22) is dependent on the form of the SOBC-OFDM scheme. A generalised form is written as:

$$\mathbf{D}(n) = \left[\, \mathbf{X}_j(n) - \hat{\mathbf{X}}_j(n) \,\right]. \tag{4.23}$$

The individual element of the channel impulse matrix $\mathbf{H}_j$ in the frequency domain can be expanded further using equations (4.3), (4.4) and (4.8). Hence $\mathbf{H}_j(n)$ is expressed as:

$$\mathbf{H}_j(n) = \left[\, h_{1j}(0) \quad \dots \quad h_{1j}(L-1) \quad h_{2j}(0)\dots h_{2j}(L-1) \,\right]_{1\times LN_t} \cdot \begin{bmatrix} \mathbf{f}(n) & 0 & \dots & 0 \\ 0 & \mathbf{f}(n) & \dots & 0 \\ \vdots & \vdots & \ddots & \vdots \\ 0 & 0 & \dots & \mathbf{f}(n) \end{bmatrix}_{LN_t\times N_t}$$

$$\mathbf{H}_j(n) = [\mathbf{h}_{1j}\ \ \mathbf{h}_{2j}]\mathbf{F}(n)$$

$$\mathbf{H}_j(n) = \mathbf{h}_j\mathbf{F}(n). \tag{4.24}$$

The conditional PEP equation (4.21) can be written with respect to the n^{th} subcarrier

as:

$$P(\mathbf{X}\rightarrow\hat{\mathbf{X}}|\mathbf{H}) = \frac{1}{2}\text{erfc}\left(\sqrt{\frac{E_s}{2N_o}\sum_{j=1}^{N_r}\sum_{n=1}^{N}\mathbf{h}_j\mathbf{F}(n)\mathbf{D}(n)(\mathbf{D}(n))^H(\mathbf{F}(n))^H\mathbf{h}_j{}^H}\right). \quad (4.25)$$

The above expression in equation (4.25) can be simplified further using the results in [72] and following the steps enumerated in Section 2.4 of Chapter 2 to give equation (4.26).

$$P(\mathbf{X}\rightarrow\hat{\mathbf{X}}) = \frac{1}{\pi}\int_0^{\infty}\frac{1}{t^2+1}\prod_{j=1}^{N_r}\frac{dt}{\det[\mathbf{I}_{LN_t}+\frac{E_s}{4N_o}\mathbf{Z}(t^2+1)]_j} \quad (4.26)$$

where $\mathbf{Z}$ is the error difference matrix for the overall subcarriers with expression:

$$\mathbf{Z} = \sum_{n=1}^{N}\mathbf{F}(n)\mathbf{D}(n)(\mathbf{D}(n))^H(\mathbf{F}(n))^H. \quad (4.27)$$

The right hand-side (RHS) of equation (4.26) can be reduced to the form:

$$RHS = \frac{1}{\pi}\int_0^{\infty}\frac{1}{t^2+1}f(t^2+1)dt \quad (4.28)$$

where:

$$f(t^2+1) = \prod_{j=1}^{N_r}\frac{1}{\det[\mathbf{I}_{LN_t}+\frac{E_s}{4N_o}\mathbf{Z}(t^2+1)]_j}. \quad (4.29)$$

Substituting $c = \frac{1}{t^2+1}$ into (4.28), one obtain:

$$RHS = \frac{1}{2\pi}\int_0^{1}\frac{1}{\sqrt{c(1-c)}}f(1/c)dc. \quad (4.30)$$

Equation (4.30) is in the orthogonal polynomial form [105] and Gauss-Chebyshev quadrature technique of the first kind [104] can be used to solve it, using:

$$\int_{-1}^{1}\frac{f(p)}{\sqrt{1-p^2}}dp = \sum_{i=1}^{m}\text{G}_i f(p_i)+\xi_m \quad (4.31)$$

where

$$p_i = \cos\frac{(2i-1)}{2m}, \tag{4.32}$$

$$\mathrm{G}_i = \frac{\pi}{m}, \tag{4.33}$$

and

$$\xi_m \leq \max_{-1<p<+1} \frac{\pi}{(2m)!2^{2m-1}} |f^{2m}(p)|. \tag{4.34}$$

Substituting $p = 2c-1$ into equation (4.30), one can reduce it to the generic Gauss-Chebyshev quadrature form shown in equation (4.31) Hence:

$$\begin{aligned} 2c-1 &= \cos\frac{(2i-1)\pi}{2m} \\ 2c &= \cos\frac{(2i-1)\pi}{2m} + 1 \\ \frac{1}{c} &= \sec^2\frac{(2i-1)\pi}{4m}. \end{aligned} \tag{4.35}$$

Therefore

$$\begin{aligned} RHS &= \sum_{i=1}^{m} \mathrm{G}_i f(p_i) + \xi_m \\ RHS &= \frac{1}{2m}\sum_{i=1}^{m} f(\sec^2\frac{(2i-1)\pi}{4m}) + \xi_m. \end{aligned} \tag{4.36}$$

The closed-form expression of the PEP for the SOBC-OFDM system using the Gauss-Chebyshev quadrature formula as given above is now given by:

$$P(\mathbf{X}\rightarrow\hat{\mathbf{X}}) = \frac{1}{2m}\sum_{i=1}^{m}\prod_{j=1}^{N_r}\frac{1}{\det[\mathbf{I}_{LN_t} + \frac{E_s}{4N_o}\mathbf{Z}\sec^2\frac{(2i-1)\pi}{4m}]_j} + \xi_m. \tag{4.37}$$

From the closed-form PEP expression for SOBC-OFDM, the following deductions can be made:

1. The PEP expression is a function of the error difference matrix $\mathbf{Z}$.

2. The PEP expression can be used for any number of transmit or receive antenna.

3. The PEP expression is not dependent on the modulation scheme, i.e. can be used for any M-PSK.

The remainder term ξ_m is negligible for the Gauss-Chebushev m-point integral formula [104].

4.2.2 Numerical Example

As an example, a simple two-state BPSK trellis shown in Figure 4.1 will be considered to obtain numerical values for the derived PEP. The code transmission is based on an SOSFTC-OFDM scheme.

The trellis contains two parallel paths converging/diverging from each state. Each of the paths is labelled $(a,\ b)/\mathbf{X}(x_1,\ x_2,\ \theta)$, where $(a,\ b)$ represent the input bits and $\mathbf{X}(x_1,\ x_2,\ \theta)$ represent the output transmitted symbols function of the SOSFTC-OFDM scheme.

In this example the system parameters are given as: $N_t = 2, N_r = 1,\ L = 2$ and N= 64. The OFDM system has a bandwidth of 1 MHz and the tone spacing of the OFDM system is 15.625 KHz. The FFT coeficienct matix $\mathbf{F}(n)$ can be obtained based on the above parameters.

$$\mathbf{F}(n) \quad = \quad \begin{bmatrix} \mathbf{f}(n) & \mathbf{0} \\ \mathbf{0} & \mathbf{f}(n) \end{bmatrix} \tag{4.38}$$

The different expressions of the error difference matrix $\mathbf{Z}$ based on equation (4.27) are given below and then these expressions are used to get a numerical PEP expression for the SOSFTC-OFDM scheme for different error event scenario.

For an error event of 1, $\mathbf{Z}$ in (4.27) is given as $\mathbf{Z}(1)$.

$$\mathbf{Z}(1) \quad = \quad Z_1 + Z_2, \tag{4.39}$$

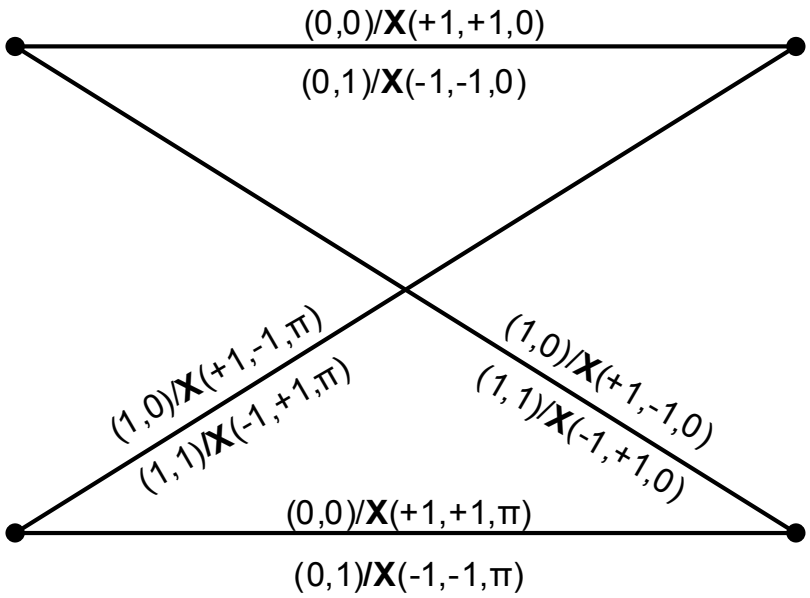

Figure 4.1: 2-State BPSK SOBC trellis

where:

$$Z_1 = \begin{bmatrix} 1 & 0 \\ f(1) & 0 \\ 0 & 1 \\ 0 & f(1) \end{bmatrix} \bullet \begin{bmatrix} 2 \\ 2 \end{bmatrix} \bullet \begin{bmatrix} 2 & 2 \end{bmatrix} \bullet \begin{bmatrix} 1 & f(1) & 0 & 0 \\ 0 & 0 & 1 & f(1) \end{bmatrix} \tag{4.40}$$

and

$$Z_2 = \begin{bmatrix} 1 & 0 \\ f(1) & 0 \\ 0 & 1 \\ 0 & f(1) \end{bmatrix} \bullet \begin{bmatrix} -2 \\ 2 \end{bmatrix} \bullet \begin{bmatrix} -2 & 2 \end{bmatrix} \bullet \begin{bmatrix} 1 & f(1) & 0 & 0 \\ 0 & 0 & 1 & f(1) \end{bmatrix} \tag{4.41}$$

For an error event of length 2 with respect to the all zero path as the correct path, $\mathbf{Z}$ in (4.27) is given as $\mathbf{Z}(2)$.

$$\mathbf{Z}(2) = Z_1 + Z_2 + Z_3 + Z_4 \tag{4.42}$$

where:

$$Z_1 = \begin{bmatrix} 1 & 0 \\ f(1) & 0 \\ 0 & 1 \\ 0 & f(1) \end{bmatrix} \bullet \begin{bmatrix} 0 \\ 2 \end{bmatrix} \bullet \begin{bmatrix} 0 & 2 \end{bmatrix} \bullet \begin{bmatrix} 1 & f(1) & 0 & 0 \\ 0 & 0 & 1 & f(1) \end{bmatrix}, \quad (4.43)$$

$$Z_2 = \begin{bmatrix} 1 & 0 \\ f(2) & 0 \\ 0 & 1 \\ 0 & f(2) \end{bmatrix} \bullet \begin{bmatrix} -2 \\ 0 \end{bmatrix} \bullet \begin{bmatrix} -2 & 0 \end{bmatrix} \bullet \begin{bmatrix} 1 & f(2) & 0 & 0 \\ 0 & 0 & 1 & f(2) \end{bmatrix}, \quad (4.44)$$

$$Z_3 = \begin{bmatrix} 1 & 0 \\ f(3) & 0 \\ 0 & 1 \\ 0 & f(3) \end{bmatrix} \bullet \begin{bmatrix} 0 \\ 0 \end{bmatrix} \bullet \begin{bmatrix} 0 & 0 \end{bmatrix} \bullet \begin{bmatrix} 1 & f(3) & 0 & 0 \\ 0 & 0 & 1 & f(3) \end{bmatrix}, \quad (4.45)$$

and

$$Z_4 = \begin{bmatrix} 1 & 0 \\ f(4) & 0 \\ 0 & 1 \\ 0 & f(4) \end{bmatrix} \bullet \begin{bmatrix} -2 \\ 2 \end{bmatrix} \bullet \begin{bmatrix} -2 & 2 \end{bmatrix} \bullet \begin{bmatrix} 1 & f(4) & 0 & 0 \\ 0 & 0 & 1 & f(4) \end{bmatrix}. \quad (4.46)$$

For an error event of length 3 with respect to the all zero path as the correct path, $\mathbf{Z}$ in (4.27) is given as $\mathbf{Z}(3)$.

$$\mathbf{Z}(3) = Z_1 + Z_2 + Z_3 + Z_4 + Z_5 + Z_6, \quad (4.47)$$

where:

$$Z_1 = \begin{bmatrix} 1 & 0 \\ f(1) & 0 \\ 0 & 1 \\ 0 & f(1) \end{bmatrix} \bullet \begin{bmatrix} 0 \\ 2 \end{bmatrix} \bullet \begin{bmatrix} 0 & 2 \end{bmatrix} \bullet \begin{bmatrix} 1 & f(1) & 0 & 0 \\ 0 & 0 & 1 & f(1) \end{bmatrix}, \quad (4.48)$$

$$Z_2 = \begin{bmatrix} 1 & 0 \\ f(2) & 0 \\ 0 & 1 \\ 0 & f(2) \end{bmatrix} \bullet \begin{bmatrix} -2 \\ 0 \end{bmatrix} \bullet \begin{bmatrix} -2 & 0 \end{bmatrix} \bullet \begin{bmatrix} 1 & f(2) & 0 & 0 \\ 0 & 0 & 1 & f(2) \end{bmatrix}, \quad (4.49)$$

$$Z_3 = \begin{bmatrix} 1 & 0 \\ f(3) & 0 \\ 0 & 1 \\ 0 & f(3) \end{bmatrix} \bullet \begin{bmatrix} 0 \\ 2 \end{bmatrix} \bullet \begin{bmatrix} 0 & 2 \end{bmatrix} \bullet \begin{bmatrix} 1 & f(3) & 0 & 0 \\ 0 & 0 & 1 & f(3) \end{bmatrix}, \quad (4.50)$$

$$Z_4 = \begin{bmatrix} 1 & 0 \\ f(4) & 0 \\ 0 & 1 \\ 0 & f(4) \end{bmatrix} \bullet \begin{bmatrix} 0 \\ 2 \end{bmatrix} \bullet \begin{bmatrix} 0 & 2 \end{bmatrix} \bullet \begin{bmatrix} 1 & f(4) & 0 & 0 \\ 0 & 0 & 1 & f(4) \end{bmatrix}, \quad (4.51)$$

$$Z_5 = \begin{bmatrix} 1 & 0 \\ f(5) & 0 \\ 0 & 1 \\ 0 & f(5) \end{bmatrix} \bullet \begin{bmatrix} 0 \\ 0 \end{bmatrix} \bullet \begin{bmatrix} 0 & 0 \end{bmatrix} \bullet \begin{bmatrix} 1 & f(5) & 0 & 0 \\ 0 & 0 & 1 & f(5) \end{bmatrix}, \quad (4.52)$$

and

$$Z_6 = \begin{bmatrix} 1 & 0 \\ f(6) & 0 \\ 0 & 1 \\ 0 & f(6) \end{bmatrix} \bullet \begin{bmatrix} -2 \\ 2 \end{bmatrix} \bullet \begin{bmatrix} -2 & 2 \end{bmatrix} \bullet \begin{bmatrix} 1 & f(6) & 0 & 0 \\ 0 & 0 & 1 & f(6) \end{bmatrix}. \quad (4.53)$$

For an error event of length 4 with respect to the all zero path as the correct path, $\mathbf{Z}$ in (4.27) is given as $\mathbf{Z}(4)$.

$$\mathbf{Z}(4) = Z_1 + Z_2 + Z_3 + Z_4 + Z_5 + Z_6 + Z_7 + Z_8, \quad (4.54)$$

where:

$$Z_1 = \begin{bmatrix} 1 & 0 \\ f(1) & 0 \\ 0 & 1 \\ 0 & f(1) \end{bmatrix} \bullet \begin{bmatrix} 0 \\ 2 \end{bmatrix} \bullet \begin{bmatrix} 0 & 2 \end{bmatrix} \bullet \begin{bmatrix} 1 & f(1) & 0 & 0 \\ 0 & 0 & 1 & f(1) \end{bmatrix}, \quad (4.55)$$

$$Z_2 = \begin{bmatrix} 1 & 0 \\ f(2) & 0 \\ 0 & 1 \\ 0 & f(2) \end{bmatrix} \bullet \begin{bmatrix} -2 \\ 0 \end{bmatrix} \bullet \begin{bmatrix} -2 & 0 \end{bmatrix} \bullet \begin{bmatrix} 1 & f(2) & 0 & 0 \\ 0 & 0 & 1 & f(2) \end{bmatrix}, \quad (4.56)$$

$$Z_3 = \begin{bmatrix} 1 & 0 \\ f(3) & 0 \\ 0 & 1 \\ 0 & f(3) \end{bmatrix} \bullet \begin{bmatrix} 0 \\ 2 \end{bmatrix} \bullet \begin{bmatrix} 0 & 2 \end{bmatrix} \bullet \begin{bmatrix} 1 & f(3) & 0 & 0 \\ 0 & 0 & 1 & f(3) \end{bmatrix}, \quad (4.57)$$

$$Z_4 = \begin{bmatrix} 1 & 0 \\ f(4) & 0 \\ 0 & 1 \\ 0 & f(4) \end{bmatrix} \bullet \begin{bmatrix} 0 \\ 2 \end{bmatrix} \bullet \begin{bmatrix} 0 & 2 \end{bmatrix} \bullet \begin{bmatrix} 1 & f(4) & 0 & 0 \\ 0 & 0 & 1 & f(4) \end{bmatrix}, \quad (4.58)$$

$$Z_5 = \begin{bmatrix} 1 & 0 \\ f(5) & 0 \\ 0 & 1 \\ 0 & f(5) \end{bmatrix} \bullet \begin{bmatrix} 0 \\ 2 \end{bmatrix} \bullet \begin{bmatrix} 0 & 2 \end{bmatrix} \bullet \begin{bmatrix} 1 & f(5) & 0 & 0 \\ 0 & 0 & 1 & f(5) \end{bmatrix}, \quad (4.59)$$

$$Z_6 = \begin{bmatrix} 1 & 0 \\ f(6) & 0 \\ 0 & 1 \\ 0 & f(6) \end{bmatrix} \bullet \begin{bmatrix} 0 \\ 2 \end{bmatrix} \bullet \begin{bmatrix} 0 & 2 \end{bmatrix} \bullet \begin{bmatrix} 1 & f(6) & 0 & 0 \\ 0 & 0 & 1 & f(6) \end{bmatrix}, \quad (4.60)$$

$$Z_7 = \begin{bmatrix} 1 & 0 \\ f(7) & 0 \\ 0 & 1 \\ 0 & f(7) \end{bmatrix} \bullet \begin{bmatrix} 0 \\ 0 \end{bmatrix} \bullet \begin{bmatrix} 0 & 0 \end{bmatrix} \bullet \begin{bmatrix} 1 & f(7) & 0 & 0 \\ 0 & 0 & 1 & f(7) \end{bmatrix}, \quad (4.61)$$

and

$$Z_8 = \begin{bmatrix} 1 & 0 \\ f(8) & 0 \\ 0 & 1 \\ 0 & f(8) \end{bmatrix} \bullet \begin{bmatrix} -2 \\ 2 \end{bmatrix} \bullet \begin{bmatrix} -2 & 2 \end{bmatrix} \bullet \begin{bmatrix} 1 & f(8) & 0 & 0 \\ 0 & 0 & 1 & f(8) \end{bmatrix}. \quad (4.62)$$

For an error event of length 5 with respect to the all zero path as the correct path, $\mathbf{Z}$ in (4.27)

is given as $\mathbf{Z}(5)$.

$$\mathbf{Z}(5) = Z_1 + Z_2 + Z_3 + Z_4 + Z_5 + Z_6 + Z_7 + Z_8 + Z_9 + Z_{10}, \tag{4.63}$$

where:

$$Z_1 = \begin{bmatrix} 1 & 0 \\ f(1) & 0 \\ 0 & 1 \\ 0 & f(1) \end{bmatrix} \bullet \begin{bmatrix} 0 \\ 2 \end{bmatrix} \bullet \begin{bmatrix} 0 & 2 \end{bmatrix} \bullet \begin{bmatrix} 1 & f(1) & 0 & 0 \\ 0 & 0 & 1 & f(1) \end{bmatrix}, \tag{4.64}$$

$$Z_2 = \begin{bmatrix} 1 & 0 \\ f(2) & 0 \\ 0 & 1 \\ 0 & f(2) \end{bmatrix} \bullet \begin{bmatrix} -2 \\ 0 \end{bmatrix} \bullet \begin{bmatrix} -2 & 0 \end{bmatrix} \bullet \begin{bmatrix} 1 & f(2) & 0 & 0 \\ 0 & 0 & 1 & f(2) \end{bmatrix}, \tag{4.65}$$

$$Z_3 = \begin{bmatrix} 1 & 0 \\ f(3) & 0 \\ 0 & 1 \\ 0 & f(3) \end{bmatrix} \bullet \begin{bmatrix} 0 \\ 2 \end{bmatrix} \bullet \begin{bmatrix} 0 & 2 \end{bmatrix} \bullet \begin{bmatrix} 1 & f(3) & 0 & 0 \\ 0 & 0 & 1 & f(3) \end{bmatrix}, \tag{4.66}$$

$$Z_4 = \begin{bmatrix} 1 & 0 \\ f(4) & 0 \\ 0 & 1 \\ 0 & f(4) \end{bmatrix} \bullet \begin{bmatrix} 0 \\ 2 \end{bmatrix} \bullet \begin{bmatrix} 0 & 2 \end{bmatrix} \bullet \begin{bmatrix} 1 & f(4) & 0 & 0 \\ 0 & 0 & 1 & f(4) \end{bmatrix}, \tag{4.67}$$

$$Z_5 = \begin{bmatrix} 1 & 0 \\ f(5) & 0 \\ 0 & 1 \\ 0 & f(5) \end{bmatrix} \bullet \begin{bmatrix} 0 \\ 2 \end{bmatrix} \bullet \begin{bmatrix} 0 & 2 \end{bmatrix} \bullet \begin{bmatrix} 1 & f(5) & 0 & 0 \\ 0 & 0 & 1 & f(5) \end{bmatrix}, \quad (4.68)$$

$$Z_6 = \begin{bmatrix} 1 & 0 \\ f(6) & 0 \\ 0 & 1 \\ 0 & f(6) \end{bmatrix} \bullet \begin{bmatrix} 0 \\ 2 \end{bmatrix} \bullet \begin{bmatrix} 0 & 2 \end{bmatrix} \bullet \begin{bmatrix} 1 & f(6) & 0 & 0 \\ 0 & 0 & 1 & f(6) \end{bmatrix}, \quad (4.69)$$

$$Z_7 = \begin{bmatrix} 1 & 0 \\ f(7) & 0 \\ 0 & 1 \\ 0 & f(7) \end{bmatrix} \bullet \begin{bmatrix} 0 \\ 2 \end{bmatrix} \bullet \begin{bmatrix} 0 & 2 \end{bmatrix} \bullet \begin{bmatrix} 1 & f(7) & 0 & 0 \\ 0 & 0 & 1 & f(7) \end{bmatrix}, \quad (4.70)$$

$$Z_8 = \begin{bmatrix} 1 & 0 \\ f(8) & 0 \\ 0 & 1 \\ 0 & f(8) \end{bmatrix} \bullet \begin{bmatrix} 0 \\ 2 \end{bmatrix} \bullet \begin{bmatrix} 0 & 2 \end{bmatrix} \bullet \begin{bmatrix} 1 & f(8) & 0 & 0 \\ 0 & 0 & 1 & f(8) \end{bmatrix}, \quad (4.71)$$

$$Z_9 = \begin{bmatrix} 1 & 0 \\ f(9) & 0 \\ 0 & 1 \\ 0 & f(9) \end{bmatrix} \bullet \begin{bmatrix} 0 \\ 0 \end{bmatrix} \bullet \begin{bmatrix} 0 & 0 \end{bmatrix} \bullet \begin{bmatrix} 1 & f(9) & 0 & 0 \\ 0 & 0 & 1 & f(9) \end{bmatrix}, \quad (4.72)$$

and

$$Z_{10} = \begin{bmatrix} 1 & 0 \\ f(10) & 0 \\ 0 & 1 \\ 0 & f(10) \end{bmatrix} \bullet \begin{bmatrix} -2 \\ 2 \end{bmatrix} \bullet \begin{bmatrix} -2 & 2 \end{bmatrix} \bullet \begin{bmatrix} 1 & f(10) & 0 & 0 \\ 0 & 0 & 1 & f(10) \end{bmatrix} \quad (4.73)$$

Other error event lengths can be calculated using the above examples.

4.3 BER OF SOSFTC-OFDM

In most digital communication systems, the BER (or FER) of the system offers a better way than the PEP for analysing the performance of such a system.

The BER can be upper bounded by using the transfer function approach [106]. This can be done when its PEP is expressed in a product form [24].

The transfer function approach is a method that uses a code state diagram to obtain the error rate performance of trellis-based codes. A truncation of the transfer function method can be done by accounting for error event paths up to a pre-determined value using the equation given below [107],

$$\text{BER} \approx \frac{1}{b} \sum_{\mathbf{X} \neq \hat{\mathbf{X}}} q(\mathbf{X} \to \hat{\mathbf{X}}) P(\mathbf{X} \to \hat{\mathbf{X}}) \quad (4.74)$$

where b is the number of input bits per trellis path and $q(\mathbf{X} \to \hat{\mathbf{X}})$ is the number of bit errors corresponding to each error event. The truncation of the infinite series used in calculating the union bound of the BER for the high SNR region can be obtained by considering the error event up to a chosen value.

Determining the maximum length of error is essential in obtaining a tighter estimate of the BER. The maximum length chosen should contain the dominant error event for the SNR region of interest. Computational complexity increases with the choice of the maximum error event to be accounted for.

In this example a maximum error event of length 5 will be considered. The BER of the SOSFTC-OFDM scheme will then be calculated using equation (4.74). The derived

closed-form expression for the PEP, i.e. equation (4.37), is used in the equation.

Starting with an error event of length one, only one bit has errors in the error event path, i.e. {(0,1)}, when an all-zero sequence, viz, {(0,0)}, is transmitted.

For an error event of length two, there is a total of 12 bits in error from the four error event paths i.e. {(1,0)(1,0), (1,0)(1,1), (1,1)(1,0) and (1,1)(1,1)}, when an all-zero sequence, i.e. {(0,0)(0,0)}, are transmitted.

For an error event of length three, there is a total of 28 bits in error from the eight error event paths, i.e. {(1,0)(0,0)(1,0), (1,0)(0,0)(1,1), (1,0)(0,1)(1,0), (1,0)(0,1)(1,1), (1,1)(0,1)(1,0), (1,1)(0,1)(1,1), (1,1)(0,0)(1,0), (1,1)(0,0)(1,1)}, when an all zero sequence, i.e.{(0,0), (0,0), (0,0)}, are transmitted.

For an error event of length four, there is a total of 64 bits in error from the 16 error event paths, i.e.{ (1,0)(0,0)(0,0)(1,0), (1,0)(0,0)(0,0)(1,1), (1,0)(0,0)(0,1)(1,0), (1,0)(0,0)(0,1)(1,1), (1,0)(0,1)(0,0)(1,0), (1,0)(0,1)(0,0)(1,1), (1,0)(0,1)(0,1)(1,0), (1,0)(0,1)(0,1)(1,1), (1,1)(0,0)(0,0)(1,0), (1,1)(0,0)(0,0)(1,1), (1,1)(0,0)(0,1)(1,0), (1,1)(0,0)(0,1)(1,1), (1,1)(0,1)(0,0)(1,0), (1,1)(0,1)(0,0)(1,1), (1,1)(0,1)(0,1)(1,0) and (1,1)(0,1)(0,1)(1,1)}, when an all-zero sequence, i.e.{(0,0), (0,0), (0,0), (0,0)} are transmitted.

For an error event of length five, there is a total of 144 bits in error from the 32 error event paths, i.e.{ (1,0)(0,0)(0,0)(0,0)(1,0), (1,0)(0,0)(0,0)(0,0)(1,1), (1,0)(0,0)(0,0)(0,1)(1,0), (1,0)(0,0)(0,0)(0,1)(1,1), (1,0)(0,0)(0,1)(0,0)(1,0), (1,0)(0,0)(0,1)(0,0)(1,1), (1,0)(0,0)(0,1)(0,1)(1,0), (1,0)(0,0)(0,1)(0,1)(1,1), (1,0)(0,1)(0,0)(0,0)(1,0), (1,0)(0,1)(0,0)(0,0)(1,1), (1,0)(0,1)(0,0)(0,1)(1,0), (1,0)(0,1)(0,0)(0,1)(1,1), (1,0)(0,1)(0,1)(0,0)(1,0), (1,0)(0,1)(0,1)(0,0)(1,1), (1,0)(0,1)(0,1)(0,1)(1,0), (1,0)(0,1)(0,1)(0,1)(1,1), (1,1)(0,0)(0,0)(0,0)(1,0), (1,1)(0,0)(0,0)(0,0)(1,1), (1,1)(0,0)(0,0)(0,1)(1,0), (1,1)(0,0)(0,0)(0,1)(1,1), (1,1)(0,0)(0,1)(0,0)(1,0), (1,1)(0,0)(0,1)(0,0)(1,1), (1,1)(0,0)(0,1)(0,1)(1,0), (1,1)(0,0)(0,1)(0,1)(1,1),

(1,1)(0,1)(0,0)(0,0)(1,0), (1,1)(0,1)(0,0)(0,0)(1,1), (1,1)(0,1)(0,0)(0,1)(1,0), (1,1)(0,1)(0,0)(0,1)(1,1), (1,1)(0,1)(0,1)(0,0)(1,0), (1,1)(0,1)(0,1)(0,0)(1,1), (1,1)(0,1)(0,1)(0,1)(1,0) and (1,1)(0,1)(0,1)(0,1)(1,1)}, when an all-zero sequence, i.e.{(0,0), (0,0), (0,0), (0,0), (0,0) }, is transmitted.

All other error events can be calculated using the above methods.

The error events of length one, two, three, four and five can be expressed in terms of the PEP as PEP_1, PEP_2, PEP_3, PEP_4 and PEP_5, respectively.

To approximate the BER by considering only the error event path of one, two, three, four and five, the $BER_1, BER_2, BER_3, BER_4,$ and BER_5 respectively, are used.

$$BER_1 \approx \frac{1}{2}(PEP_1) \tag{4.75}$$

$$BER_2 \approx \frac{1}{2}(PEP_1 + 12 * PEP_2) \tag{4.76}$$

$$BER_3 \approx \frac{1}{2}(PEP_1 + 12 * PEP_2 + 28 * PEP_3) \tag{4.77}$$

$$BER_4 \approx \frac{1}{2}(PEP_1 + 12 * PEP_2 + 28 * PEP_3 + 64 * PEP_4) \tag{4.78}$$

$$BER_5 \approx \frac{1}{2}(PEP_1 + 12 * PEP_2 + 28 * PEP_3 + 64 * PEP_4 + 144 * PEP_5) \tag{4.79}$$

4.4 PERFORMANCE RESULT

The simulated and the calculated performance of an SOSFTC-OFDM system in a quasi-static frequency selective fading channel are presented. The same parameter stated in Section 4.2.2 is used for the calculated and simulated code. The derived closed form PEP expression for the various SNR regions is presented in Figure 4.2 for various error event lengths. An error

event of length 2 has the worst PEP compared to error events of length 1, 3, 4 and 5. This is because for the chosen SOSFTC-OFDM code, the dominant error event is concentrated at error event path of length 2. This is the worst case PEP scenario for the code.

In Figure 4.3, the simulated BER for N=64 is compared with the calculated BER for various error events: 1, 2, 3, 4 and 5, which correspond to N = 2, 4, 6, 8 and 10, respectively. The graph shows that an increase in the error events (i.e. from 1 to 5) gives a more accurate and tighter BER evaluation compared with the simulated one. The graph shows that for a maximum error event of length 5, the analysis and the simulation are very close, therefore for the high SNR region, the calculated BER values can be used instead of simulation, which can be time- consuming.

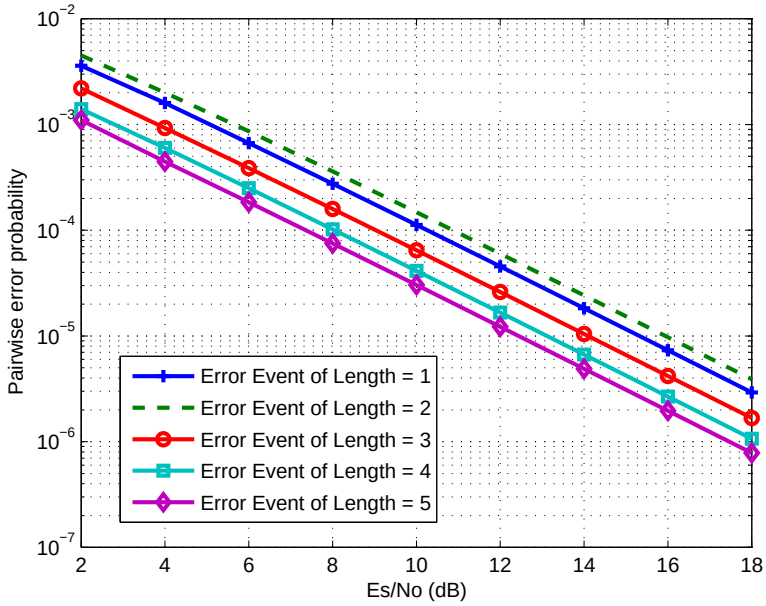

Figure 4.2: PEP performance for a two-state BPSK SOSFTC-OFDM scheme

4.5 SUMMARY

In this chapter, the derivation of a closed-form PEP expression is given for an SOBC-OFDM scheme using the Gauss Chebyshev quadrature technique. The derived PEP is a function of the codeword difference matrix between the transmitted and the erroneously decoded codeword matrix. The method proposed in this chapter is not limited to only SOSFTC-

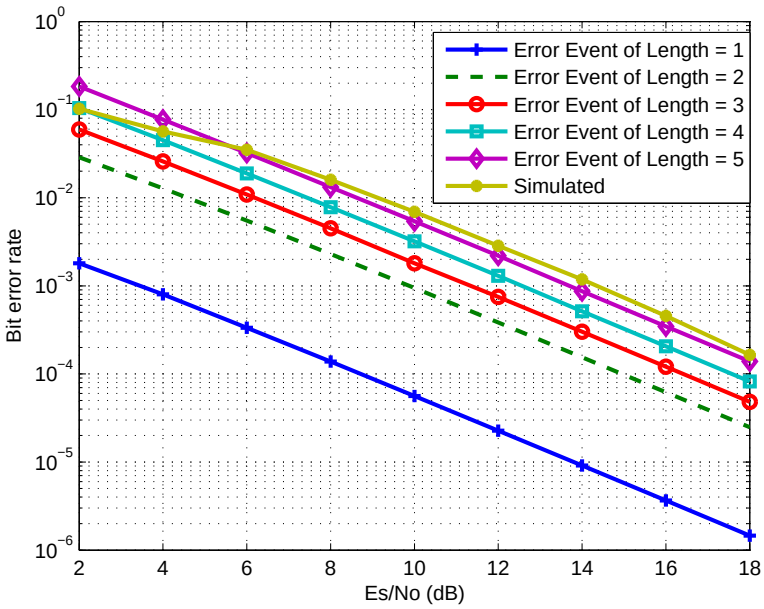

Figure 4.3: BER for a two-state BPSK SOSFTC-OFDM scheme

OFDM, schemes but can be extended to other kinds of space-frequency coded schemes, e.g. [108] where there is no angular rotation of the orthogonal block code.

CHAPTER 5

BER ANALYSIS OF SOBC-OFDM WITH ESTIMATION ERRORS

The performance of SOBC-OFDM schemes has been studied in this thesis, with the assumption that perfect channel state information is available at the receiver so that coherent decoding is possible. In most practical scenarios [109], some form of estimation is done for the channel state information and decoding is done based on the estimated channel state information. Estimation of the channel state information can either be by using training (i.e. pilot) symbols (i.e. pilot-based channel estimation [90], [92]) or by using second or higher order statistics of the transmitted signals (i.e. blind channel estimation [78], [79]).

Pilot-based channel estimation algorithms have been observed to have lower complexity than the blind channel estimation algorithm, since there is no need for a long data record [110]. When pilot symbols are used in channel estimation, the estimated channel consists of estimation errors that can affect the performance of the communication system. It is therefore relevant to study the effect of channel estimation errors on SOBC-OFDM.

In this chapter, an LS estimation technique is applied to an SOBC-OFDM scheme in quasi-static FS fading channel. Sequences of pilot code vector are used to estimate the channel matrix. Using the Gauss Chebychev quadrature technique previously described in Chapter 4, a closed form expression for the PEP is derived by assuming the statistical property of the channel estimation error. The expression is used to calculate the BER of a two BPSK SOSTTC-OFDM scheme.

5.1 SYSTEM MODEL

A SOBC-OFDM transmission system with N_t transmit antennas, N_r receive antennas and N subcarriers is considered. At the n^{th} subcarrier index, the encoder encodes the information symbols $s(n)$ into N_t coded symbols $x_1(n), x_2(n), \ldots, x_{N_t}(n)$, which are transmitted by the N_t. The signal received for a generic OFDM transmission at the j^{th} received antenna, on the n^{th} subcarrier, is given as:

$$r_j(n) = \sum_{i=1}^{N_t} H_{ij}(n)x_i(n) + \eta_j(n), \qquad j = 1,2,\ldots,N_r \tag{5.1}$$

where $H_{ij}(n)$ is the channel impulse in frequency domain from the i^{th} transmit antenna to the j^{th} receive antenna on the n^{th} subcarrier. The term $\eta_{ij}(n)$ is an AWGN from the i^{th} transmit antenna to the j^{th} receive antenna on the n^{th} subcarrier. The noise component is zero-mean vector and variance $\sigma^2/2$ per dimension. The channel coefficients are assumed to be Rayleigh fading channel.

The signal received equation (5.1) can be rewritten in matrix form for a full rate $N_t = 2$ SOBC-OFDM scheme on the nth subcarrier as:

$$\mathbf{r}_j(n) = \mathbf{X}(n)\mathbf{H}_j(n) + \boldsymbol{\eta}_j(n), \tag{5.2}$$

where $\mathbf{H}_j(n) = [H_{1j}(n)\ H_{2j}(n)]^T$ and for an entire frame of N subcarries, equation (5.2) can be written as:

$$\mathbf{R}_j = \mathbf{X}_j\mathbf{H}_j + \tilde{\mathbf{N}}_j, \tag{5.3}$$

with the individual elements given by,

$$\mathbf{R}_j = [\mathbf{r}_j(1)\ \mathbf{r}_j(2)\ \mathbf{r}_j(3)\ \cdots\ \mathbf{r}_j(N)]^T, \tag{5.4}$$

$$\mathbf{X}_j = \begin{bmatrix} \mathbf{X}(1) & 0 & \dots & 0 \\ 0 & \mathbf{X}(2) & \dots & 0 \\ \vdots & \vdots & \ddots & \vdots \\ 0 & 0 & \dots & \mathbf{X}(N) \end{bmatrix}, \tag{5.5}$$

$$\mathbf{H}_j = [\mathbf{H}_j(1)\ \mathbf{H}_j(2)\ \mathbf{H}_j(3)\ \cdots\ \mathbf{H}_j(N)]^T, \tag{5.6}$$

and

$$\tilde{\mathbf{N}}_j = [\boldsymbol{\eta}_j(1)\ \boldsymbol{\eta}_j(2)\ \boldsymbol{\eta}_j(3)\ \cdots\ \boldsymbol{\eta}_j(N)]^T. \tag{5.7}$$

In an OFDM system the channel impulse in the frequency domain can be expressed as:

$$H_{ij}(n) = \sum_{l=0}^{L-1} h_{ij}(l,t)\exp(-j2\pi n n_l/N), \tag{5.8}$$

where $h_{ij}(l,t)$, for $l = 0,1,2,\cdots,L-1$, are narrowband zero-mean complex Gaussian processes for the different i transmit antenna and j receive antennas. Equation (5.8) can be rewritten in matrix form as:

$$H_{ij}(n) = \mathbf{h}_{ij}\mathbf{f}(n), \tag{5.9}$$

where $\mathbf{h}_{ij} = [h_{ij}(0)\ h_{ij}(1)\ \cdots\ h_{ij}(L-1)]$ is the channel vector, $\mathbf{f}(n) = [f(0)\ f(1)\ \cdots\ f(L-1)]^T$ is the FFT coefficient vector (note that $f(k) = e^{-j2\pi nk/N}$) and T denotes the transpose operation.

5.2 CHANNEL ESTIMATION

Based on equation (5.2), the signal received at the pilot subcarrier p for transmit antenna i and receive antenna j can be written as:

$$\mathbf{r}_j(p) = \mathbf{X}(p)\mathbf{H}_j(p) + \boldsymbol{\eta}_j(p), \tag{5.10}$$

where $\boldsymbol{\eta}_j(p)$ consists of i.i.d complex Gaussian random noise vectors, $\mathbf{X}(p)$ is the orthogonal pilot symbols matrix and $\mathbf{r}_j(p)$ is the received pilot matix at the pilot instance. From equation (5.10) , the least squares estimate [111] of the channel matrix at the pilot subcarrier is given by :

$$\tilde{\mathbf{H}}(p) = \frac{(\mathbf{X}(p))^H \mathbf{r}_j(p)}{\mathbf{X}(p)(\mathbf{X}(p))^H}, \tag{5.11}$$

where $(\bullet)^H$ denotes the conjugate transpose operator. The pilot symbols must be chosen such that $\mathbf{X}(p)(\mathbf{X}(p))^H$ is invertible. In the remainder of the analysis, the pilot index p in equation (5.11) can be omited for notation convenience.

Using equation (5.10) and equation (5.11), the estimated channel impulse in the frequency domain $\tilde{\mathbf{H}}$ can be rewritten as:

$$\tilde{\mathbf{H}} = \mathbf{H} + \frac{\mathbf{X}^H \boldsymbol{\eta}}{\mathbf{X}\mathbf{X}^H}. \tag{5.12}$$

The denominator in equation (5.13) can be written as $\mathbf{X}\mathbf{X}^H = N_t \mathbf{I}_{N_t}$, since all the transmitted orthogonal training symbols are selected from a constellation where each member has normalised unit energy, e.g. PSK.

Therefore equation (5.12) can be rewriten as:

$$\tilde{\mathbf{H}} = \mathbf{H} + \frac{\mathbf{X}^H \boldsymbol{\eta}}{N_t \mathbf{I}_{N_t}}. \tag{5.13}$$

The estimate of the channel written in equation (5.13) can be seen to be perturbed by zero-mean Gaussian noise and can be rewritten as:

$$\tilde{\mathbf{H}} = \mathbf{H} + \underbrace{\frac{\mathbf{X}^H \boldsymbol{\eta}}{N_t \mathbf{I}_{N_t}}}_{\mathbf{E}} = \mathbf{H} + \mathbf{E}. \tag{5.14}$$

When the estimate of the channel impulse in the frequency domain is perfect, the channel frequency domain estimation error matrix $\mathbf{E} = \mathbf{0}$ and

$$\tilde{\mathbf{H}} = \mathbf{H}. \tag{5.15}$$

For an entire frame of N transmitted subcarriers the estimated channel impulse in the frequency domain can be expanded as follow:

$$\begin{aligned} \tilde{\mathbf{H}} &= [\tilde{\mathbf{H}}(1)\ \tilde{\mathbf{H}}(2)\ \tilde{\mathbf{H}}(3)\ \cdots\ \tilde{\mathbf{H}}(N)] \\ \tilde{\mathbf{H}} &= \begin{bmatrix} \tilde{\mathbf{h}}_j\mathbf{F}(0) & \mathbf{0} & \dots & \mathbf{0} \\ \mathbf{0} & \tilde{\mathbf{h}}_j\mathbf{F}(2) & \dots & \mathbf{0} \\ \dots & \dots & \ddots & \vdots \\ \mathbf{0} & \mathbf{0} & \dots & \tilde{\mathbf{h}}_j\mathbf{F}(N) \end{bmatrix} \end{aligned} \tag{5.16}$$

where the estimated channel impulse in the time domain is written as:

$$\begin{aligned} \tilde{\mathbf{h}}_j &= [\tilde{\mathbf{h}}_{1j}\ \tilde{\mathbf{h}}_{2j}] \\ \tilde{\mathbf{h}}_j &= [\tilde{h}_{1j}(0)\ \cdots\ \tilde{h}_{1j}(L-1)\ \tilde{h}_{2j}(0)\ \cdots\ \tilde{h}_{2j}(L-1)] \end{aligned} \tag{5.17}$$

and $\mathbf{F}(n)$ is the FFT coefficient matrix.

An alternative expression of the estimated channel impulse in the time domain as a function of the time domain channel impulse error $\mathbf{e}$ is written as:

$$\tilde{\mathbf{h}} = \mathbf{h} + \underbrace{\frac{\mathbf{X}^H \boldsymbol{\eta}}{N_t \mathbf{I}_{N_t} \otimes \mathbf{F}(n)}}_{\mathbf{e}} = \mathbf{h} + \mathbf{e} \tag{5.18}$$

where $\otimes$ is the Kronecker product operator.

5.3 PERFORMANCE ANALYSIS

To evaluate the performance of the SOBC-OFDM system with imperfect channel estimation, the PEP is used. This is the probability of selecting the codeword

$$\hat{\mathbf{X}} = [\hat{x}(1) \;\; \hat{x}(2) \;\; \cdots \;\; \hat{x}(N)], \tag{5.19}$$

when the codeword

$$\mathbf{X} = [x(1) \;\; x(2) \;\; \cdots \;\; x(N)], \tag{5.20}$$

was transmitted after the channel had been estimated.

The ML decoding metric that represents the actual transmitted codeword (i.e. $m(\mathbf{R},\mathbf{X})$) and the wrongly decoded codeword (i.e. $m(\mathbf{R},\hat{\mathbf{X}})$) will be used.

The ML metrics corresponding to the actual and the wrongly decoded codeword, based on equation (5.3), for $j = 1$ are given by equation (5.21) and equation (5.22), respectively.

$$m(\mathbf{R},\mathbf{X}) = ||\mathbf{R} - (\tilde{\mathbf{H}}\mathbf{X})||^2, \tag{5.21}$$

$$m(\mathbf{R},\hat{\mathbf{X}}) = ||\mathbf{R} - (\tilde{\mathbf{H}}\hat{\mathbf{X}})||^2, \tag{5.22}$$

where $\tilde{\mathbf{H}}$ is expressed in (5.16).

The PEP over the entire N subcarriers and for the estimated channel in the frequency domain is written as:

$$\begin{aligned} P(\mathbf{X} \to \hat{\mathbf{X}}|\tilde{\mathbf{H}}) &= Pr\{m(\mathbf{R},\mathbf{X}) > m(\mathbf{R},\hat{\mathbf{X}})\} \\ &= Pr\{(m(\mathbf{R},\mathbf{X}) - m(\mathbf{R},\hat{\mathbf{X}})) > 0\}. \end{aligned} \tag{5.23}$$

Simplifying (5.23) by substituting (5.21) and (5.21) gives the following expression:

$$\begin{aligned} P(\mathbf{X}\rightarrow\hat{\mathbf{X}}|\tilde{\mathbf{H}}) &= Pr\{||\mathbf{R}-(\tilde{\mathbf{H}}\mathbf{X})||^2)-||\mathbf{R}-(\tilde{\mathbf{H}}\hat{\mathbf{X}})||^2>0\} \\ &= Pr\{||\tilde{\mathbf{H}}\mathbf{X}||^2-||\tilde{\mathbf{H}}\hat{\mathbf{X}}||^2>0\} \\ &= Pr\{||\tilde{\mathbf{H}}(\mathbf{X}-\hat{\mathbf{X}})||^2>0\} \\ &= Pr\{||\tilde{\mathbf{H}}\boldsymbol{\Delta}||^2>0\} \end{aligned} \tag{5.24}$$

where $\boldsymbol{\Delta}$ is the codeword difference matrix that represents the difference between the codeword that was actually transmitted and the codeword that was decoded in error after the channel had been estimated.

The conditional PEP in equation (5.24) can now be expressed in terms of the complementary error function i.e. erfc as:

$$P(\mathbf{X}\rightarrow\hat{\mathbf{X}}|\tilde{\mathbf{H}}) = \frac{1}{2}\text{erfc}\left(\sqrt{\frac{E_s}{4N_o}\tilde{\mathbf{H}}\boldsymbol{\Delta}\boldsymbol{\Delta}^H\tilde{\mathbf{H}}^H}\right). \tag{5.25}$$

Expanding equation (5.25) will result in:

$$P(\mathbf{X}\rightarrow\hat{\mathbf{X}}|\tilde{\mathbf{h}}) = \frac{1}{2}\text{erfc}\left(\sqrt{\frac{E_s}{4N_o}\sum_{n=1}^{N}\tilde{\mathbf{h}}\mathbf{F}(n)\Delta(n)(\Delta(n))^H(\mathbf{F}(n))^H(\tilde{\mathbf{h}})^H}\right), \tag{5.26}$$

where the expression for $\mathbf{F}(n)$ has been given in (4.24) and $\boldsymbol{\Delta}\boldsymbol{\Delta}^H$ is the codeword difference matrix with detailed expression in (5.27) and (5.28).

$$\boldsymbol{\Delta}\boldsymbol{\Delta}^H = \begin{bmatrix} \boldsymbol{\Delta}(1)(\boldsymbol{\Delta}(1))^H & 0 & \dots & 0 \\ 0 & \boldsymbol{\Delta}(2)(\boldsymbol{\Delta}(2))^H & \dots & 0 \\ \vdots & \vdots & \ddots & \vdots \\ 0 & 0 & \dots & \boldsymbol{\Delta}(N)(\boldsymbol{\Delta}(N))^H \end{bmatrix}, \tag{5.27}$$

and where

$$\boldsymbol{\Delta}(n) = \mathbf{X}(n)-\hat{\mathbf{X}}(n). \tag{5.28}$$

The intergral expression for the efrc [105] is written:

$$\text{erfc}(b) = \frac{2}{\pi}\int_0^{\infty} \frac{e^{-b^2(t^2+1)}}{t^2+1}\,dt. \tag{5.29}$$

Based on the above intergral expression of the efrc, the averaging of the conditional probability in equation (5.26) can be written as:

$$P(\mathbf{X}\rightarrow\hat{\mathbf{X}}|\tilde{\mathbf{h}}) = \frac{1}{\pi}E\left\{\int_0^{\infty}\frac{\exp[-(t^2+1)\frac{E_s}{4N_o}\tilde{\mathbf{h}}\mathbf{Q}(\tilde{\mathbf{h}})^H]}{t^2+1}\,dt\right\}, \tag{5.30}$$

where

$$\mathbf{Q}=\sum_{n=1}^{N}\mathbf{F}(n)\boldsymbol{\Delta}(n)(\boldsymbol{\Delta}(n))^H(\mathbf{F}(n))^H. \tag{5.31}$$

The averaged conditional probability given in equation (5.30) can be simplified based on the results in [72] i.e.

$$E[\exp(-\mathbf{z}\mathbf{M}(\mathbf{z}^*)^T)] = \frac{\exp[-\boldsymbol{\mu}\mathbf{M}(\mathbf{I}+\sigma_{\mathbf{z}}^2\mathbf{M})^{-1}(\boldsymbol{\mu}^*)^T]}{\det(\mathbf{I}+\boldsymbol{\sigma}_{\mathbf{z}}^2\mathbf{M})}, \tag{5.32}$$

where $\mathbf{z}$ is a Gaussian random row matric, $\boldsymbol{\mu}$ is the mean, $\boldsymbol{\sigma}_{\mathbf{z}}^2$ is the variance of $\mathbf{z}$ and $\mathbf{M}$ is a Hermittian matrix.

To solve equation (5.30), using equation (5.32), one need to obtain the mean and variance of the estimated channel matrix $\tilde{\mathbf{h}}$. The estimated channel matrix in the time domain $\tilde{\mathbf{h}}$ is a function of the channel matrix $\mathbf{h}$ and the channel estimation error matrix $\mathbf{e}$ as given in equation (5.18), which are uncorrelated and independent of each other.

In [106], the sum D of any two independent random variables $\text{A}\sim C(\mu_{\text{A}},\sigma_{\text{A}}^2)$ and $\text{B}\sim C(\mu_{\text{B}},\sigma_{\text{B}}^2)$ that are normally distributed is also normally distributed i.e.

$$\begin{aligned}\text{D} &= \text{A}+\text{B}\\ \text{D} &\sim C(\mu_{\text{A}}+\mu_{\text{B}},\sigma_{\text{A}}^2+\sigma_{\text{B}}^2).\end{aligned} \tag{5.33}$$

Based on equation (5.33), the mean and the variance of the elements of the estimated channel

matrix $\tilde{\mathbf{h}}$ is therefore the addition of the mean and variance of $\mathbf{h}$ and $\mathbf{e}$. The mean of $\tilde{\mathbf{h}}$ is expressed as:

$$\mu_{\tilde{\mathbf{h}}} = \mu_{\mathbf{h}} + \mu_{\mathbf{e}} \tag{5.34}$$

while the variance is expressed as:

$$\sigma^2_{\tilde{\mathbf{h}}} = \sigma^2_{\mathbf{h}} + \sigma^2_{\mathbf{e}}. \tag{5.35}$$

For the purpose of this analysis, one can assume that $\mathbf{h}$ and $\mathbf{e}$ have the same normal distribution and based on this assumption the mean of $\tilde{\mathbf{h}}$ will be an all-zero matrix and the variance will be the sum of the variance of $\mathbf{h}$ and $\mathbf{e}$ as given in equation (5.35).

Using equation (5.32) and substituting the mean and the variance of $\tilde{\mathbf{h}}$, the conditional PEP in (5.30) can be written as:

$$P(\mathbf{X} \to \hat{\mathbf{X}}) = \frac{1}{\pi}\int_0^{\infty} \frac{1}{t^2+1} \frac{1}{\det[\mathbf{I} + \frac{E_s}{4N_o}\sigma^2_{\tilde{\mathbf{h}}}\mathbf{Q}(t^2+1)]}\, dt, \tag{5.36}$$

To solve (5.36), one can follow the same process as described in Section 4.2.1, Chapter 4 to obtain the closed-form expression using the Gauss-Chebychev quadrature technique. The closed-form expression of the PEP with estimation error can therefore be written as:

$$P(\mathbf{X} \to \hat{\mathbf{X}}) = \frac{1}{2m}\sum_{i=1}^{m} \frac{1}{\det[\mathrm{I}_{LN_t} + \frac{E_s}{4N_o}\sigma^2_{\tilde{\mathbf{h}}}\mathbf{Q}\sec^2\frac{(2i-1)\pi}{4m}]} + \xi_m. \tag{5.37}$$

The main difference between the closed-form PEP expression for the case with perfect channel knowledge as given in Chapter 4 and equation (5.37) is the variance of the channel used and the codeword difference matrices. In Chapter 4 the variance of the channel is an identity matrix of size LN_t while in equation (5.37) the variance of estimated channel used will be an identity matrices of size LN_t with diagonal element of 0.5. This is as a result of the normalisation of the variance.

5.4 NUMERICAL EXAMPLE

To demonstrate the closed-form expression for the SOBC-OFDM scheme with channel estimation error, the two-state BPSK trellis described earlier in Section 4.2.1 of Chapter 4 will be used as an example. The trellis transmission will assume an SOSTTC-OFDM scheme instead of the SOSFTC-OFDM, as had been used as example in Chapter 4. The trellis in Figure 4.1 is constructed using the same concept of set-partitioning as explained in [39]. Two sets, each containing two pairs of BPSK symbols, are assigned to each state, i.e. there is a pair of parallel paths between each pair of states. The orthogonal pilot transmitted to estimate the channel are of the form:

$$\mathbf{X}(p) = \begin{bmatrix} x_1(p)e^{j\theta} & x_2(p) \\ -x_{2j}^*(p)e^{j\theta} & x_1^*(p) \end{bmatrix}. \tag{5.38}$$

After the orthogonal pilots had been used to estimate the channel, the information-carrying symbol is transmitted. In this example $N_t = 2, N_r = 1$, $L = 2$, the OFDM system has a bandwidth of 1 MHz and there are 64 OFDM subcarriers (N=64). The tone spacing of the OFDM system is 15.625 KHz. Based on these parameters $\mathbf{F}(n)$ is given as:

$$\mathbf{F}(n) = \begin{bmatrix} 1 & 0 \\ f(n) & 0 \\ 0 & 1 \\ 0 & f(n) \end{bmatrix}. \tag{5.39}$$

First the parallel paths, where $n = 1$, which corresponds to an error event length of 1 are considered. The codeword matrix obtained from the trellis and $\mathbf{F}(n)$ values is written as:

$$\mathbf{Q}(1) = \begin{bmatrix} 1 & 0 \\ f(1) & 0 \\ 0 & 1 \\ 0 & f(1) \end{bmatrix} \bullet \begin{bmatrix} 2 & -2 \\ 2 & 2 \end{bmatrix} \bullet \begin{bmatrix} 2 & 2 \\ -2 & 2 \end{bmatrix} \bullet \begin{bmatrix} 1 & f(1) & 0 & 0 \\ 0 & 0 & 1 & f(1) \end{bmatrix}. \tag{5.40}$$

For an error event of length 2, the codeword matrix obtained from the trellis based on the addition of the dominant error paths is expressed as:

$$\mathbf{Q}(2) = Q_1 + Q_2, \tag{5.41}$$

where

$$Q_1 = \begin{bmatrix} 1 & 0 \\ f(1) & 0 \\ 0 & 1 \\ 0 & f(1) \end{bmatrix} \bullet \begin{bmatrix} 0 & -2 \\ 2 & 0 \end{bmatrix} \bullet \begin{bmatrix} 0 & 2 \\ -2 & 0 \end{bmatrix} \bullet \begin{bmatrix} 1 & f(1) & 0 & 0 \\ 0 & 0 & 1 & f(1) \end{bmatrix}, \tag{5.42}$$

and

$$Q_2 = \begin{bmatrix} 1 & 0 \\ f(2) & 0 \\ 0 & 1 \\ 0 & f(2) \end{bmatrix} \bullet \begin{bmatrix} 0 & -2 \\ 0 & 2 \end{bmatrix} \bullet \begin{bmatrix} 0 & 0 \\ -2 & 2 \end{bmatrix} \bullet \begin{bmatrix} 1 & f(2) & 0 & 0 \\ 0 & 0 & 1 & f(2) \end{bmatrix}. \tag{5.43}$$

For an error event of length 3, the codeword matrix obtained from the trellis based on the addition of the dominant error paths is expressed as:

$$\mathbf{Q}(3) = Q_1 + Q_2 + Q_3, \tag{5.44}$$

where

$$Q_1 = \begin{bmatrix} 1 & 0 \\ f(1) & 0 \\ 0 & 1 \\ 0 & f(1) \end{bmatrix} \bullet \begin{bmatrix} 0 & -2 \\ 2 & 0 \end{bmatrix} \bullet \begin{bmatrix} 0 & 2 \\ -2 & 0 \end{bmatrix} \bullet \begin{bmatrix} 1 & f(1) & 0 & 0 \\ 0 & 0 & 1 & f(1) \end{bmatrix}, \tag{5.45}$$

$$Q_2 = \begin{bmatrix} 1 & 0 \\ f(2) & 0 \\ 0 & 1 \\ 0 & f(2) \end{bmatrix} \bullet \begin{bmatrix} 0 & 0 \\ 2 & 2 \end{bmatrix} \bullet \begin{bmatrix} 0 & 2 \\ 0 & 2 \end{bmatrix} \bullet \begin{bmatrix} 1 & f(2) & 0 & 0 \\ 0 & 0 & 1 & f(2) \end{bmatrix}, \quad (5.46)$$

and

$$Q_3 = \begin{bmatrix} 1 & 0 \\ f(3) & 0 \\ 0 & 1 \\ 0 & f(3) \end{bmatrix} \bullet \begin{bmatrix} 0 & -2 \\ 0 & 2 \end{bmatrix} \bullet \begin{bmatrix} 0 & 0 \\ -2 & 2 \end{bmatrix} \bullet \begin{bmatrix} 1 & f(3) & 0 & 0 \\ 0 & 0 & 1 & f(3) \end{bmatrix}. \quad (5.47)$$

For an error event of length 4, the codeword matrix obtained from the trellis based on the addition of the dominant error paths is expressed as:

$$\mathbf{Q}(4) = Q_1 + Q_2 + Q_3 + Q_4, \quad (5.48)$$

where

$$Q_1 = \begin{bmatrix} 1 & 0 \\ f(1) & 0 \\ 0 & 1 \\ 0 & f(1) \end{bmatrix} \bullet \begin{bmatrix} 0 & 2 \\ -2 & 0 \end{bmatrix} \bullet \begin{bmatrix} 0 & -2 \\ 2 & 0 \end{bmatrix} \bullet \begin{bmatrix} 1 & f(1) & 0 & 0 \\ 0 & 0 & 1 & f(1) \end{bmatrix}, \quad (5.49)$$

$$Q_2 = \begin{bmatrix} 1 & 0 \\ f(2) & 0 \\ 0 & 1 \\ 0 & f(2) \end{bmatrix} \bullet \begin{bmatrix} 0 & 2 \\ 0 & 2 \end{bmatrix} \bullet \begin{bmatrix} 0 & 0 \\ 2 & 2 \end{bmatrix} \bullet \begin{bmatrix} 1 & f(2) & 0 & 0 \\ 0 & 0 & 1 & f(2) \end{bmatrix}, \quad (5.50)$$

$$Q_3 = \begin{bmatrix} 1 & 0 \\ f(3) & 0 \\ 0 & 1 \\ 0 & f(3) \end{bmatrix} \bullet \begin{bmatrix} 0 & 2 \\ 0 & 2 \end{bmatrix} \bullet \begin{bmatrix} 0 & 0 \\ 2 & 2 \end{bmatrix} \bullet \begin{bmatrix} 1 & f(3) & 0 & 0 \\ 0 & 0 & 1 & f(3) \end{bmatrix}, \quad (5.51)$$

and

$$Q_4 = \begin{bmatrix} 1 & 0 \\ f(4) & 0 \\ 0 & 1 \\ 0 & f(4) \end{bmatrix} \bullet \begin{bmatrix} 0 & 0 \\ -2 & 2 \end{bmatrix} \bullet \begin{bmatrix} 0 & 0 \\ -2 & 2 \end{bmatrix} \bullet \begin{bmatrix} 1 & f(4) & 0 & 0 \\ 0 & 0 & 1 & f(4) \end{bmatrix}. \quad (5.52)$$

For an error event of length 5, the codeword matrix obtained from the trellis based on the addition of the dominant error paths is expressed as:

$$\mathbf{Q}(5) = Q_1 + Q_2 + Q_3 + Q_4 + Q_5, \quad (5.53)$$

where

$$Q_1 = \begin{bmatrix} 1 & 0 \\ f(1) & 0 \\ 0 & 1 \\ 0 & f(1) \end{bmatrix} \bullet \begin{bmatrix} 0 & 2 \\ -2 & 0 \end{bmatrix} \bullet \begin{bmatrix} 0 & -2 \\ 2 & 0 \end{bmatrix} \bullet \begin{bmatrix} 1 & f(1) & 0 & 0 \\ 0 & 0 & 1 & f(1) \end{bmatrix}, \quad (5.54)$$

$$Q_2 = \begin{bmatrix} 1 & 0 \\ f(2) & 0 \\ 0 & 1 \\ 0 & f(2) \end{bmatrix} \bullet \begin{bmatrix} 0 & 2 \\ 0 & 2 \end{bmatrix} \bullet \begin{bmatrix} 0 & 0 \\ 2 & 2 \end{bmatrix} \bullet \begin{bmatrix} 1 & f(2) & 0 & 0 \\ 0 & 0 & 1 & f(2) \end{bmatrix}, \quad (5.55)$$

$$Q_3 = \begin{bmatrix} 1 & 0 \\ f(3) & 0 \\ 0 & 1 \\ 0 & f(3) \end{bmatrix} \bullet \begin{bmatrix} 0 & 2 \\ 0 & 2 \end{bmatrix} \bullet \begin{bmatrix} 0 & 0 \\ 2 & 2 \end{bmatrix} \bullet \begin{bmatrix} 1 & f(3) & 0 & 0 \\ 0 & 0 & 1 & f(3) \end{bmatrix}, \quad (5.56)$$

$$Q_4 = \begin{bmatrix} 1 & 0 \\ f(4) & 0 \\ 0 & 1 \\ 0 & f(4) \end{bmatrix} \bullet \begin{bmatrix} 0 & 2 \\ 0 & 2 \end{bmatrix} \bullet \begin{bmatrix} 0 & 0 \\ 2 & 2 \end{bmatrix} \bullet \begin{bmatrix} 1 & f(4) & 0 & 0 \\ 0 & 0 & 1 & f(4) \end{bmatrix}, \quad (5.57)$$

and

$$Q_5 = \begin{bmatrix} 1 & 0 \\ f(5) & 0 \\ 0 & 1 \\ 0 & f(5) \end{bmatrix} \bullet \begin{bmatrix} 0 & 0 \\ -2 & 2 \end{bmatrix} \bullet \begin{bmatrix} 0 & 0 \\ -2 & 2 \end{bmatrix} \bullet \begin{bmatrix} 1 & f(5) & 0 & 0 \\ 0 & 0 & 1 & f(5) \end{bmatrix}. \quad (5.58)$$

Other codeword matrices can be calculated with respect to the error event path.

For different SNR, the calculated codeword matrix is then substituted into the closed-form PEP equation given in (5.37). The variance of the estimated channel will be an identity matrix whose diagonal elements is 0.5, since the channel power has been normalised to one. The PEP curve in Figure 5.1 is generated for $m = 2$.

Figure 5.1 shows the PEP curve for a two-state BPSK SOSTTC-OFDM for various error events. An error event of length 2 has the worst PEP compared to error event of length 1, 3, 4 and 5. This is because for the chosen SOSTTC-OFDM transmission, the dominant error event is concentrated at error event path of length 2. This is the worst case PEP scenario for the code.

Since a BER is of greater importance in digital communication than the PEP, an estimation of the BER for SOSTTC-OFDM with channel estimation error is obtained.

The BER of the SOSTTC-OFDM systems with a channel estimation error can be approxim-

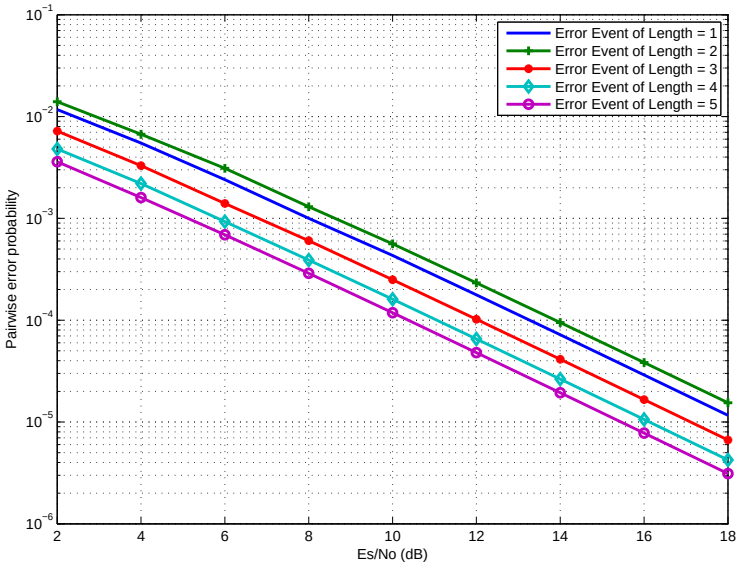

Figure 5.1: PEP performance of two-state BPSK SOSTTC-OFDM .

ated based on the truncated transfer function approach as explained in Section 4.3 of Chapter 4. The BER equations, i.e. (4.75), (4.76), (4.77), (4.78) and (4.79), can be used to obtain the approximated BER.

5.5 PERFORMANCE RESULT

The performance of the SOSTTC-OFDM with channel estimation error is evaluated using the same parameters for both simulation and analysis. Analytical BER was obtained using the previously derived closed-form PEP expression. In the closed-form PEP derivation, the variance of the estimated channel, i.e. $\sigma^2_{\tilde{\mathbf{h}}}$, is obtained by assuming that the channel impulse in the time domain and the channel estimation error are uncorellated zero-mean Gaussian random variables.

Monte Carlo simulation was used to simulate the BER of SOSTTC-OFDM with channel estimation error. The following parameters were used; $N_t = 2$, $N_r = 1$, $L = 2$, $N = 64$ and orthogonal pilots were used at the pilot instances. The channel is modelled as a quasi-static FS fading channel.

The graph in Figure 5.2 shows both the analytical BER (i.e. for an error event of length 1, 2, 3, 4 and 5) and the simulated BER. From Figure 5.2 it is observed that the accuracy of the

analytical BER and simulated BER is a function of the error event path chosen and the SNR region. For low SNR region fewer error event paths are needed, while for high SNR region more error event paths are needed.

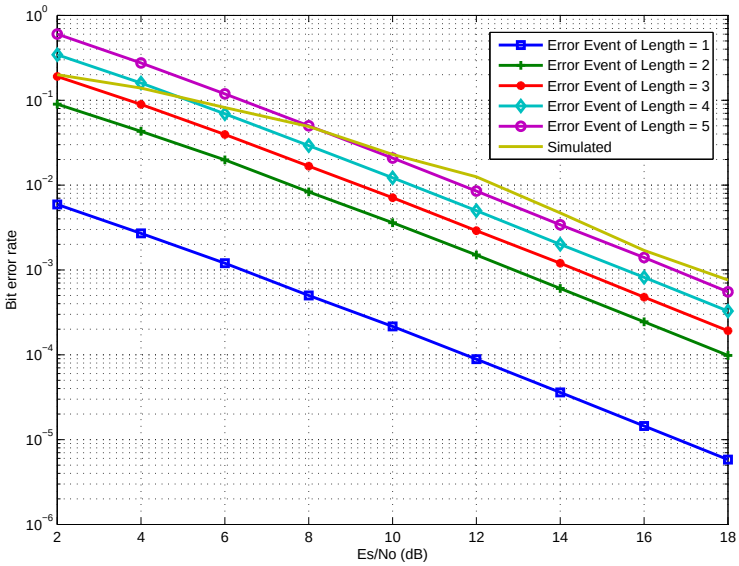

Figure 5.2: BER of SOSTTC-OFDM with imperfect channel estimation.

5.6 CONCLUSION

The analysis of the PEP and the BER performance of a SOSTTC-OFDM scheme, with channel estimation error in a quasi-static FS fading channel, is considered. By assuming the statistical distribution of the estimated channel information, a closed-form expression for the PEP was derived. The derived closed-form PEP was used to calculate the BER using the truncated transfer function method. The result shows that the analytical and simulated BER are the same for most SNR regions.

CHAPTER 6

CONCLUSION AND FUTURE RESEARCH

6.1 CONCLUSION

This thesis focuses on the performance of channel codes for multiple antenna-OFDM schemes in a coherent and non-coherent detection environment. A chapterwise summary and conclusion of the results presented in this thesis and possible future research work are given below.

In Chapter 1, a brief historical overview of the wireless industry is given, as well as the challenges faced in designing a robust network that can yield the performance needed to support emerging trends in the wireless industry. Current literature techniques on various transmit diversity techniques as a way of overcoming some of the challenges faced by signals in wireless networks were discussed. It was established that the capacity obtainable in the wireless network is a function of the diversity technique used and the number of transmit and receive antennas.

The concept of channel codes for multiple antenna systems, i.e. space-time codes, was introduced. These are codes that are used to increase the quality of signals in multiple antenna systems. The four main primary approaches to space-time coding as discussed in the literature were mentioned.

Lastly, the motivation and the objective of the research, original contributions of this thesis and the outline of the thesis were presented.

In Chapter 2, the error rate performance of channel codes for multiple antenna systems in both FS and flat fading channel were discussed. In FS fading channel, two main methods to mitigate the effect of symbol interference i.e. equalisation and orthogonal frequency division multiplexing were discussed.

A new receiver structure for SOSTTC with multichannel equalisation was proposed. Simulation results show that even though SOSTTC were designed for flat fading channel, it provides at least the same diversity order when applied to FS fading channel.

A new super-orthogonal block coding scheme in an OFDM environment was proposed, i.e. SOSFTC-OFDM that takes advantage of the spatial and frequency diversity possible for SOBCs in frequency selective fading channel. A performance comparison of SOSFTC-OFDM with other coded OFDM schemes (i.e. SOSTTC-OFDM, STTC-OFDM, STBC-OFDM and SFBC-OFDM) for various delay spreads was made. The FER curve shows that SOSFTC-OFDM outperforms other coded OFDM schemes. Lastly, the effect of channel delay spread on SOSFTC-OFDM system was shown. An increase in channel delay spread gives a better code performance.

In Chapter 3, simplified channel estimation algorithms were proposed for STTC-OFDM and SOBC-OFDM schemes i.e. SOSTTC-OFDM and SOSFTC-OFDM.

A non-overlapping pilot structure was applied to STTC-OFDM and orthogonal pilot structure was used for both SOSTTC-OFDM and SOSFTC-OFDM schemes. The proposed channel estimation algorithms were based on the premise of having an equal number of received equation and unknown channels at the pilot instance so that the channel impulse in the frequency domain can be easily estimated. Simulation results for various delay spreads and pilot intervals were given. Simulation results show that an increase in the number of pilot symbols used, which corresponds to a smaller pilot interval, gives a more accurate code performance when compared with the case of ideal channel state information, while a decrease in the number of pilots used, which corresponds to a higher pilot interval, gives a less accurate code performance when compared with the case of ideal channel state information.

In Chapter 4, a closed-form expression for the PEP of a SOBC-OFDM scheme was given for perfect channel state information. The closed-form PEP expression was obtained by using the Gauss Chebychev quadrature technique to solve the complementary error function of the conditional PEP. The closed-form PEP obtained was found to be a function of the codeword diference matrix between the transmitted codeword and the erroneously decoded codeword. The closed-form PEP expression was then used to calculate the BER. The simulated and analytical results for the SOSFTC-OFDM system are asymptotic at an error event of 5.

In Chapter 5, the performance analysis of a SOBC-OFDM scheme with channel estimation error was presented. A closed-form PEP expression was given for the SOBC-OFDM scheme with channel estimation error. The closed-form PEP expression was obtained by assuming that the statistical property of the channel impulse in the time domain and the channel estimation error are uncorrelated. The closed-form PEP expression obtained was found to be a function of the variance of the estimated channel impulse in the time domain and the codeword diference matrix between the transmitted codeword and the erroneously decoded codeword after the channel had been estimated. The derived PEP was used to calculate the BER of the SOSTTC-OFDM scheme. The analytical BER was close to the simulated BER for an error event of 5.

6.2 FUTURE RESEARCH

In this thesis, possible future work could be categorised into three main research areas, viz encoding schemes, the channel environment and receiver structure.

6.2.1 Encoding Schemes

This thesis concentrated on the SOBC that ensures orthogonality and gives a full-rate code, i.e. $N_t = 2$. Recently, in [112], [113], it has been proven that by relaxing some of the conditions on the conventional SOBCs, other codes could be generated for N_t greater than 2 with slightly improved code rates. Based on these new codes, other codes could be generated

that would take advantage of not only the space and time diversity but also the space and frequency diversity for such codes in an OFDM environment.

6.2.2 Channel Environment

The fading channel model used in this thesis was Rayleigh in its statistical distribution. The performance of the SOBC in other fading models e.g. Ricean fading channel and Nakagami fading channel, needs to be investigated. For both the Ricean and Nakagami fading channel, simplified channel estimation algorithms will have to be proposed. Also,an optimum channel estimation technique for multiple antenna systems still needs to discovered by comparing various channel estimation techniques and their perfomance in various fading channels. The performance of the new codes (i.e. [112], [113]) in an FS fading also channel needs to be investigated.

6.2.3 Receiver Structure

Research on optimum receiver structure for transmit diversity based OFDM continues. Possible future work will be to design an optimum receiver, with low complexity, for both super-quasi-orthogonal block code [112] and silver codes [113] for any number of transmit antennas in an OFDM environment.

REFERENCES

[1] M. R. Bhalla and A. V. Bhalla, "Generations of mobile wireless technology: A survey," *International Journal of Computer Application*, vol. 5, no. 4, pp. 26–32, August 2010.

[2] A. Kumar, Y. Liu, J. Sengupta, and G. Divya, "Evolution of mobile wireless communication Networks: 1G to 4G," *International Journal of Electronic and Communication Technologies*, vol. 1, no. 1, pp. 68–72, December 2010.

[3] S. M. Redl, M. K. Webber, and M. W. Oliphant, *An introduction to GSM*. Boston, USA: Artech House, 1995.

[4] F. Hilebrand, *GSM and UMTS: The creation of global communication*. Chichester, UK: John Wiley and Sons, 2001.

[5] M. J. Arshad, A. Farooq, and A. Shah, "Evolution and development towards 4th Generation (4G) mobile communication systems," *Journal of American Science*, vol. 6, no. 12, pp. 63–68, August 2010.

[6] T. S. Rappaport, *Wireless communications: Principles and Practice*. Second Edition, Prentice Hall, 2002.

[7] B. Li, "A survey on mobile WiMax," *IEEE Communications Magazine*, vol. 45, no. 12, pp. 70–75, December 2007.

[8] I. F. Akyildiz, D. M. Gutierrez-Estevez, and E. C. Reyes, "A survey on mobile

WiMax," *ELSEVIER Journal on Physical Communication*, vol. 3, pp. 217–244, August 2010.

[9] Wimax forum. [Online]. Available : `http://www.wimaxforum.org`.

[10] Technical White Paper: Long term evolution (LTE): A technical overview. [Online]. Available : `http://www.motorola.com`.

[11] H. Jafarkhani, *Space-time coding theory and practice*. Cambridge University Press, 2005.

[12] E. Biglieri, J. Proakis, and S. Shamai, "Fading channels: Information theoretic and communication aspects," *IEEE Transactions on Information Theory*, vol. 44, no. 6, pp. 2619–2692, October 1998.

[13] B. Sklar, "Rayleigh fading channels in mobile digital communication systems part 1:Charaterisation," *IEEE Communications Magazine*, vol. 35, no. 7, pp. 90–100, July 1997.

[14] N. Srivastava, "Diversity schemes for wireless communication: A short review," *Journal of Theoretical and Applied Information Technology*, vol. 15, no. 2, pp. 134–142, May 2010.

[15] C. B. Dietrich, K. Dietze, J. R. Nealy, and W. L. Stutzman, "Spatial, polarisation, and pattern diversity for wireless handheld terminals," *IEEE Transactions on Antenna and Propagation*, vol. 49, no. 9, pp. 1271–1281, September 2001.

[16] T. Eng, N. Kong, and L. B. Milstein, "Comparison of diversity combining techniques for Rayleigh fading channels," *IEEE Transactions on Communications*, vol. 44, no. 9, pp. 1117–1129, September 1996.

[17] D. G. Brennan, "Linear diversity combining techniques," *Proceeding of Institute of Radio Engineers*, vol. 47, no. 1, pp. 1075–1102, June 1959.

[18] N. Kong and L. B. Milstein, "Average SNR of a generalised diversity selection combining scheme," *IEEE Communications Letters*, vol. 3, no. 3, pp. 57–59, March 1999.

[19] I. E. Telatar, "Capacity of multi-antenna gaussian channels," *European Transactions on Telecommunication*, vol. 10, no. 6, pp. 585–595, Nov 1999.

[20] G. J. Foschini and M. J. Gans, "On limits of wireless communications in a fading environment when using multiple antennas," *IEEE Wireless Communications Magazine*, vol. 6, pp. 311–335, Mar 1998.

[21] W. Feller, *An introduction to probability theory and its applications*. Chichester, UK: John Wiley and Sons, 1971.

[22] H. Bengt, "On the capacity of the MIMO channel: A tutorial introduction," *IEEE Norwegian Symposium on Signal Processing*, pp. 167–172, May 2001.

[23] A. Paulraj, R. Nabar, and D. Gore, *Introduction to space-time wireless communication*. Cambridge University Press, 2003.

[24] V. Tarokh, H. Jafarkhani, and A. R. Calderbank, "Space-time codes for high data rate wireless communication; Performance analysis and code construction," *IEEE Transactions on Information Theory*, vol. 44, no. 2, pp. 744–756, March 1998.

[25] G. J. Foschini, "Layered space-time architecture for wireless communication in a fading environment when using multi-element antenna," *Bell Labs Technical Journal*, vol. 1, no. 2, pp. 41–59, Autumn 1996.

[26] A. J. Jameel, H. Adnan, Y. Xiaohu, and A. Hussain, "Layered space time codes in wireless communication channels: System design and performance analysis," in *Proceedings of Second International Conference on Developments in eSystems Engineering*, Abu Dhabi, December 2009, pp. 77–83.

[27] D. Shiu and J. Kahn, "Layered space-time codes for wireless communication using multiple transmit antennas ," in *Proceedings of the IEEE International Conference on*

Communications, Vancouver, Canada, June 1999, pp. 436–440.

[28] S. Alamouti, "Space-time block coding: A simple transmitter diversity technique for wireless communications," *IEEE Journal on Selected Areas in Communications*, vol. 16, pp. 1451–1458, October 1998.

[29] V. Tarokh, H. Jafarkhani, and A. R. Calderbank, "Space-time block codes from orthogonal designs," *IEEE Transactions on Information Theory*, vol. 45, pp. 1456–1467, July 1999.

[30] A. V. Geramita and J. Seberry, "Orthogonal designs, quadratic forms and Hadmard Matrices," *Lecture notes in Pure and Applied Mathematics*, vol. 43, June 1979.

[31] W. Su and X. G. Xia, "Two generalized complex orthogonal space-time block code of rates 7/11 and 3/5 for 5 and 6 transmit antennas," *IEEE Transactions on Information Theory*, vol. 49, no. 1, pp. 313–316, January 2003.

[32] ——, "A systematic design of high rate complex orthogonal space-time block codes," *IEEE Communications Letters*, vol. 6, no. 6, pp. 380–382, June 2004.

[33] A. Wittneben, "Base station modulation diversity for digital SIMULCAST," *Proceedings of IEEE Vehicular Technology Conference*, pp. 848–853, May 1991.

[34] N. Seshadri and J. H. Winters, "Two signaling schemes for improving the error performance of frequency division duplex (FDD) transmission systems using transmit antenna diversity," *International Journal on Wireless Information Networks*, vol. 1, no. 1, pp. 49–60, January 1994.

[35] S. Baro, G. Bauch, and A. Hansmann, "Improved codes for space-time trellis coded modulation," *IEEE Communications Letters*, pp. 20–22, January 2000.

[36] J. Grimm, M. Fitz, and J. Krogmeier, "Further results in space time coding for Rayleigh fading," in *Proceedings of Annual Allerton Communications, Control and Computing Conference*, Monticello, Illinois, Sepember 1998, pp. 391–400.

[37] Q. Yan and R. S. Blum, "Optimum space-time convolutional codes," *IEEE Wireless Communications and Networking Conference*, pp. 1351–1355, September 2000.

[38] A. J. Viterbi, "Error bounds for convolutional codes and an asymptotically optimum decoding algorithm," *IEEE Transactions on Communications*, pp. 260–269, April 1967.

[39] H. Jafarkhani and N. Seshadri, "Super-orthogonal space-time trellis codes," *IEEE Transactions on Information Theory*, vol. 49, pp. 937–950, April 2003.

[40] S. Siwamogsatham and M. P. Fitz, "Improved high rate space time codes via orthogonality and set partitioning," in *Proceedings of the IEEE Wireless Communications and Networking Conference*, vol. 1, Orlando, Florida, March 2002, pp. 264–270.

[41] M. Bale, B. Laska, D. Dunwell, F. Chan, and H. Jafarkhani, "Computer design of super-orthogonal space-time trellis codes," *IEEE Transactions on Wireless Communication*, vol. 6, no. 2, pp. 463–467, February 2007.

[42] E. R. Hartling, F. Chan, and H. Jafarkhani, "Design rules for extended super orthogonal space time trellis codes," in *Proceedings of the Canadian Conference of Electrical and Computer Engineering*, Niagara Falls, Ontario, May 2008, pp. 001 621–001 626.

[43] Y. Yang, Z. Zhong, and G. Xu, "Delay spread characteristics of wideband MIMO channel based on outdoor NLOS measurement," in *Proceedings of the IEEE Global Telecommunications Conference*, Washington DC, USA, November 2007, pp. 3745–3749.

[44] Y. Liu, M. Fitz, and Y. Takeshita, "Space time codes performance criteria and design for frequency selective fading channels ," in *Proceedings of the IEEE International Conference on Communications*, vol. 9, Helsinki, Finland, June 2001, pp. 2800–2804.

[45] S. Zhou and G. B. Giannakis, "Space time coding with maximun diversity gain over

frequency selective fading channels," *IEEE Signal Processing Letters*, vol. 8, no. 10, pp. 269–272, October 2001.

[46] D. Gore, S. Sandhu, and A. Paulraj, "Delay diversity code for frequency selective channels," *IEEE Electronics Letters*, vol. 37, pp. 1230–1231, September 2001.

[47] A. R. Hammons and H. E. Gamal, "On the theory of space-time codes for PSK modulation," *IEEE Transactions on Information Theory*, vol. 46, no. 2, pp. 524–542, March 2000.

[48] H. Y. Liang and W. Wu, "Improved design of criterion for good space-time trellis codes under block fading channel," in *Proceedings of the International Conference on Communications Technology*, vol. 2, April 2003, pp. 1111–1113.

[49] G. Kang, C. Elena, Q. Binghua, J. Xianglan, and Z. Ping, "Searching good space-time trellis codes of high complexity," in *Proceedings of the IEEE Wireless Communications and Networking Conference*, vol. 1, March 2002, pp. 109–113.

[50] Y. Gong and K. B. Letaief, "Performance evaluation and analysis of space-time coding in unequalised multipath fading links," *IEEE Transactions on Communications*, vol. 48, no. 11, pp. 1778–1782, November 2000.

[51] P. Luo and Y. Guan, "Optimum receiver for space-time trellis code in multipath fading channel," *International Zurich Seminar on Broadband Communications*, pp. 43–1–43–5, February 2002.

[52] E. Lindskog and A. Paulraj, "A Transmit diversity scheme for channels with intersymbol interference," in *Proceedings of IEEE International Conference on Communications*, vol. 1, June 2000, pp. 307–311.

[53] K. Amis and D. L. Roux, "Predictive decision feedback equalisation for space-time block codes with orthogonality in frequency domain ," in *Proceedings of IEEE Personal, Indoor and Mobile Radio Communication Conference*, vol. 2, Berlin, Germany,

September 2005, pp. 1140–1144.

[54] K. Zangi, "Physical layer issues for deploying transmit diversity in GPRS/EGPRS networks," in *Proceedings of the IEEE Vehicular Technology Conference*, vol. 2, October 2001, pp. 538–542.

[55] R. Asokan and H. Arslan, "Detection of STBC signal in frequency selective fading channels," in *Proceedings of World Wireless Congress*, San Francisco, USA, May 2003.

[56] Y. Rahayu, T. A. Rahman, R. Ngah, and P. S. Hall, "Ultra wideband technology and its applications," in *Proceedings of the 5th IFIP international Conference on Wireless and Optical Communications Networks*, May 2008, pp. 1–5.

[57] I. F. Akyildiz, W. Y. Lee, M. C. Vuran, and S. Mohanty, "NeXt generation/dynamic spectrum access/cognitive radio wireless networks: A survey," *Computer Networks*, vol. 50, no. 13, pp. 2127–2159, September 2006.

[58] T. Hwang, C. Yang, G. Wu, S. Li, and G. Y. Li, "OFDM and its wireless application: A survey," *IEEE Transactions on Vehicular Technology*, vol. 58, no. 4, pp. 1673–1694, May 2009.

[59] ETSI, "Radio Broadcasting Systems; Digital Audio Broadcasting (DAB) to Mobile, Portable and Fixed Receivers," in *European Telecommunications Standards Institute ETS 300 401*, vol. 300 401, Valbonne, France, 1997, pp. 1089–1093.

[60] ——, "Digital Video Broadcasting (DVB); Framing Structure, Channel Coding and Modulation for Digital Terrestrial Television," in *European Telecommunications Standards Institute ETS EN 300 744*, vol. 1.1.2, Valbonne, France, 1997.

[61] Part 11 Wireless LAN Medium Access control (MAC) and Physical Layer (PHY) Specifications: High-Speed Physical Layer in the 5 GHz band : *IEEE Standards 802.11a*.

[62] Part 16 Local and Metropolitan Area Networks: Air Interface for fixed broadband

Wireless Access Systems *IEEE Standards 802.16a*.

[63] Y. Hong, J. Choi, and X. Shao, "Performance analysis of space-time trellis coded OFDM over quasi-static frequency selective fading channel," in *Proceedings of the 2003 Joint Conference of the Fourth International Conference on Information, Communications and Signal Processing and Fourth Pacific Rim Conference on Multimedia*, vol. 3, Singapore, December 2003, pp. 1478–1482.

[64] G. Bauch, "Space-time block codes versus space-frequency block codes," in *Proceedings of the IEEE Vehicular Technology Conference*, Seoul, Korea, April 2003, pp. 567–571.

[65] K. Aksoy and U. Aygolu, "Super-orthogonal space-time frequency trellis coded OFDM," *IET Communication*, vol. 1, no. 3, pp. 317–324, June 2007.

[66] Y. Hong, J. Choi, and X. Shao, "Robust space-time trellis codes for OFDM systems over quasi-static frequency selective fading channels," in *Proceedings of IEEE Personal, Indoor and Mobile Radio Communications Conference*, vol. 1, Beijing, China, September 2003, pp. 434–439.

[67] H. Bolcskei and A. J. Paulraj, "Space-frequency coded broadband OFDM systems," in *Proceedings of IEEE Wireless Communications and Networking Conference*, Chicago, USA, September 2000, pp. 1–6.

[68] M. J. Dehghani, R. Aavind, S. Jam, and K. M. M. Prabhu, "Space-frequency block coding in OFDM systems," in *Proceedings of IEEE Region 10 Conference TENCON*, vol. 1, November 2004, pp. 543–546.

[69] M. K. Simon and H. Jafarkhani, "Performance evaluation of super-orthogonal space-time trellis codes using a moment generating function based approach," *IEEE Transactions on Signal Processing*, vol. 51, no. 11, pp. 2739–2751, February 2002.

[70] M. K. Simon and M. S. Alouini, *Digital communication over fading channels: A*

unified approach to performance analysis. Hoboken, NJ: Wiley, 2001.

[71] A. Dogandžić, "Chernoff bound on PEP of space-time codes," *IEEE Transactions on information theory*, vol. 49, no. 5, pp. 1327–1336, May 2003.

[72] G. L. Turin, "The Characteristic function of Hermetian quadratic forms in complex normal random variables," *Biometrika*, pp. 199–201, June 1960.

[73] D. Agrawal and et al., "Space-time coded OFDM for high rate data rate wireless communication over wideband channels," in *Proceedings of IEEE Vehicular Technology Conference*, vol. 3, Ontario, Canada, May 1998, pp. 2232–2236.

[74] M. K. Ozdemir and H. Arslan, "Channel estimation for wireless OFDM systems," *IEEE Communications Surveys and Tutorials*, vol. 9, no. 2, pp. 18–48, Second Quarter 2007.

[75] G. L. Stuber, J. R. Barry, S. W. McLaughlin, Y. G. Li, M. A. Ingram, and T. G. Pratt, "Broadband MIMO-OFDM wireless communications," in *Proceedings of the IEEE*, vol. 92, February 2004, pp. 271–294.

[76] Y. Li, N.Seshadri, and S. Ariyavistakul, "Channel estimation for OFDM systems with transmitter diversity in mobile wireless channels," *IEEE Journal on Selected Areas in Communication*, vol. 17, pp. 461–471, March 1999.

[77] M. Biguesh and A. B. Gershman, "On channel estimation and optimum training for MIMO systems," July 2004.

[78] W. Bai, "Blind channel estimation in MIMO-OFDM systems," *IECE Transaction on Communication*, vol. E85-B, no. 9, pp. 1849–1853, October 2002.

[79] S. Yatawatta and A. Petropulu, "Blind channel estimation in MIMO-OFDM systems," in *Proceedings of the IEEE Workshop Statistical Signal Process*, September 2003, pp. 363–366.

[80] T. Wo, P. A. Hoeher, A. Scherb, and K. D. Kammeyer, "Performance analysis of maximum-likelihood semiblind estimation of MIMO channels," in *Proceedings of the IEEE Vehicular Technology Conference*, Melbourne, Australia, May 2006, pp. 1738–1742.

[81] M. Abuthinien, S. Chen, and L. Hanzo, "Semiblind joint maximum likelihood channel estimation and data detection for MIMO systems," *IEEE Signal Processing Letters*, vol. 15, pp. 202–205, 2008.

[82] M. W. Numan, M. T. Islam, and N. Misran, "Performance and complexity improvement of training based channel estimation in MIMO systems," *Progress in Electromangnetic Research*, vol. 10, pp. 1–13, July 2009.

[83] J. J. van de Beek, O. Edfors, M. Sandell, S. Wilson, and P. Borjesson, "On channel estimation in OFDM systems," in *Proceedings of the IEEE Global Telecommunication Conference*, vol. 3, Chicago, USA, July 1995, pp. 815–819.

[84] P. Hoecher, S. Kaiser, and P. Robertson, "Pilot-symbol aided channel estimation in time and frequency," in *Proceedings of the IEEE Globecom Communications Theory Mini-Conference*, vol. 3, USA, November 1997, pp. 90–96.

[85] K. P. Bagadi and S. Das, "MIMO-OFDM channel estimation using pilot carriers," *International Journal on Computer Applications*, vol. 2, no. 3, pp. 81–88, May 2010.

[86] Y. Li, "Simplified channel estimation estimation for OFDM systems with multiple transmit antennas," *IEEE Transactions on Wireless Communications*, vol. 1, pp. 67–75, January 2002.

[87] S. M. Lee and H. J. Choi, "On channel estimation for space-time trellis coded OFDM systems," *IEICE Transactions on Communications*, vol. E85-B, November 2002.

[88] K. F. Lee and D. B. Williams, "Pilot symbol assisted channel for space time coded OFDM systems," *EURASIP Journal on Applied Signal Processing*, vol. 5, pp. 507–

516, 2002.

[89] M. A. Khojastepour and K. Gomadam, "Pilot assisted channel estimation for MIMO-OFDM systems using theory of sparse signal recovery," in *Proceedings of the IEEE International Conference on Acoustics Speech and Signal Processing*, Taipei, Taiwan, April 2009, pp. 2693–2696.

[90] B. C. Chen, W. J. Lin, and J. S. Lin, "Pilot assisted channel estimation for STBC based wireless MIMO-OFDM systems," in *Proceedings of the International Conference on Wireless Communications and Mobile Computing*, New York, USA, 2007, pp. 411–416.

[91] Y. Shen and E. Martinez, "Channel estimation in OFDM systems," *Freescale Semiconductor Inc. : Application Notes*.

[92] M. H. Hsieh and C. H. Wei, "Channel estimation for OFDM systems based comb-type pilot arrangement in frequency selective fading channels," *IEEE Transactions on Consumer Electronic*, vol. 44, no. 1, pp. 217–225, February 1998.

[93] Y. Zhao and A. Huang, "A novel channel estimation method for OFDM mobile communications systems based on pilot signals and transform domain processing," in *Proceedings of the IEEE 47th Vehicular Technology Conference*, USA, May 1997, pp. 2089–2093.

[94] A. V. Oppenhein and R. W. Schafer, *Discrete-time signal processing*. Prentice-Hall Inc. New Jersey, 1999.

[95] O. Sokoya and B. T. Maharaj, "Super-orthogonal block codes with multichannel equalisation and OFDM in frequency selective fading," *EURASIP Journal on Wireless Communication and Networking*, August 2010.

[96] G. Taricco and E. Biglieri, "Exact pairwise error probability of space-time codes," *IEEE Transactions on Information Theory*, vol. 48, no. 2, pp. 510–513, February

2002.

[97] M. Uysal and C. N. Geoghiades, "Error performance analysis of space-time codes over Rayleigh fading channels," *Journal of Communication and Network*, vol. 2, no. 4, pp. 351–356, December 2000.

[98] M. K. Simon, "Evaluation of average bit error probability for space-time coding based on a simple exact evaluation of pairwise error probability," *International Journal on Communications and Networks*, vol. 3, no. 3, pp. 257–264, September 2001.

[99] F. Xu and D. W. Yue, "Closed capacity and outage probability expression for orthogonal space time block codes," in *Proceedings of International Conference on ITS Telecommunications*, June 2006, pp. 507–510.

[100] J. K. Cavers and P. Ho, "Analysis of the error performance of trellis coded modulation in Rayleigh fading channels," *IEEE Transactions on Communications*, vol. 40, no. 1, pp. 74–83, January 1992.

[101] P. Ho and D. K. P. Fung, "Error performance of interleaved trellis coded PSK modulations in correlated Rayleigh fading channels," *IEEE Transactions on Communications*, vol. 40, no. 12, pp. 1800–1809, December 1992.

[102] R. U. Mahesh and A. K. Charurvedi, "Closed-form BER expression for BPSK OFDM systems with frequency offset," *IEEE Communications Letters*, vol. 14, no. 8, pp. 731–733, August 2010.

[103] P. Dharmawansa and N. Rajatheva, "An exact error probability analysis of OFDM systems with frequency offset," *IEEE Transactions on Communications*, vol. 57, no. 1, pp. 26–31, January 2009.

[104] C. Tellambura, "Evaluation of exact union bound for trellis coded modulation over fading channels," *IEEE Transactions on Communications*, vol. 44, no. 12, pp. 1693–1699, December 1996.

[105] M. Abramovitz and I. A. Stegun, *Handbook of mathematic functions*. Dover, New York, 1972.

[106] J. Proakis, *Digital Communication*. McGraw-Hill Higher, 2000.

[107] C. Ling, "Generalized union bound for space-time codes," *IEEE Transactions on Communications*, vol. 55, no. 1, pp. 90–99, January 2007.

[108] M. Torabi, "On the BER performance of space-frequency block coded OFDM systems in fading MIMO Channels," *IEEE Transactions on Wireless Communications*, vol. 6, no. 2, pp. 1366–1373, April 2007.

[109] W. M. Gifford, M. Z. Win, and M. Chiani, "Diversity with practical channel estimation," *IEEE Transaction on Wireless Communications*, vol. 4, pp. 1935–1947, July 2005.

[110] S. Coleri, M. Ergen, A. Puri, and A. Bahai, "Channel estimation techniques based on pilot arrangement in OFDM systems," *IEEE Transactions on Broadcast*, vol. 48, no. 3, pp. 223–208, 2002.

[111] M. Biguesh and A. B. Gershman, "Training-based MIMO channel estimation: A study of estimator tradeoffs and optimal training signals," *IEEE Transactions on Signal Processing*, vol. 54, no. 3, pp. 884–893, March 2006.

[112] H. Jafarkhani and N. Hassanpour, "Super-quasi orthogonal space-time trellis codes for four transmit antennas," *IEEE Transactions on Wireless Communications*, vol. 4, pp. 215–227, January 2005.

[113] Y. Wu and R. Calderbank, "Construction of high rate super-orthogonal space time block codes," in *Proceedings of IEEE International Conference on Communications*, Dresden, Germany, June 2009, pp. 1938–1883.